

---

Electronic Thesis and Dissertation Repository

---

12-6-2022 1:00 PM

# Noninvasive Quantification of Tissue Sodium Concentration in the Kidney Disease Spectrum using $^{23}\text{Na}$ Magnetic Resonance Imaging

Fabio R. Salerno, *The University of Western Ontario*

Supervisor: McIntyre, Christopher W., *The University of Western Ontario*

Co-Supervisor: Parraga, Grace, *The University of Western Ontario*

A thesis submitted in partial fulfillment of the requirements for the Doctor of Philosophy degree in Medical Biophysics

© Fabio R. Salerno 2022

Follow this and additional works at: <https://ir.lib.uwo.ca/etd>



Part of the [Cardiovascular Diseases Commons](#), [Medical Physiology Commons](#), [Nephrology Commons](#), and the [Physiological Processes Commons](#)

---

## Recommended Citation

Salerno, Fabio R., "Noninvasive Quantification of Tissue Sodium Concentration in the Kidney Disease Spectrum using  $^{23}\text{Na}$  Magnetic Resonance Imaging" (2022). *Electronic Thesis and Dissertation Repository*. 9025.

<https://ir.lib.uwo.ca/etd/9025>

This Dissertation/Thesis is brought to you for free and open access by Scholarship@Western. It has been accepted for inclusion in Electronic Thesis and Dissertation Repository by an authorized administrator of Scholarship@Western. For more information, please contact [wlsadmin@uwo.ca](mailto:wlsadmin@uwo.ca).

## Abstract

Chronic kidney disease (CKD), especially when requiring kidney replacement therapy (hemodialysis (HD) and peritoneal dialysis (PD)), is associated with extracellular water expansion with increased total body sodium. Sodium can also be accumulated in tissues independently of extracellular water. Sodium-23 magnetic resonance imaging ( $^{23}\text{Na}$  MRI) can quantify the concentration of sodium nuclei in tissues. Applied to the human leg, quantification of tissue sodium concentrations mainly at the skin and muscle level is possible. We hypothesized that increased tissue sodium concentrations exert toxic effects in CKD and dialysis. We aimed to (1) compare tissue sodium concentrations in adults, children and adolescents with CKD, HD and PD against healthy individuals, (2) identify their predictors, (3) understand their connection to left ventricular structure in patients receiving HD and (4) observe their relationship with adverse cardiovascular events and mortality in patients receiving HD and PD. Tissue sodium concentrations were increased in adult patients receiving HD and PD, with respect to healthy individuals. In children and adolescents with CKD, tissue sodium concentrations varied depending on CKD etiology, suggesting kidney disorders can be associated with either sodium wasting or accumulation. Tissue sodium concentrations were associated with older age and overweight in healthy individuals; in patients with CKD and receiving dialysis, hypoalbuminemia was an important predictor of tissue sodium concentrations. In pediatric CKD, proteinuria was also positively associated with tissue sodium concentrations, suggesting a role of proteinuria in increased sodium reabsorption. In patients receiving HD, dialysate sodium concentration was strongly positively associated with skin sodium concentrations.

In patients receiving HD, tissue sodium concentrations were associated with left ventricular hypertrophy and dilatation, with tissue sodium concentrations being highest in patients with a dilated heart. Skin sodium concentration was associated with major cardiovascular adverse events and mortality in patients receiving HD or PD. These findings expand our understanding on the toxicity of sodium in CKD and point out critical issues of current dialysis treatment practices. Future studies should explore improved technical applications of  $^{23}\text{Na}$  MRI and experiment with new therapies and treatment strategies to reduce tissue sodium concentration in patients with CKD and those receiving dialysis.

**Keywords:** sodium-23, magnetic resonance imaging, chronic kidney disease, hemodialysis, peritoneal dialysis, tissue sodium concentration

## Lay Summary

Sodium, one of the two constituents of table salt along with chloride, is the main ion contained in extracellular water. One of the main functions of the kidneys is to control extracellular water balance by excreting excess sodium and water. With sodium-23 magnetic resonance imaging ( $^{23}\text{Na}$  MRI) sodium concentration in human leg tissues can be measured. We hypothesized that diseased kidneys, especially when kidney replacement therapy is necessary, are associated with increased tissue sodium concentration. Our goals are to (1) compare tissue sodium concentrations in adults and children with kidney disease and receiving dialysis against healthy individuals, (2) identify what factors are associated with them, (3) understand their connection to heart structure in patients receiving dialysis and (4) observe their relationship with heart disease such as myocardial infarction and death in patients receiving dialysis.

In the first project, we found that adult patients receiving dialysis had higher tissue sodium concentrations compared with healthy individuals. Tissue sodium concentrations were higher in older, overweight individuals and when serum levels of the protein albumin were lower. In the second project, we found that tissue sodium concentrations in children and adolescents with kidney disease differed depending on what kind of kidney disease they had, suggesting that some forms of kidney disease lose sodium through the urine, whereas others reabsorb too much sodium from the urine. In the third project, we found that tissue sodium concentrations in patients receiving hemodialysis were mirrored by alterations in the heart structure, such as ventricle dilatation and increased wall thickness. In the fourth project, we observed that higher tissue sodium concentrations in the skin of patients receiving dialysis was associated with more occurrences of heart disease and death. We also found out that hemodialysis using high sodium concentration in

the dialysis fluid led to higher skin sodium concentration, suggesting hemodialysis itself may lead to tissue sodium accumulation.

These findings suggest that tissue sodium in kidney disease and dialysis is toxic. These results should prompt a change in dialysis prescriptions to reduce the amount of sodium accumulation, and future studies should design new treatments using tissue sodium as a target.

## Co-Authorship Statement

This work contains four manuscripts, either published or currently under peer review for publication. I am either the first author or joint first author in all these manuscripts, as a proof to my significant contribution to all aspects of this research. I was responsible for submitting all the manuscripts as well as addressing the questions raised during the peer review process. I wrote the original study manuscripts in three out of four studies, and significantly contributed to writing one. The original study design was devised by Dr. Christopher McIntyre, Dr. Elena Qirjazi, Dr. Alireza Akbari and Dr. Timothy Scholl. I later contributed by amending the original study protocol and taking over the study analyses after Dr. Elena Qirjazi completed her MSc degree.

I was responsible for management of study visits, echocardiography image acquisition and acquisition of participant data. I devised a standardized procedure for  $^{23}\text{Na}$  MR image analysis that was applied in all studies, and was responsible for study database management, statistical analysis and clinical/physiological interpretation of the data, as well as drafting the original manuscripts (in three out of four manuscripts) and final approval of all four manuscripts.

Dr. Christopher W. McIntyre MD, PhD, was my senior supervisor as well as Principal Investigator of these studies. He provided guidance and financial support, was responsible for the initial study conception, provided intellectual support for the final manuscripts and helped during the peer review process. He was also clinically responsible for the study procedures.

Dr. Elena Qirjazi, MD, MSc, was a nephrologist who devised the original study as a part of her MSc graduate degree. She developed the original study protocol and wrote the first draft manuscript of the study (Chapter 2).

Dr. Sandrine Lemoine MD, PhD, was a visiting professor from the University of Lyon, France. She collaborated in the later studies of this thesis project, and provided support in data management and interpretation, as well as final manuscript drafting.

Dr. Alireza Akbari, PhD, was responsible for developing the  $^{23}\text{Na}$  MRI transmit/receive coil and the MRI dedicated pulse sequence, as well as image acquisition and post-processing. He provided valuable help reviewing the technical details in the draft manuscripts as well as addressing some questions raised during the peer review process.

Dr. Timothy Scholl, PhD, provided technical and intellectual support when drafting the final manuscripts.

Dr. Guido Filler, MD, PhD, is a pediatric nephrologist, provided support in recruiting children and adolescents affected by chronic kidney disease in relation to the manuscript published in Chapter 3. He also provided intellectual support when interpreting the data, as well as drafting for the final manuscripts. He was also clinically responsible for the study procedures.

Organization and management of the study visits occurred with the collaboration of Ms. Jarrin Penny, RN and PhD Candidate, Mr. Justin Dorie, RPN, and Ms. Tanya Tamasi, RPN. MRI acquisition for all research participants was performed by Dr. Alireza Akbari, PhD and David Reese.

All co-authors approved the final manuscripts published in this thesis work and their contributions are explained below.

**Chapter 2** is an original research article entitled “Tissue sodium concentrations in chronic kidney disease and dialysis patients by lower leg sodium-23 magnetic resonance imaging” and was published in the journal *Nephrology, Dialysis, Transplantation* in 2020. This manuscript was authored as joint first authors by Elena Qirjazi and Fabio R. Salerno. Other co-authors were Alireza Akbari, Lisa Hur, Jarrin Penny, Timothy Scholl and Christopher W. McIntyre. Alireza Akbari developed and implemented the  $^{23}\text{Na}$  MRI acquisition and reconstruction technique, produced the concentration maps, mentored the image analysis process and contributed to the methods section. Lisa Hur contributed to the statistical analysis and analyzed the images for reproducibility along with Jarrin Penny. Timothy Scholl provided mentoring and technical insight into the  $^{23}\text{Na}$  MRI development and image acquisition. Christopher W. McIntyre conceived the original study idea, was medically responsible for the study, provided funding and supervision and approved the final manuscript.

**Chapter 3** is an original research article entitled “*Effects of pediatric chronic kidney disease and its etiology on tissue sodium concentration: a pilot study*” and was published in the journal *Pediatric Nephrology* in 2022. This manuscript was authored by Fabio R. Salerno, Alireza Akbari, Sandrine Lemoine, Timothy Scholl, Christopher W. McIntyre and Guido Filler.

Alireza Akbari developed and implemented the  $^{23}\text{Na}$  MRI acquisition and reconstruction technique, produced the concentration maps, and mentored the image analysis process. Sandrine Lemoine provided intellectual insight to the study conduct and data interpretation. Timothy Scholl provided mentoring and technical insight for the  $^{23}\text{Na}$  MRI development and image acquisition. Christopher W. McIntyre conceived the original study idea and provided funding, intellectual insight, and supervision. Guido Filler was responsible for the investigational visits; facilitated

recruitment; and provided clinical support, medical supervision, and intellectual insight on the interpretation of the results.

**Chapter 4** is an original research article entitled “*Tissue Sodium and Cardiac Structure in Chronic Hemodialysis Patients*” is currently under consideration for publication on Hemodialysis International. This manuscript was authored by Fabio R. Salerno, Alireza Akbari, Sandrine Lemoine and Christopher W. McIntyre.

Alireza Akbari developed and implemented the  $^{23}\text{Na}$  MR acquisition and reconstruction technique and produced the concentration maps for analysis. Sandrine Lemoine contributed to echocardiography data acquisition and to the interpretation of the study results. Christopher W. McIntyre conceived the original study idea, was medically responsible for the study, provided funding and supervision.

**Chapter 5** is an original research article entitled “*Outcomes and predictors of skin sodium concentration in dialysis patients*” and was published on the *Clinical Kidney Journal* in 2022. This manuscript was authored by Fabio R. Salerno, Alireza Akbari, Sandrine Lemoine, Guido Filler, Timothy Scholl and Christopher W. McIntyre. Alireza Akbari developed and implemented the  $^{23}\text{Na}$  MRI acquisition and reconstruction technique, produced the concentration maps, mentored the image analysis process and contributed to the methods section. Sandrine Lemoine was responsible for database maintenance, provided intellectual insight on imaging and data analysis. Guido Filler provided intellectual insight on result interpretation. Timothy Scholl provided mentoring and technical insight for the  $^{23}\text{Na}$  MRI development and image acquisition. Christopher

W. McIntyre conceived the original study idea, was medically responsible for the study, provided funding, supervision, verified the validity of the study data, and approved the final manuscript.

## Acknowledgements

I thank Dr. Christopher W. McIntyre, my senior supervisor, for his support. He inspired me to pursue a career in clinical research, and it allowed me to develop a wider perspective in the field of nephrology, my medical specialty, and medicine in general. He supported me when I took a leave of absence from the Program, as I returned to Italy during the first wave of the COVID-19 pandemic, despite all the difficulties everyone was facing at the time. He still supported me when I considered dropping out of the Medical Biophysics Ph.D. program in the face of burnout and supported me to this very moment.

I thank Dr. Grace Parraga, my co-supervisor. I have struggled to have a balanced relationship with her, and yet she provided scholarly guidance and support throughout the Ph.D. experience, especially during the first wave of the COVID-19 pandemic, up to now. Although she was not directly involved in the drafting and publishing of the thesis manuscripts, her support was essential, nonetheless. Thanks to her, I now understand what it takes to be successful in the academia.

I would like to thank the other two members of my advisory committee, Dr. Timothy Scholl and Dr. David McCormack. Dr. Scholl's always supportive and optimistic view lightened the atmosphere during the tensest moments during my advisory committee meetings. Conversely, Dr. McCormack's skeptical approach to my research always made me strive to look for a better answer and better solutions to the questions he posed.

I would also like to thank Dr. Aaron Ward and Dr. Charles McKenzie for their help and their willingness to listen and address the issues that came up during the course of the Ph.D.

I would also like to thank my lab members, without whose help it would not have been possible to complete this Ph.D. In particular, I would like to thank:

Jarrin Penny, RN and Ph.D. candidate, for being the best friend I could ask for, a wonderful colleague and exceptional nurse. Thank you for listening to all my ravings and rants. For inviting me over to celebrate the Canadian holidays with your family and Steve. And for everything else you (and Steve) have done.

Janice Gomes, Ph.D. candidate, for being an honest and patient friend.

Dr. Alireza Akbari, for being a good friend, mentor, colleague.

Justin Dorie, Patricia Jarosz, Kathleen Koyle, Tanya Tamasi for their help coordinating and organizing the study visits and data acquisition. Diane, for your unwavering support.

All the students and staff at the Robarts Research Institute: Rachel Eddy, Alex Matheson, Marrison McIntosh, Maksym Sharma, Nourhan Shalaby, Danielle Knipping, David Reese.

All the members of the London Chess Club, especially Jim and Steve, all the members of the Aikido London club, especially Sensei Ashley Hennessy for his support in the last months I spent in Canada.

Lastly, I would like to thank my former colleagues, friends and family from home.

Dr. Federico Pieruzzi M.D., Ph.D., for being my long-standing mentor and friend, for believing in me during my time as a student, trainee and physician during my time working in the hospital during the first wave of the COVID-19 pandemic.

Silvia, simply for being there, pretty much every day. Marcello, for the long phone calls. Alberto, for your advice. Selena, for the opportunity you gave me. Veronica, for your strength and honest character. As well as Stefania, Chiara, Susie, Ileana.

Mom and dad. I know it has been hard for you, with me being far, especially during the pandemic.

Luca and Giulia, although we did not chat much, I know you were still there.

# Table of Contents

Abstract.....	ii
Lay Summary.....	v
Co-Authorship Statement.....	vii
Acknowledgements.....	xii
Table of Contents.....	xiv
List of Tables.....	xviii
List of Figures.....	xx
List of Appendices.....	xxiii
List of Abbreviations.....	xxiv
Chapter 1.....	1
1.1 Sodium and Compartment Physiology.....	1
Compartment physiology and the Starling Equation.....	2
Fluid Balance between the Extracellular and Intracellular Compartments.....	5
Fluid Balance within ECV Subcompartments.....	5
Total Body Sodium and Sodium Distribution within the Body Compartments.....	8
Exchangeable vs Nonexchangeable Sodium.....	9
Osmotically Active and Osmotically Inactive Sodium.....	10
Sodium Accumulation in Excess of Water and “Osmotically Inactive” Sodium.....	11
1.2 Sodium and the Kidneys.....	16
Glomerular Filtration Rate.....	19
Regulation of Renal Sodium Excretion: Glomerulo-tubular balance.....	19
Sodium Balance and Kidney Disorders.....	20
1.3 Physiology of renal replacement therapies – HD and PD.....	24
The Physiology of Sodium Removal in Renal Replacement Therapy.....	25
Sodium Accumulation: extracellular volume expansion and outcomes.....	29

Extracellular volume management with dialysis .....	30
1.4 Introduction to $^{23}\text{Na}$ MRI.....	32
Sodium quantification.....	35
Mechanisms Underlying Increased Tissue $[\text{Na}^+]$ and Potential Applications .....	36
Leg $^{23}\text{Na}$ MRI .....	38
1.5 Overarching Hypothesis and Rationale .....	41
1.6 Bibliography .....	43
Chapter 2.....	58
2.1 Introduction.....	58
2.2 Materials and Methods.....	61
Study Design.....	61
Subjects.....	61
Biochemical Measurements .....	61
$^{23}\text{Na}$ MRI Acquisition and Quantification of Tissue $[\text{Na}^+]$ .....	62
Data Analysis .....	64
2.3 Results.....	66
Baseline Characteristics and Medications .....	66
$^{23}\text{Na}$ MRI Analysis.....	69
Correlation Analysis .....	71
Interobserver Variability.....	78
2.4 Discussion.....	79
Conclusions.....	82
2.5 Bibliography .....	84
Chapter 3.....	88
3.1 Introduction.....	88
3.2 Materials and Methods.....	89
Study design.....	89
Study participants.....	90
Magnetic Resonance Imaging and Image Analysis .....	90
Laboratory Analysis.....	91
Statistical Analysis.....	92
3.3 Results.....	93
Correlations.....	99

3.4 Discussion .....	101
Limitations .....	106
Conclusions .....	107
3.5 Bibliography .....	108
Chapter 4 .....	113
4.1 Introduction .....	113
4.2 Materials and Methods .....	114
Sample Size Justification and Statistical Methods .....	116
4.3 Results .....	116
4.4 Discussion .....	123
4.5 Bibliography .....	126
Chapter 5 .....	130
5.1 Introduction .....	130
5.2 Materials and Methods .....	132
Study design .....	132
Study participants .....	132
Dialysate [Na <sup>+</sup> ] prescription .....	132
Magnetic Resonance Imaging and Image Analysis .....	133
Laboratory Analysis .....	134
Outcomes and Statistical Analysis .....	134
5.3 Results .....	136
Linear Regression Models .....	140
Outcomes .....	141
5.4 Discussion .....	145
5.5 Bibliography .....	149
Chapter 6 .....	152
6.1 Overview and Research Questions .....	152
6.2 Summary and Conclusions .....	153
6.3 Limitations .....	155
6.4 Significance of the Results .....	156
6.5 Future Steps .....	158
6.6 Bibliography .....	160

Appendices.....	166
Appendix A: HSREB Full Board Initial Approval Notice. ....	166
Appendix B: Oxford University press license – Nephrology Dialysis Transplantation.....	167
Appendix C: Springer Nature press licence – Pediatric Nephrology. ....	170
Appendix D: Oxford University press licence – Clinical Kidney Journal.....	175
Appendix E: Radiology licence. ....	178
Appendix F: Curriculum Vitae .....	179

## List of Tables

Table 2.1: Baseline characteristics in the four groups (Controls, CKD, HD, PD). .....	67
Table 2.2: Biomarker levels in the four groups (Controls, CKD, HD, PD).....	68
Table 2.3: Tissue [Na <sup>+</sup> ] in the four groups (Controls, CKD, HD, PD). Data presented as mean (SD).....	69
Table 2.4: Correlation analysis between skin, soleus and tibial [Na <sup>+</sup> ] with demographics, anthropometrics and biomarkers in the control group. ....	71
Table 2.5: Correlation analysis between skin, soleus and tibial sodium concentration with demographics, anthropometrics and biomarkers in the CKD group.....	72
Table 2.6: Correlation analysis between skin, soleus and tibial [Na <sup>+</sup> ] with demographics, anthropometrics and biomarkers in the HD group.....	73
Table 2.7: Correlation analysis between skin, soleus and tibial [Na <sup>+</sup> ] with biomarkers and demographics in the PD group.....	74
Table 2.8: Bonferroni correction for significant findings. ....	75
Table 3.1: Demographics, anthropometry and tissue [Na <sup>+</sup> ] according to study group.....	93
Table 3.2: Clinical features, blood and urine biochemistry of the CKD patient group. ....	94
Table 3.3: Individual demographics, clinical features and tissue [Na <sup>+</sup> ] of the CKD patient group. ....	97
Table 3.4: Associations between demographics, anthropometry and clinical variables with tissue [Na <sup>+</sup> ] in healthy children and adolescents and CKD patients.....	99
Table 4.1: Characteristics of the study sample, stratified by left ventricular hypertrophy. ....	117
Table 4.2: Imaging data, stratified by left ventricular hypertrophy.....	118

Table 5.1: Demographics, anthropometrics, clinical information and medications of the overall study sample and after Skin [Na <sup>+</sup> ] quartile stratification.....	136
Table 5.2: Multiple Linear Regression models to explain Skin [Na <sup>+</sup> ].....	141
Table 5.3: Summary of follow-up times, survival and clinical events, in the overall study sample and after Skin [Na <sup>+</sup> ] quartile stratification.....	142
Table 5.4: Cox proportional hazard regression to model the association between Skin [Na <sup>+</sup> ] and clinical outcomes, before and after confounder adjustment. ....	143

## List of Figures

Figure 1.1: Summary of water distribution within body compartments. ....	3
Figure 1.2: The main forces driving net capillary filtration according to the Starling equation. ...	7
Figure 1.3: Schematic representation of the kidney nephron. ....	17
Figure 1.4: Summary of the 1979 study by Sellars et al, showing incremental exchangeable sodium deposits as dialysate $[Na^+]$ increased and weekly treatment time decreased. <sup>85</sup> .....	29
Figure 1.5: A representation of k-space as acquired by two-dimensional radial imaging.....	35
Figure 1.6: $^{23}Na$ signal as a function of the extracellular to intracellular volume ratio, due to the partial volume effect. White circles stand for cell mass within the extracellular space. ....	37
Figure 1.7: Summary of the leg cross-section with $^{23}Na$ MRI. ....	38
Figure 2.1: Schematic summary of proton (Panel A) and $^{23}Na$ MRI (Panel B) acquisition. Proton and $^{23}Na$ images are acquired separately and superimposed (Panel C) after acquisition for software analysis. ....	63
Figure 2.2: Superimposed Proton and $^{23}Na$ MRI of the leg for the anatomical selection of Regions of Interest (Tibia, Soleus Muscle, Skin). The different Regions of Interest are represented by different colored sections. ....	64
Figure 2.3: Sample $^{23}Na$ MR images of the leg in 4 sample subjects from each group. The color bar on the right represents $[Na^+]$ in mmol/L. Panel A: Healthy control. Panel B: CKD patient. Panel C: HD patient. Panel D: PD patient. The images show a progressive increase in the sodium signal eminently in the skin and in the muscle, especially evident in Panels C and D. A notable increase in tibial sodium can be observed in Panel D.....	69
Figure 2.4: Between group comparison in mean Tissue $[Na^+]$ (Skin, panel A; Soleus, panel B; Tibia, panel C). ....	70

Figure 2.5: Correlation analysis for the relationship between eGFR and Skin, Soleus and Tibial [Na <sup>+</sup> ] (Panels A, B and C respectively) in both Control and CKD group.....	75
Figure 2.6: Correlation analysis for the relationship between Hemoglobin and Soleus [Na <sup>+</sup> ] (Panels A, B), and Tibial [Na <sup>+</sup> ] (Panel C, D) in CKD and HD patients. ....	77
Figure 2.7: Correlation analysis for the relationship between serum Albumin and Soleus [Na <sup>+</sup> ] in HD patients. ....	78
Figure 3.1: Tissue [Na <sup>+</sup> ] according to the three groups: in healthy children and adolescents vs CKD patients vs healthy adults. (A: Whole leg [Na <sup>+</sup> ]; B: Skin [Na <sup>+</sup> ]; C: Muscle [Na <sup>+</sup> ]) .....	96
Figure 3.2: Scatterplots showing the relationship between age with whole leg [Na <sup>+</sup> ] (Panel A), skin [Na <sup>+</sup> ] (Panel B) and muscle [Na <sup>+</sup> ] (Panel C) in healthy children, adolescents and adults (n=36).....	100
Figure 3.3: Scatterplots showing the relationship between serum albumin (Panels A-C) and uPCR (Panels D-F) with tissue [Na <sup>+</sup> ] in pediatric CKD patients (n=19). ....	100
Figure 4.1: Correlation between tissue [Na <sup>+</sup> ] (skin, whole-leg [Na <sup>+</sup> ]) with LVMI (A, B) and LVEDV/BSA (C, D), respectively.....	121
Figure 4.2: Tissue [Na <sup>+</sup> ] (skin, whole-leg [Na <sup>+</sup> ]) according to LVH (A, B) and to LV geometry category (C, D), ordered by known escalating influence on negative cardiovascular outcomes. ....	122
Figure 5.1: Dialysate [Na <sup>+</sup> ] prescription in HD patients, according to skin [Na <sup>+</sup> ] quartiles. Data is presented as median (bars) and individual values.....	139
Figure 5.2: Kaplan-Meier curves for overall survival (A) and event-free survival as a composite of all-cause mortality and major adverse cardiovascular events (B), after skin [Na <sup>+</sup> ] quartile stratification. ....	142

Figure 6.1: Anatomic  $^1\text{H}$  (A) and  $^{23}\text{Na}$  (B) MRI scans in a healthy volunteer and (C)  
corresponding overlaid  $^1\text{H}$  and  $^{23}\text{Na}$  images for region of interest analysis. .... 160

## **List of Appendices**

Appendix A: HSREB Full Board Initial Approval Notice. ....	166
Appendix B: Oxford University press license – Nephrology Dialysis Transplantation.....	167
Appendix C: Springer Nature press licence – Pediatric Nephrology. ....	170
Appendix D: Oxford University press licence – Clinical Kidney Journal.....	175
Appendix E: Radiology licence. ....	178
Appendix F: Curriculum Vitae .....	179

## List of Abbreviations

<sup>1</sup>H: hydrogen-1

<sup>23</sup>Na: sodium-23

<sup>24</sup>Na: sodium-24

*95% CI: 95% confidence interval*

ACEi: angiotensin-converting enzyme inhibitor

ARB: angiotensin receptor blocker

BMI: body mass index

BP: blood pressure

BSA: body surface area

CAKUT: congenital anomalies of kidney and urinary tract

CCI: Charlson comorbidity index

CH: concentric hypertrophy

CKD: chronic kidney disease

CNI: calcineurin inhibitor

COPD: chronic obstructive pulmonary disease

CR: concentric remodelling

ECV: extracellular volume

eGFR: estimated glomerular filtration rate

ENaC: distal tubular epithelial sodium channel

ESA: erythropoiesis-stimulating agent

FSGS: focal segmental glomerulosclerosis

GFR: glomerular filtration rate

EH: eccentric hypertrophy

HD: hemodialysis

HR: hazard ratio

HSREB: health sciences research ethics board

HUBES: Human Behavior Study

HUS: hemolytic uremic syndrome

ICV: intracellular volume

IDWG: interdialytic weight gain

IQR: interquartile range

LV: left ventricular

LVEDV: left ventricular end-diastolic volume

LVH: left ventricular hypertrophy

LVM: left ventricular mass

LVMI: left ventricular mass index

MACE: major adverse cardiovascular events

MPGN: membranoproliferative glomerulonephritis

MR: magnetic resonance

MRI: magnetic resonance imaging

NG: normal geometry

PD: peritoneal dialysis

PTH: parathyroid hormone

SD: standard deviation

spKt/V: single pool urea clearance\*time/total body water volume

TBW: total body water

UFR: ultrafiltration rate

uPCR: urinary protein-to-creatinin ratio

UTE: ultrashort echo time

UTI: urinary tract infection

VEGF-C: vascular endothelial growth factor C

[HCO<sub>3</sub><sup>-</sup>]: hydrogen carbonic acid or hydrogen carbonic acid concentration

[K<sup>+</sup>]: potassium concentration

[Na<sup>+</sup>]: sodium concentration

# Chapter 1

## 1.1 Sodium and Compartment Physiology

*Traditional physiology explains sodium balance in mammals and humans as essentially regulated at two levels: (1) at a body compartment level, where sodium is tightly linked with water and potassium, as a function of tissue composition and driving hydrostatic and osmotic forces, regulating fluid shifts between body compartments; (2) at the kidney level, where a fraction of the sodium contained in the blood plasma (intravascular compartment) is finally excreted from the body, finely regulated by mechanisms of filtration, reabsorption and secretion. Other pathways of sodium loss, via the gastrointestinal system and through sweating, are - from a physiological standpoint – marginal and have been therefore omitted from discussion in this chapter. More recently, a third level of sodium regulation has been described – accumulated in the dermal skin layer without commensurate water, bound to negatively charged proteoglycans – as osmotically inactive sodium.*

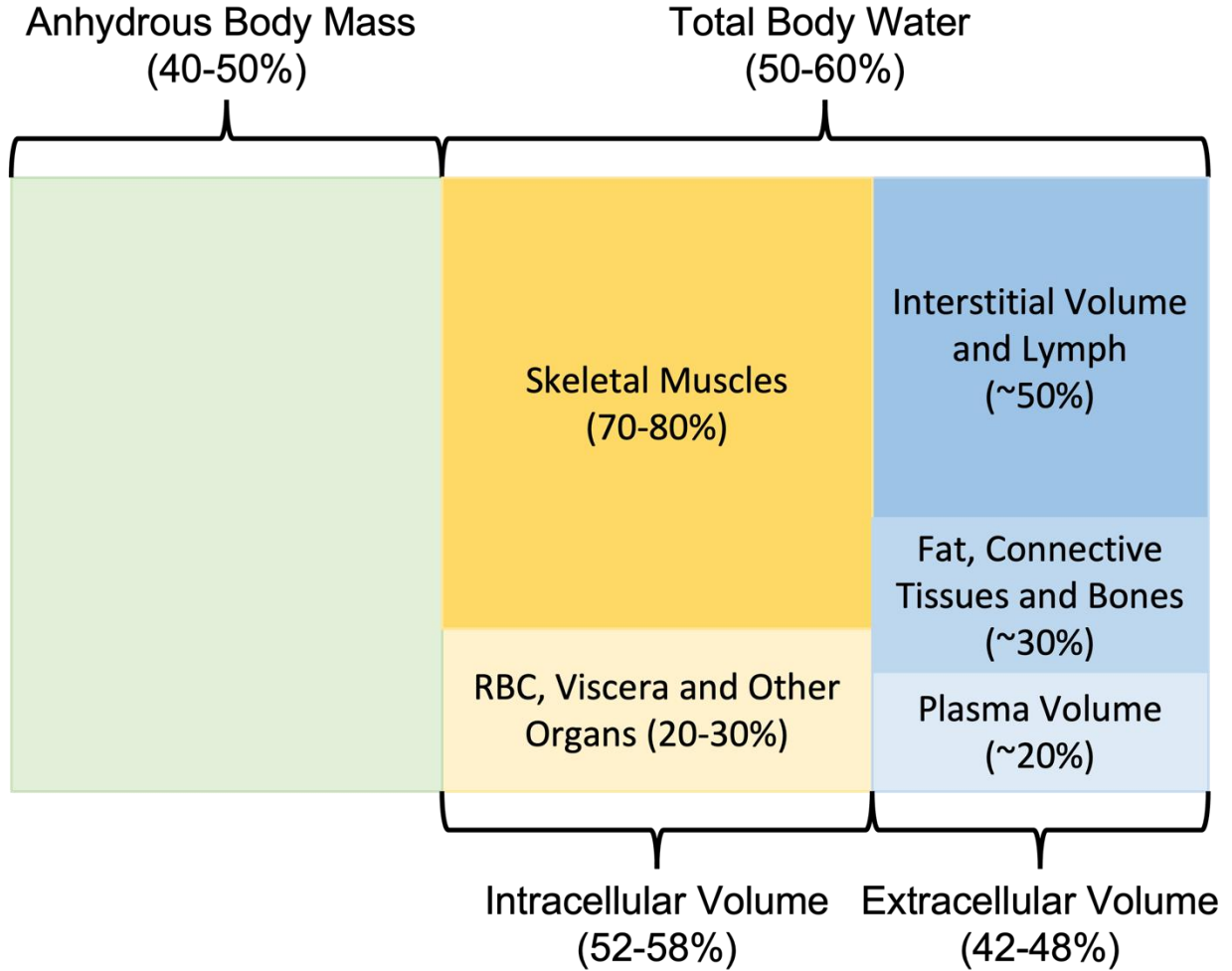
## *Compartment physiology and the Starling Equation*

*Compartment physiology describes the distribution and behavior of fluids within the human body.*

*It is key to understanding the physiology of sodium, as the main extracellular ion, and its relationship with the surrounding environment.*

The human body is composed by 50 (in women) to 60% (in men) of water, with a physiological decline with aging. Furthermore, visceral organs, brain, muscles and the skin consist of ~75% water, as opposed to 10-20% in fat tissue and skeletal bones.<sup>1</sup> According to compartment physiology, total body water is divided into two compartments: the extracellular volume (ECV) and the intracellular volume (ICV). The ECV is composed of five subcompartments: (1) the intravascular (plasma) space, (2) the interstitial and lymph fluids, (3) connective tissue and bones, (4) transcellular fluid (contained in cavities such as the pleural space, the peritoneal cavity, the cerebrospinal fluid system), and (5) fat tissue (**Figure 1.1**).

Figure 1.1: Summary of water distribution within body compartments.



The ECV contains 45-48% of total body water in women, as opposed to 42-45% in men, who have a larger ICV due to a greater muscle mass.<sup>1</sup> The ICV constitutes 53-58% of total body water, with almost 75% being represented by skeletal muscles (**Figure 1.1**). For this reason, loss of muscle mass causes a redistribution of total body water from the ICV to the ECV.

Water movements between compartments are regulated by a balance of hydrostatic and osmotic forces, according to the following formula:

$$P_{ic} - P_{ec} = \Pi_{ic} - \Pi_{ec}$$

Where P stands for the hydrostatic forces,  $\Pi$  for the osmotic forces, ic for intracellular and ec for extracellular. In animal cells, the presence of a flexible cellular membrane (phospholipid bilayer) causes the water shifts between the ECV and ICV to be mediated only by the balance of extracellular and intracellular osmotic forces, as the extracellular and intracellular hydrostatic forces cancel each other out at equilibrium. The osmotic movement of water across a semipermeable membrane can be described by the following relationship:

$$\text{Osmotic Water Flux} \propto L_p * \Delta[c] * \sigma$$

Where  $L_p$  is the hydraulic permeability of the semipermeable membrane,  $\Delta[c]$  the concentration difference of the solute of interest at the two sides of the membrane and  $\sigma$  Staverman's reflection coefficient.

Briefly,  $\sigma$  describes the behavior of a solute, as the ratio of the observed difference in osmotic pressure ( $\Delta\Pi_{\text{obs}}$ ) at the two sides of the membrane and the ideal difference in osmotic pressure ( $\Delta\Pi_{\text{ideal}}$ ) generated by an impermeable solute. Ranging from 0 to 1, when  $\sigma \rightarrow 1$ , then the solute is completely impermeable and generates maximum osmotic water flux; when  $\sigma \rightarrow 0$ , then the solute is maximally permeable, and no osmotic water flux is generated.

Based on their ability to generate osmotic water flux, solutes can be divided into ineffective osmoles, i.e. solutes with a  $\sigma \rightarrow 0$  and/or not able to generate a concentration difference across a given semipermeable membrane, and as such do not generate osmotic water flux, and effective osmoles, i.e. molecules with a  $\sigma > 0$  and generate a concentration difference across the semipermeable membrane, and are able to generate osmotic water flux.

## *Fluid Balance between the Extracellular and Intracellular Compartments*

*Key concepts in understanding compartment physiology pertain to solute and water distribution between the ECV and the ICV, and within the ECV subcompartments, mainly between the vascular space and the interstitium.*

Fluids in the ECV and ICV compartments are in a dynamic balance: the ICV is rich in fixed anions, such as adenosine tri-phosphate (ATP), phospho-creatine and sulfate anion. In order to maintain electroneutrality, these negative charges attract the two main body cations – sodium and potassium – with accompanying osmotic water influx, as the cellular membrane is permeable to both sodium and potassium. Without intervention, these two ions would enter the intracellular space, causing the cell to swell and burst from the osmotic water influx. To prevent this from happening, the relative distribution of sodium and potassium is highly regulated by a membrane protein, the sodium/potassium ( $\text{Na}^+/\text{K}^+$ ) ATPase. This protein extrudes three sodium ions from the cell and imports two potassium ions into the cell, so that in practice, an osmotic gradient in sodium and potassium is generated and these two ions become effective osmoles. As a consequence, 95% of total body sodium has been estimated to be distributed in the ECV and 98% of total body potassium distributed in the ICV. The extrusion of sodium in the ECV is then balanced by a passive outflux of chloride, the main extracellular anion accompanying sodium.

## *Fluid Balance within ECV Subcompartments*

The ECV subcompartments are in close communication with one another. The intravascular compartment contains 15-20% of the ECV water: intravascular water is tightly regulated as it is essential for the maintenance of an effective circulation. Intravascular water mainly depends on:

(a) balance of hydrostatic and osmotic forces between the ECV subcompartments, (b) lymphatic system, (c) the kidneys in concert with (d) neurohormonal mechanisms. These regulatory systems closely interact and communicate with one another.

a. Small molecules (e.g. urea, creatinine) and electrolytes (e.g. sodium, potassium and chloride) diffusive freely and therefore are ineffective osmoles in the ECV subcompartments. Therefore, the most important effective osmoles are represented by albumin and other plasma proteins. Net capillary filtration, as the balance of forces regulating water shifts between the intravascular and interstitial subcompartment, is described by the Starling equation as follows:

$$\text{Net Capillary Filtration (J}_v\text{)} = L_p * [(P_c - P_i) - \sigma (\Pi_c - \Pi_i)]$$

where  $L_p$  stands for hydraulic permeability,  $P_c$  and  $P_i$  are capillary and interstitial hydrostatic pressures,  $\Pi_c$  and  $\Pi_i$  are capillary and interstitial colloid osmotic pressures, and  $\sigma$  represents Staverman's reflection coefficient. As a result of the Starling equation, a positive net fluid filtration into the extravascular subcompartments throughout the whole capillary has been observed experimentally.<sup>2</sup> The result is a continuous net fluid loss from the intravascular subcompartment to the extravascular subcompartments (**Figure 1.2**). At steady state, this loss is counterbalanced by the lymphatic system.

Figure 1.2: The main forces driving net capillary filtration according to the Starling equation.

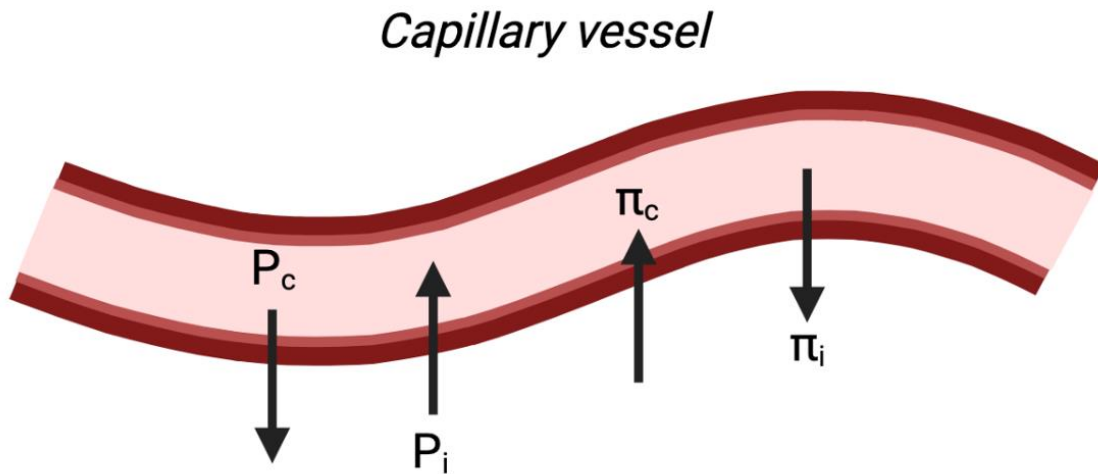


Figure generated at BioRender.com

b. The lymphatic system has both an immune and circulatory support function. It is composed of a specialized vessel network and organs (e.g. lymph nodes), whose main function is to return the interstitial fluid (lymph) from the tissues back into the circulatory system. About 8 liters/day of capillary filtrate is transported by the lymphatic vessels back into the intravascular compartment, with about 4 liters of filtrate transiting through the lymph nodes and the remainder returning into the circulation through the thoracic duct.

c. The kidneys regulate the intravascular volume mainly by affecting the sodium balance – this aspect will be covered in detail further below (see paragraph: **1.2 Sodium and the Kidneys**). Intravascular sodium balance regulation, as operated by the kidneys, ultimately affects all ECV subcompartments.

d. Neurohormonal regulation of the intravascular volume occurs as the result of an interaction between input systems (nervous and cardiovascular system) and output systems (the kidneys).

Cardiopulmonary baroreceptors, located in the pulmonary artery and cardiac atria sense wall strain due to filling the pressures and activate compensatory mechanisms to stimulate water and sodium excretion at the kidney level, by secreting hormones such as the atrial natriuretic peptides.

Renin angiotensin-aldosterone system: a specialized structure located in the kidney tubules (the *macula densa*) is able to sense the tubular chloride load and regulate kidney filtration by altering the vascular tone of the glomerular afferent arteriole via the renin-angiotensin pathway. This way, the kidney is able to maintain a constant sodium chloride excretion in spite of even large changes to kidney blood flow, preserving an adequate intravascular volume. Aldosterone acts favoring distal tubular sodium reabsorption by regulating the expression of sodium transporter proteins, thus maintaining the intravascular volume. It is partially upregulated by angiotensin II and partially by other systems. These systems are described more in detail further below (see paragraph: **1.2 Sodium and the Kidneys**).

### *Total Body Sodium and Sodium Distribution within the Body Compartments*

*As the intravascular compartment is the most easily accessible compartment of the human study, the first total body ionic (sodium and potassium) balance studies were performed from inferences based on the ionic content of the intravascular compartment as delineated further below.*

In mammals, intracellular tonicity is considered equivalent to the extracellular environment. This equates to the physiological assumption that intracellular, plasma, interstitial and total body tonicity are similar. As explained above, sodium and potassium are the two main cations in the

human body, responsible for ~50% of total body tonicity, the remainder of the total body tonicity being represented by the associated anions (mainly chloride and bicarbonate, with smaller amounts represented by inorganic anions such as phosphate, sulphate, etc). Total body sodium and potassium balance studies by Edelman et al<sup>3</sup> have estimated that the ~98% of total body sodium is contained within the ECV compartment, with the remaining ~2% confined within the intracellular compartment. This almost mirrors the behavior of potassium, with ~95% located intracellularly and ~5% extracellularly. Sodium is also the main cation of human plasma, where its physiological concentrations range ~150 mmol/L, as opposed to potassium at ~4 mmol/L. Early physiology studies, therefore, posited that tissue sodium and potassium content essentially reflect the balance between the ECV and the ICV.<sup>3</sup>

### *Exchangeable vs Nonexchangeable Sodium*

In order to estimate total body sodium, Forbes and other authors devised short-term balance studies using radioisotope dilution techniques.<sup>4,5</sup> The principle behind these methods assumed that a small amount of radioactive isotope (sodium and potassium), after intravenous injection, would dilute within all ECV and ICV subcompartments. Measuring residual plasma radioactivity due to these isotopes, after a relatively short period of time (18-24 hours), would yield an estimate of total body cations available for exchange between subcompartments. The total body pool of exchangeable sodium and potassium were thus measured. Total body sodium in humans was estimated by the radioisotope sodium-24 ( $t_{1/2} = 15$  hours) dilution techniques. A known amount of radioactive sodium was allowed to equilibrate within the body for 18-24 hours; at the end of the equilibration period a plasma sample was taken, while urine was collected continuously during the equilibration period. Assuming that radioactivity in the plasma, after equilibration, would equate total body

radioactivity, total body sodium content was calculated as “total exchangeable sodium”, according to the formula:

$$\text{Total exchangeable sodium} = ({}^{24}\text{Na}_{\text{injected}} - {}^{24}\text{Na}_{\text{excreted}})/([{}^{24}\text{Na}]_{\text{serum}}/[\text{Na}]_{\text{serum}})$$

then indexed by body weight, returning an estimate of tissue sodium content. The isotopic dilution method, therefore, measures that portion of the total body sodium which is available for short-term exchange between body subcompartments. Notably, total exchangeable sodium is opposed to “non-exchangeable” sodium or “osmotically inactive” sodium, that is the amount of sodium not available for short-term equilibration: longer-term equilibration studies (up to four weeks, using sodium-22, with a  $t_{1/2} = 2.6$  years) coupled with bone biopsies and ashing techniques showed that a relevant fraction of total body sodium (20-30% of total body sodium) is fixed in crystalized form within the mineralized skeletal bone matrix.<sup>6,7</sup> At the time, however, the metabolic significance of those sodium deposits in the longer term had not been clearly defined. Normal total body sodium per kilogram of body weight (including both exchangeable and non-exchangeable sodium) and exchangeable sodium/kg body weight values were calculated at 54 mEq/kg and 40 mEq/kg, equating to 0.12% and 0.09% of body weight, respectively.<sup>1</sup> Similar techniques were used for total body potassium using potassium-42, albeit potassium exchange occurred mainly within the ICV subcompartments.

### *Osmotically Active and Osmotically Inactive Sodium*

Osmotic equilibrium between body compartments is assumed to be mainly determined by the balance of exchangeable cations (sodium and potassium) and body water, or total body tonicity. Sodium-24, potassium-42 as well as deuterium water dilution studies in healthy individuals

allowed the calculation of total body tonicity. The resulting linear equation, initially enunciated by Edelman et al,<sup>3</sup> related the sodium contained in plasma to the amount of exchangeable sodium and potassium contained in the total body water:

$$[\text{Na}^+]_p = 1.11 (\text{Na}_e + \text{K}_e)/\text{TBW} - 25.6$$

The advantage of this formula is that it relates a parameter simply measured in clinical practice (plasma sodium concentration or plasma  $[\text{Na}^+]$ ) with three parameters measured as the result of operationally complex dilution studies. Furthermore, it postulated a predictable quantitative relationship between sodium balance to potassium and water balance. The slope of the linear formula predicted a change in a plasma  $[\text{Na}^+]$  of 1.11 mmol/L per unit change in total body tonicity. The y-intercept (-25.6) in this formula was calculated to be determined by several elements originally unaccounted for by the original Edelman equation: the presence of comorbid states (heart, liver, kidney and hormonal disorders), measurement error relative to dilution studies, non-sodium and non-potassium osmotically active solutes such as glucose, serum potassium concentration and, importantly, sodium and potassium stored in excess of water.<sup>8</sup> As a result of these considerations, this equation has been the subject of a considerable body of subsequent physiological and mathematical investigations leading to further implementations and specifications, and its validity is a matter of animated ongoing debate.<sup>9,10</sup>

### *Sodium Accumulation in Excess of Water and “Osmotically Inactive” Sodium*

*In addition to non-exchangeable sodium deposits at the skeletal level, two other organs have been suggested to accumulate sodium in excess of water – articular cartilage, the skin and the vascular*

*endothelium. Whereas the articular cartilage accumulates sodium in an osmotically active, albeit hypertonic fashion, the skin and the vascular endothelium are thought to be able to store sodium in a “non-osmotic” or “osmotically inactive” fashion, as they are considered inactive with respect to plasma  $[Na^+]$  and total body tonicity, according to the traditional Edelman equation. The existence of such deposits, especially at the skin level, have been suggested in humans by long-term balance studies, observing that urinary sodium excretion over the long term (days to weeks) did not match sodium intake, leading to apparent, sizeable sodium accumulation without commensurate water retention.*

### *Cartilage*

The cartilage microenvironment has been long recognized to be hypertonic compared to plasma: the extremely high intra-articular sodium content (>200 mmol/L) is bound to negatively-charged glycosaminoglycans (GAG), long linear polysaccharide chains containing sulfate groups (responsible for the negatively-charged portion). This sodium-GAG complexes are *osmotically active*, and osmotic swelling is counteracted by the high hydrostatic pressure generated by a network of collagen chains.<sup>11</sup> These features are responsible for the high degree of cartilage hydration, its functional and mechanical properties.

### *Skin*

In the second half of 1970, a Russian group of researchers first identified the skin as being another source of sodium deposition in rats.<sup>12</sup> Usual radioisotope dilution studies identified these deposits as rapidly exchangeable, though outside of the sodium pool contained in the ECV or ICV,

suggesting the existence of a relevant third compartment able to store exchangeable sodium.<sup>13</sup> More than two decades later, subsequent studies led by Titze and colleagues rediscovered that rats fed a high sodium diet would accumulate sodium in excess of water and potassium at the skin dermis level, were bound to interstitial glycosaminoglycans, similarly to the cartilage tissue.<sup>14-16</sup> In support of these findings, a high-sodium diet was found to increase the sulfate glycosaminoglycan content in the skin in several studies, both in rats and humans.<sup>17</sup> Skin hypertonicity was speculated to occur by intradermal kidney-like countercurrent concentrating mechanisms.<sup>18,19</sup> Skin sodium accumulation was found to be immunologically regulated by resident macrophages sensitive to changes in local changes in interstitial fluid tonicity via a signaling pathway mediated by the tonicity-enhanced binding protein (TonEBP), which would upregulate glycosaminoglycan synthesis by interstitial fibroblast as a result of increased interstitial fluid tonicity.<sup>17,20,21</sup> This mechanism also regulates local fluid clearance mechanisms, through the secretion of vascular-endothelial growth factor C, which stimulates lymphangiogenesis to increase local lymphatic fluid clearance.<sup>22,23</sup>

In humans, the existence of a third compartment for hypertonic sodium accumulation has been suggested by a spaceflight simulation studies, the Human Behaviour Study (HUBES) and the Mars500 study, where simulating the conditions of a metabolic ward, participants received food with a known amount of salt urine was collected daily for the whole duration of the simulation.<sup>24-</sup><sup>26</sup> The HUBES study showed the long term behaviour of total body sodium to water intake, after changing from a low-salt diet to a high-salt diet. Human participants, following an abrupt increase in dietary sodium intake, underwent an initial increase in body weight for the first 80 days, only to keep accumulating sodium without changes in body weight, up to 134 days.<sup>24</sup> The Mars500 studies showed that under a constant dietary salt intake, urinary sodium excretion exhibited large

fluctuations about the mean, following 7-day cycles. Increasing salt intake was immediately followed by sodium accumulation and an increase in extracellular water, and was eventually followed by increased salt intake. These large, weekly fluctuations in urinary sodium excretion, however, were not followed by commensurate extracellular water retention. Altogether, these studies suggest that sodium can be stored in excess of water and released rhythmically.<sup>26</sup>

From an evolutionary perspective, these sodium reservoirs act as a buffer system in response to acute hypotonic and hypertonic loading, preventing acute shifts in plasma osmolarity (harmful to the central nervous system), or to prevent sudden ECV expansion. Indeed, the skin's inability to "sequester" sodium via these mechanisms was associated with intravascular volume expansion, and sodium-sensitive hypertension.<sup>27</sup> Recent studies have also shown that hypertonic skin sodium reservoirs may serve to enhance the antimicrobial barrier provided by the skin.<sup>28</sup> Conversely, excessive skin sodium deposition, as well as defects in lymphatic clearance mechanisms, have been associated with vascular endothelial nitric-oxide synthase dysregulation and sodium-sensitive hypertension.<sup>20</sup>

### *Endothelial Glycocalyx*

Recently, an additional sodium-buffering system was also described at the vascular endothelium level: the endothelial surface layer or "endothelial glycocalyx".<sup>29</sup> This is a layer of proteins attached to glycosaminoglycan groups (such as heparan sulfate and hyaluronic acid), thought to have vasoregulatory and immune-regulatory functions.<sup>30</sup> More recently, several authors suggested that the endothelial surface layer may also have intravascular sodium buffering function, non-dissimilarly than the skin.<sup>31-33</sup> Studies showed that intravascular sodium loading, occurring either due to hypertonic saline infusion or due to high dialysate  $[Na^+]$  during hemodialysis (HD)

treatments, resulted in local osmotic stress and glycocalyx “shedding”, i.e. losing molecular components.<sup>31-33</sup> Impaired endothelial surface layer function is associated with increased microvascular permeability and has been speculated to lead to increased sodium accumulation at the skin level.<sup>30</sup>

## 1.2 Sodium and the Kidneys

One of the main functions of the kidneys is the maintenance of the water and electrolyte balance. Each of the two kidneys contains ~1,000,000 structural and functional units – the nephrons – in human adults.<sup>34</sup> A nephron is composed of a vascular subunit, the glomerulus, made of a convoluted tuft of capillaries and connected to a tubular epithelial subunit, the tubule, via Bowman's capsule.

Blood enters the glomerulus from the systemic arterial circulation via the afferent artery and exits the glomerulus via the efferent artery, through the peritubular capillaries, key in the reabsorption process, and back into the systemic venous circulation. The main function of the glomerulus is the filtration of blood plasma through a barrier made of three layers: (a) the fenestrated glomerular endothelium, (b) the glomerular basal membrane and (c) a layer of specialized cells – the podocytes. These cells have elongated foot processes forming small slits in the filtration barrier that allow the selective filtration of molecules. This barrier is selectively permeable to small solutes (such as electrolytes, small molecules such as urea and creatinine), and with limited permeability to proteins. The fluid resulting from the filtration process – ultrafiltrate – enters the tubule via Bowman's capsule.

The tubule is a hollow structure made by specialized epithelial cells with different absorption and secretive properties, mediated by specialized ionic channels and transport proteins located on the apical (luminal) and basal side of the cell. According to different epithelial cell populations accounting for specific solutes and water permeability and reabsorption properties, the tubule can be divided in several different segments (**Figure 1.3**):

Figure 1.3: Schematic representation of the kidney nephron.

In each segment of the kidney tubule, purple arrows represent primary and secondary active transport mechanisms (absorption and secretion), whereas blue arrows represent passive transport mechanisms.

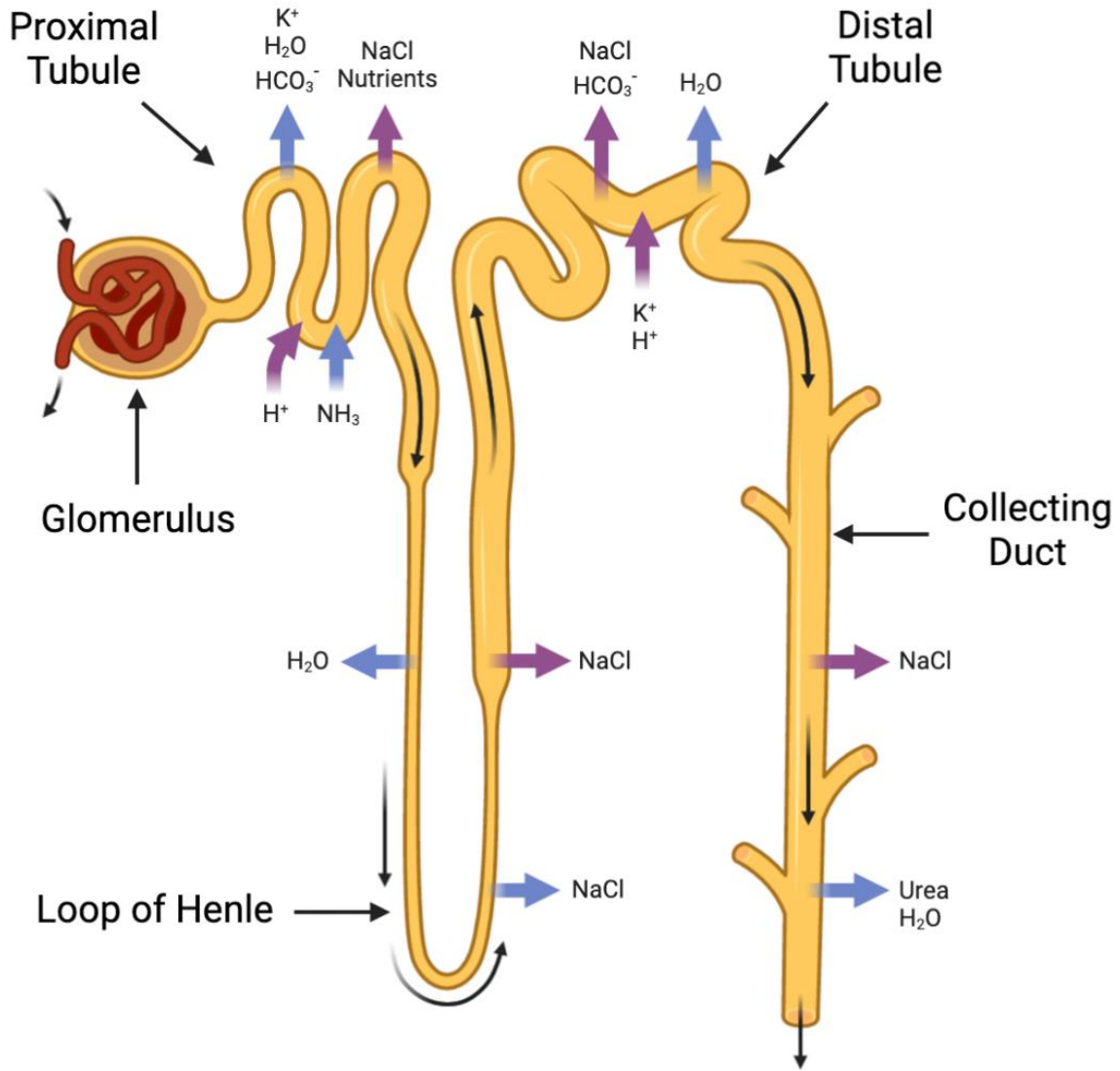


Figure generated at BioRender.com

- The proximal tubule, responsible for active mass reabsorption of several molecules that cross the glomerular filtration barrier. This process occurs via active transporters using energy in the form of adenosine triphosphate and passive transporters, exploiting transtubular solute concentration gradients. The entirety of aminoacids, glucose and small

peptides and proteins is reabsorbed at this level in normal conditions. Large amounts of sodium (~65%), potassium (~45%), chloride and bicarbonate are also reabsorbed at this level.

- The loop of Henle, comprising a thick descending limb, a thin descending and ascending limbs, the thick ascending limb, and the *macula densa*. This portion of the tubule has several functions. Firstly, it reabsorbs large amounts of electrolytes (e.g. 25-30% of sodium is reabsorbed at this level). Secondly, it is responsible for the urine concentration and dilution processes. Thirdly, it acts as a feedback mechanism *in tandem* with the glomerulus to regulate glomerular blood flow: the *macula densa* is a specialized tubular cell conglomerate belonging to the *juxtaglomerular apparatus*. It is responsible for the regulation of the vascular tone of the afferent arteriole in response to tubular salt delivery: briefly, increased tubular chloride delivery is sensed by the macula densa, which secretes vasoactive substances and causing vasoconstriction of the afferent arteriole, thus reducing glomerular blood flow and the filtered load.<sup>35</sup> Viceversa, a reduced tubular chloride delivery block secretions of these vasoactive molecules and results in vasodilation of the afferent arteriole, increasing glomerular blood flow and filtered load. This process is known as *tubulo-glomerular feedback*.
- The distal tubule, further separated into three segments – the distal convoluted tubule, the connecting tubule, the collecting tubule. The distal convoluted tubule reabsorbs sodium chloride through a thiazide diuretic-sensitive cotransporter (~5% of total reabsorbed sodium). The collecting tubule is responsible for the final portion of sodium reabsorption (~3%) via the epithelial sodium channel (ENaC), upregulated by cortical adrenal hormones – mineralocorticoids such as aldosterone, and glucocorticoids such as cortisol. This portion

of the tubule is also responsible for final urine concentration: the conditional expression of tubular water channels (aquaporins) in response to posterior pituitary gland release of the antidiuretic hormone leads to free water reabsorption of urine concentration. The connecting tubule covers an intermediate function between the two segments.

### *Glomerular Filtration Rate*

One of the main measures of kidney function used in physiology and clinical medicine is glomerular filtration rate (GFR). This is the volume of plasma filtered by the kidney glomeruli per unit of time. Normal GFR values stand between 100-120 ml/min, with a physiological decline of ~1 ml/min/year of age. Pathological declines in GFR may be due to either acute or chronic disease processes of the kidneys. GFR can be measured experimentally by measuring the clearance (i.e. the volume of blood completely cleared from a substance per unit of time) of some specific molecules by the kidneys, as long as they are freely filtered into the tubules, and their secretion and reabsorption is negligible. Examples of such molecules are the exogenous molecules inuline and iothalamate. In clinical practice, creatinine clearance is more commonly used, as creatinine is an endogenous molecule resulting from the catabolism of muscle creatine, and whose plasma levels increase with decreasing GFR. In the last decades, GFR has been clinically estimated (eGFR) from steady state plasma creatinine levels, using linear regression formulas derived from population-based studies.<sup>36,37</sup>

### *Regulation of Renal Sodium Excretion: Glomerulo-tubular balance.*

In relation to the amount of filtered sodium, only less than 1% of filtered sodium is excreted in the final urine under normal conditions. This balance is maintained even in situations of significantly

increased filtered sodium loads, meaning that tubules can regulate their reabsorption capacity even in situations of large increases in GFR. This phenomenon, called glomerulo-tubular balance, can be enunciated as: “sodium reabsorption in a given nephron segment is proportional to sodium delivery in that segment”.<sup>34</sup>

This process occurs in several tubular segments, each with specific mechanisms. At the proximal tubular level, an increase in GFR results in increased filtration fraction, with increasing oncotic pressure in the peritubular capillaries, favoring tubular reabsorption and reduced sodium excretion. The resulting increase in filtered load of glucose and aminoacids is also associated with increased sodium reabsorption. At the distal tubular level, sodium reabsorption is even more critical compared with the proximal tubule – although quantitatively less significant, distal sodium regulation is the final regulatory step before excretion and is therefore the critical step to determine final urinary sodium excretion.<sup>38</sup> This final regulatory step is mainly under the control of aldosterone and cortisol, with their regulatory function on ENaC expression and sodium reabsorption.<sup>38</sup>

### *Sodium Balance and Kidney Disorders*

Chronic kidney disease (CKD) is an umbrella term encompassing all kidney disorders that result in a sustained reduction in GFR for at least 6 months.<sup>39</sup> Numerous different etiologies underlie the development of CKD and result in widely different glomerular and tubular function derangements. Nonetheless, the general consensus is that CKD is a condition prone to developing sodium accumulation, this being reflected both from studies investigating the pathophysiology as well as the epidemiology of sodium balance in CKD.<sup>38,40</sup>

The main mechanisms underlying sodium accumulation in kidney disorders can be divided in (a) reduced filtered sodium load and (b) increased tubular sodium reabsorption. As for point (a), significant reductions in the filtered sodium load are typical of advanced CKD stages or severe acute kidney injury, where severe reductions in GFR ensue. As for point (b), conversely, several mechanisms concur to determine an increased tubular sodium reabsorption in CKD:<sup>38</sup>

1. Reductions in kidney mass (observed from experimental forms of surgical CKD with removal of 5/6<sup>th</sup> of the total kidney mass), result in an imbalance in sodium reabsorption, where it decreases in the proximal tubule,<sup>41</sup> while it increases by four to five times in the distal tubule, due to the upregulation of the sodium transport proteins therein located.<sup>42</sup>
2. CKD is associated with increased circulating aldosterone levels, both due to traditional (high plasma renin activity and hyperkalemia)<sup>43-45</sup> and non-traditional activation mechanisms (e.g. acidosis, endothelin-1, vasopressin, adrenocorticotrophic hormone secretion).<sup>46,47</sup> Aldosterone secretion is then associated with increased distal tubular sodium reabsorption.
3. Activation of the intrarenal renin-angiotensin system: indeed, proximal tubules have been shown to be able to synthesize angiotensinogen,<sup>48</sup> which can be activated into angiotensin II via renal renin and angiotensin-converting enzyme expressed throughout the nephron.<sup>49</sup> Tubular angiotensin II can activate ENaC in the distal nephron, promoting distal sodium reabsorption.<sup>50</sup> These mechanisms are overactive in CKD, especially in diabetic kidney disease.<sup>51,52</sup>
4. Increased chloride intake has been associated with increased distal sodium reabsorption in individuals with salt-sensitive hypertension: as the accompanying anion of sodium in salt,

high chloride intake activates the aldosterone receptors and distal sodium reabsorption in this subset of individuals.<sup>53,54</sup>

5. Acid loading, such as the one that normally occurs in protein-rich Western diets, stimulates several mechanisms of increased kidney proton excretion (including the renin-angiotensin system, aldosterone and endothelin-1).<sup>55</sup> In CKD, however, these mechanisms are incapable of completely excreting the ingested acid loading due to the reduction in nephron mass: the resulting metabolic acidosis further stimulates these mechanisms initiating a self-sustained vicious cycle. These mechanisms converge on distal proton secretion, mediated by H<sup>+</sup>-ATPases that require the maintenance of electroneutrality to work, thus stimulating ENaC-mediated distal sodium reabsorption.<sup>55</sup>
6. This final mechanism is extremely relevant to a subset of kidney disorders characterized by urinary protein loss (proteinuria) due to selective damage to the glomerular membrane. One such disorders is diabetic kidney disease, where chronic glucose exposure results in endothelial protein glycation and kidney glomerular capillary damage, with varying proteinuria severity. In nephrotic syndrome, congenital or acquired defects in the glomerular membrane result in massive urinary protein loss, low serum protein levels, sodium/water retention and edema formation. Proteinuria has been shown to directly activate the ENaC and subsequent sodium reabsorption: this mechanism is mediated by plasminogen, a serin-protease excreted in the urine among other proteins: plasminogen is activated into plasmin inside the tubular lumen and activates the ENaC by cleaving the ENaC  $\gamma$ -subunit, thus releasing an inhibitory peptide.<sup>56</sup> Plasminogen excretion has been shown to increase proportionally with the severity of proteinuria: therefore, kidney

disorders with more severe proteinuria have also been associated with more severe sodium retention.<sup>57-59</sup>

As CKD is an extremely heterogenous disease, different combinations of the above mechanisms may be at play to determine increase distal sodium reabsorption – if present.<sup>38</sup> Indeed, the determination of urinary sodium handling in CKD and its causes is an extremely understudied field, both at the epidemiological and experimental level. This is likely the consequence of the lack of reliable and validated tests to objectively evaluate urinary sodium excretion in clinical practice, the variability in daily dietary sodium intake and urinary sodium excretion,<sup>25,60</sup> the compliance challenges associated with long-term, complete urine collections, and the multitude of etiologies underlying CKD, with a relevant fraction of CKD having no diagnosis due to diagnostic limitations of modern-day nephrology.<sup>61</sup>

### **1.3 Physiology of renal replacement therapies – HD and PD**

*Severe impairments in renal function, up to levels of eGFR <15 ml/min/1.73m<sup>2</sup>, in presence of either ECV overload, metabolic disorders and/or symptoms of “uremia”, require the initiation renal replacement therapy in order to support life. Excluding renal transplantation, which is not going to be treated in this work, two main options of renal replacement therapy exist at present: HD and PD. The physiology of dialysis is an extremely wide topic, therefore for the purpose of this work, only the aspects relative to volume and sodium removal are going to be presented.*

Maintaining a neutral sodium balance is one of the main goals of renal replacement therapy. Sodium intake must be equal to urinary sodium excretion (when there is meaningful residual urinary output) and removal through renal replacement therapy.

Though noting the recently described incongruencies between total body sodium and the ECV due to osmotically inactive sodium deposits (see paragraph: **1.1 Sodium and Compartment Physiology**), according to traditional physiology, sodium intake is considered a fundamental determinant of the ECV status, as it determines thirst and subsequent water intake: an increase in plasma tonicity, primarily (but not only, with hyperglycemia in diabetes being a notable exception)<sup>62</sup> driven by increased plasma [Na<sup>+</sup>], is detected by the osmoceptors located in the hypothalamus, driving thirst and vasopressin secretion by the posterior pituitary gland.<sup>63,64</sup> Vasopressin secretion acts on the collecting tubules by stimulating the reabsorption of free water. This is an extremely sensitive mechanism – even a ~2% increase in plasma tonicity is sufficient to promote fluid intake, regardless of age.<sup>65</sup> Humans tend to maintain plasma [Na<sup>+</sup>] relatively constant around a fixed value, the plasma “sodium setpoint”, according to the above mechanisms. This also applies to patients requiring renal replacement therapy even in absence of a meaningful

residual kidney function – pre-dialysis plasma  $[Na^+]$  shows little variability in repeated measures over time in this population, mainly as a function of thirst regulation.<sup>66,67</sup>

Sodium intake generally encompasses: [a] dietary sodium intake, mainly by ingesting food containing naturally present or added sodium, [b] sodium contained in commonly prescribed medications (e.g. sodium bicarbonate, or antibiotics) or [c] via the infusion of intravenous fluids like saline, for hospital inpatients.

Residual urinary output is of primary relevance in patients on renal replacement therapy, and its preservation has been associated with better survival.<sup>68,69</sup> residual urinary output allows the maintenance of urinary sodium excretion in-between dialysis sessions, and better control of ECV balance due to urinary sodium excretion, preventing the hazards of high ultrafiltration rates during HD.<sup>70,71</sup>

### *The Physiology of Sodium Removal in Renal Replacement Therapy*

Sodium removal in renal replacement therapy occurs via two different biophysical principles: convection and diffusion. These principles describe solute movement across a semi-permeable membrane:

- Convection occurs when a pressure gradient (either hydrostatic or osmotic) is applied across a semi-permeable membrane: water moves across the membrane and drags sodium and other molecules along, as a function of water flow. In HD, the pressure gradient is generated by applying a negative hydrostatic pressure in the dialysate compartment, in order to remove water and sodium; in PD, the pressure gradient is generated by instilling high glucose-containing solutions inside the peritoneal cavity.

- On the other hand, diffusion occurs when sodium moves across the semi-permeable membrane as a function of the concentration gradient of sodium in the two sides of the membrane. In both HD and PD, the concentration gradient of sodium is generated by manipulating  $[\text{Na}^+]$  in the dialysate solution, according to the following formula:

$$[\text{Na}^+]_{\text{gradient}} = [\text{Na}^+]_{\text{dialysate}} - [\text{Na}^+]_{\text{plasma}}$$

Where  $[\text{Na}^+]_{\text{plasma}}$ , in this setting, is equal to the plasma sodium setpoint. A negative gradient will determine diffusive loss of sodium to the dialysate, whereas a positive gradient will result in diffusive sodium gain. In case of a null gradient, no sodium loss or gain will occur.<sup>72</sup>

Positive sodium gradients also tend to increase the plasma sodium setpoint over time, and are strongly associated with thirst and increased weight gain in-between dialyses sessions.<sup>73,74</sup>

Other factors, however, intervene in influencing the diffusion of sodium across the dialysis membrane. In principle, two main aspects need to be considered: the activity of sodium in the solution and the dialysis membrane.<sup>72</sup>

Plasma is a complex solution, containing about 94% water, electrolytes and small molecules, and 6% proteins and lipids. In this setting, not all sodium ions contained in the solution are available for diffusion, but only the sodium ions that are non-complexed (e.g. to anions such as bicarbonate, phosphate, or proteins) and electrochemically active.<sup>72</sup> In practice, dialysate  $[\text{Na}^+]$  needs to be calibrated against active plasma sodium, rather than plasma  $[\text{Na}^+]$ .

As previously mentioned, diffusive sodium transport is affected by the presence and properties of the dialysis membrane.<sup>75</sup> By interacting with the electrically charged membrane, plasma proteins coat the dialysis membrane surface and form a gel that generates resistance for sodium ions to transit across. Furthermore, because of the selective permeability of the dialysis membrane,

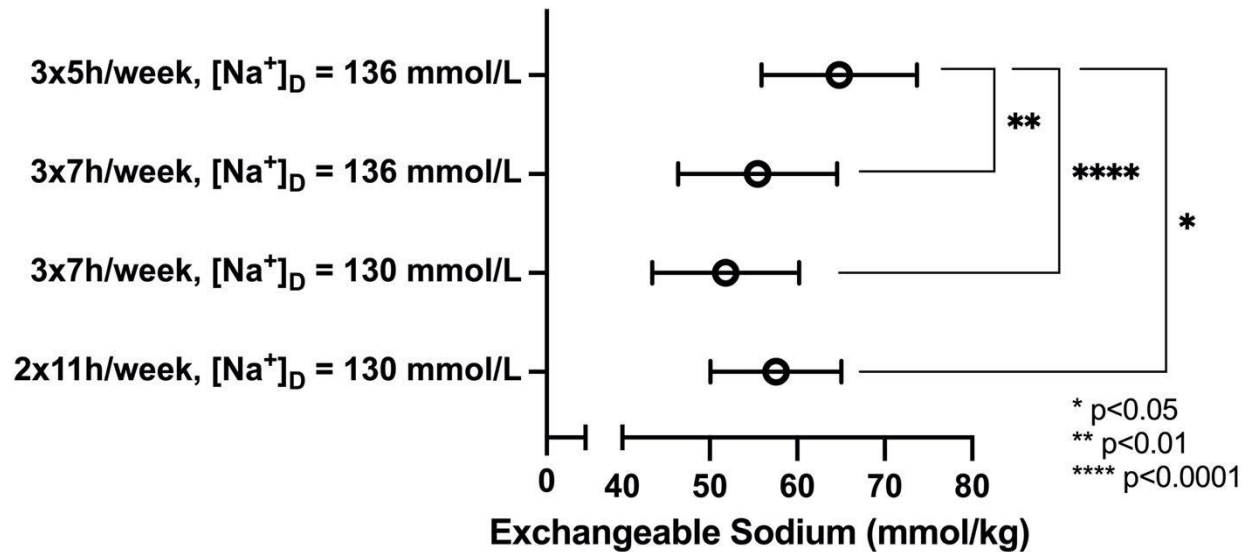
negatively charged plasma proteins like albumin do not cross the barrier; in order to maintain electroneutrality, these proteins trap cations like sodium, and blunt its activity.<sup>72</sup> This phenomenon is termed the “Gibbs-Donnan effect”. The practical consequence of the Gibbs-Donnan effect is that, when applying convection alone, the generated ultrafiltrate has a lower  $[Na^+]$  compared with the plasma.<sup>76,77</sup> To generate ultrafiltrate with the same  $[Na^+]$  as the plasma (“isonatric”), a negative diffusive gradient needs to be generated, where the dialysate  $[Na^+]$  is about 4-7% (5-10 mmol/L) lower than plasma  $[Na^+]$ .<sup>77,78</sup> If dialysate  $[Na^+]$  is maintained above the “isonatric” threshold, sodium diffuses from the dialysate compartment to the plasma, and the net result is sodium accumulation with respect to water. This phenomenon generates an imbalance between sodium and water removal – when water removal exceeds sodium removal, plasma  $[Na^+]$  rises, further stimulating thirst, weight gain and ECV expansion.<sup>66</sup> Therefore, diffusion is necessary to maintain an optimal balance between sodium and water removal.<sup>79,80</sup>

In HD, most of the sodium removal is usually achieved via convection: in one study, convection was estimated to account for at about ~80% of interdialytic sodium removal and was closely related to ultrafiltration volume; diffusion, conversely, as it closely depends on the  $[Na^+]_{\text{gradient}}$ , was highly variable (also including intradialytic diffusive sodium gain) and accounted for ~20% of interdialytic sodium removal on average.<sup>81</sup>

Determining the optimal dialysate  $[Na^+]$  is a clinical challenge. As the main plasma osmolyte, sudden reductions in plasma sodium result in reduced plasma osmolality and intravascular volume.<sup>82</sup> Thus, high dialysate  $[Na^+]$  are necessary to maintain intradialytic hemodynamic stability and to prevent brain osmotic imbalances (dialysis disequilibrium syndrome): short, highly efficient HD treatments require high ultrafiltration rates to remove excess volume and cause rapid drops in plasma osmolarity (due to uremic toxin removal, such as urea).<sup>80</sup> Both also result in a rapid

reduction of the intravascular plasma volume and are associated with significant drops in blood pressure (BP) and organ (heart, brain, kidney, gut) ischemia during HD.<sup>83,84</sup> Using high dialysate  $[\text{Na}^+]$ , however, also has important shortcomings. The effects of high dialysate  $[\text{Na}^+]$  on exchangeable total body sodium, combined with shorter dialysis treatments have been shown as far back as 1979 (**Figure 1.4**), where patients with shortest treatment times (14.8 hours per week) and highest dialysate  $[\text{Na}^+]$  (136 mmol/L) had a 25% higher mean total body exchangeable sodium per kg of lean body mass, compared with patients receiving 18-21 hours per week with a dialysate  $[\text{Na}^+]$  of 130 mmol/L.<sup>85</sup>

Figure 1.4: Summary of the 1979 study by Sellars et al, showing incremental exchangeable sodium deposits as dialysate  $[Na^+]_D$  increased and weekly treatment time decreased.<sup>85</sup>



As a modern comparison, contemporary prescription practices commonly entail 12 hours per week (or less) and dialysate  $[Na^+]_D$  of 140 mmol/L,<sup>79,80</sup> and may result in even larger ECV expansion than evidenced at the time. This hypothesis is supported by the overwhelming rates of hypertension and cardiovascular disease currently observed in patients treated with standard HD practices.<sup>86–88</sup>

In spite of suggestive evidence provided by single-center experiences such as Tassin, France, or Turkey, where optimal ECV and sodium balance is achieved via longer HD treatments with optimized convective and diffusive sodium removal, leading to better BP control and survival benefits,<sup>89,90</sup> contemporary lifestyle, structural and economic pressures have led to the common adoption of shorter dialysis sessions and high dialysate  $[Na^+]_D$ .

### *Sodium Accumulation: extracellular volume expansion and outcomes*

The expansion of the ECV is a common complication encountered in patients undergoing renal replacement therapy, manifesting itself with peripheral (e.g. ankle, lower limbs) and central (e.g. pulmonary) edema.<sup>91</sup> Expansion of the ECV and its subcompartments is associated with an

increase in total body sodium, with adverse effects on the cardiovascular system: hypertension, cardiac hypertrophy, heart failure, acute coronary syndrome and stroke.<sup>92,93</sup> This is especially relevant in patients with CKD and kidney replacement therapy, where cardiovascular disease is the main cause of death in this population.<sup>94</sup>

### *Extracellular volume management with dialysis*

One of the main goals of dialysis is maintaining an optimal ECV balance by removal of excess sodium and water. The optimal ECV corresponds to the patients' "dry weight", and is defined as "the absence of signs and symptoms of volume overload or volume depletion".<sup>79</sup> The dry weight is estimated clinically by each individual clinician using physical examination (e.g. pitting edema, jugular vein distention, pulmonary crackles, signs of pleural effusion, ascites), with the aid of several diagnostic tools, such as chest imaging (x-ray, computed tomography), point-of-care ultrasound and bioimpedance spectroscopy.

When suspecting ECV expansion, the dry weight is clinically challenged by "probing" it – attempting to remove extra sodium and water during HD.<sup>95</sup> Because of the lack of a standardized definition of dry weight, with low sensitivity and specificity of the clinical assessment and the currently available diagnostic tools, estimating the dry weight comes at the tangible risk of both over and underestimation. An overestimated dry weight is associated with ECV expansion and adverse outcomes.<sup>96</sup> Conversely, underestimating the dry weight is associated with ECV contraction and clinical complications such as intradialytic hypotension, due to reduced intravascular volume.<sup>97,98</sup>

Therefore, the achievement of a "correct" dry weight is challenging. At the same time, intradialytic volume removal is limited by the amount of volume that can be safely removed during a single

dialysis session. Indeed, excessive volume removal per unit of time during dialysis is associated with symptoms of reduced intravascular volume (e.g. hypotension, vascular access thrombosis, organ ischemia, nausea, vomiting, loss of consciousness, cardiac arrest) and is susceptible to renal replacement therapy-related factors (e.g. treatment time, modality, temperature, dialysate fluid content), as well as individual factors based on comorbidities, anthropometry and demographics.<sup>99,100</sup> This is especially true with current HD practices, characterized by relatively short, intermittent sessions – four-hour, three-time weekly HD, where the treatment time to achieve the ECV goals is limited.

## 1.4 Introduction to $^{23}\text{Na}$ MRI

Magnetic resonance imaging (MRI) is a medical imaging technique that uses a strong magnetic field and nonionizing radiofrequency energy to polarize the magnetic spins of susceptible nuclei in biological tissues. In its most commonly available form, MRI manipulates the spins of protons ( $^1\text{H}$ ) contained in biological tissues to generate medical images. Recent technological improvements, however, allow other nuclei with spin properties that make them susceptible to nuclear magnetic resonance to be imaged. Sodium-23 ( $^{23}\text{Na}$ ) is one of such nuclei. The properties that reduce the MR sensitivity of non- $^1\text{H}$  nuclei, and therefore make multi-nuclear imaging more technically challenging, are the following:

- [a] a lower gyromagnetic ratio ( $\gamma$ ), which translates into a lower Larmor frequency, according to the formula  $\omega_0 = \gamma * B_0$ , where  $B_0$  (“B-nought”) is the static magnetic field of the MR magnet;
- [b] the spin properties of the nucleus of interest, which influence its relaxation properties;
- [c] a lower in-vivo abundance of the nucleus of interest.

Sodium-23 ( $^{23}\text{Na}$ ) is by far the most prevalent sodium isotope in nature and biological systems. It represents the only stable sodium isotope in nature with an almost 100% abundance. Although twenty other sodium isotopes have been identified in trace quantities, only two have potential significance in medicine,  $^{22}\text{Na}$  and  $^{24}\text{Na}$ . They are characterized by radioactive beta decay, with a half-life of  $\sim 2.6$  years and  $\sim 15$  hours, respectively. Their use in medicine is limited to nuclear medicine for dilution studies to determine total body exchangeable sodium, as detailed previously. Conversely,  $^{23}\text{Na}$  is the only relevant sodium nucleus for MRI. Its gyromagnetic ratio is 11.26 MHz/T, approximately 26% of  $^1\text{H}$  (42.58 MHz/T). It has a spin of  $3/2$  and a quadrupolar moment. In biological tissues, this results in a relatively short longitudinal ( $T_1$ ) relaxation (ranging 12-55

msec) and a bi-exponential transverse ( $T_2$ ) decay, with  $T_{2\text{short}}$  in the order 0.5–5 msec (which constitutes 60% of the signal) and  $T_{2\text{long}}$  (which constitutes 40% of the signal) in the order 15–30 msec.<sup>101</sup> Its natural abundance in the human body is about ~0.1% of the human body weight.<sup>3</sup> All these factors net to a signal-to-noise ratio (SNR) between 3,000–20,000 times lower compared with  $^1\text{H}$  MRI.<sup>101,102</sup>

Although the first publications in sodium MRI date back to the 1970s,<sup>103,104</sup> an increasing interest in  $^{23}\text{Na}$  MRI has sparked starting from the 1990s, with the development of higher field strength magnets ( $\geq 3.0$  T) that allow a better SNR, which can be traded for an increased spatial resolution and/or decreased scanning time. With a lower Larmor frequency compared with  $^1\text{H}$ ,  $^{23}\text{Na}$  MRI requires dedicated custom-made transmit-receive radiofrequency coils. Other technological improvements entail radiofrequency coils, computational power and pulse sequences with shorter signal acquisition times.

The development of pulse sequences with ultra-short echo times (UTE) now allows the acquisition of MR signal from tissues with extremely short  $T_2$  due to their properties (e.g. cortical bones or lungs, with  $^1\text{H}$ ) or nuclei with rapid transverse decay, such as  $^{23}\text{Na}$ .

Rudimentary UTE pulse sequences utilized a nonselective hard pulse, with an echo time of 2–4 msec.<sup>105</sup> Shorter echo times ( $< 1$  msec) have been later achieved by using non-cartesian pulse sequences, with radial or spiral signal acquisition, where most of the signal is collected from the center of k-space, where all radial projections start – this allows enhanced image contrast and reduced motion artifacts. This comes at the expense of final image resolution and image blurring. At present, common pulse sequences employed for  $^{23}\text{Na}$  MRI are mainly 3D radial and twisted projection imaging, both with density adaptation to fill the k-space homogeneously and improve the point spread function of the signal acquisition methods.<sup>106</sup>

By using “long” TR and ultra-short TE, UTE pulse sequences allow the collection of sodium-23 spin density-weighted images. This is the simplest way to quantify tissue  $[\text{Na}^+]$ . Such is also the pulse sequence employed for this research work.

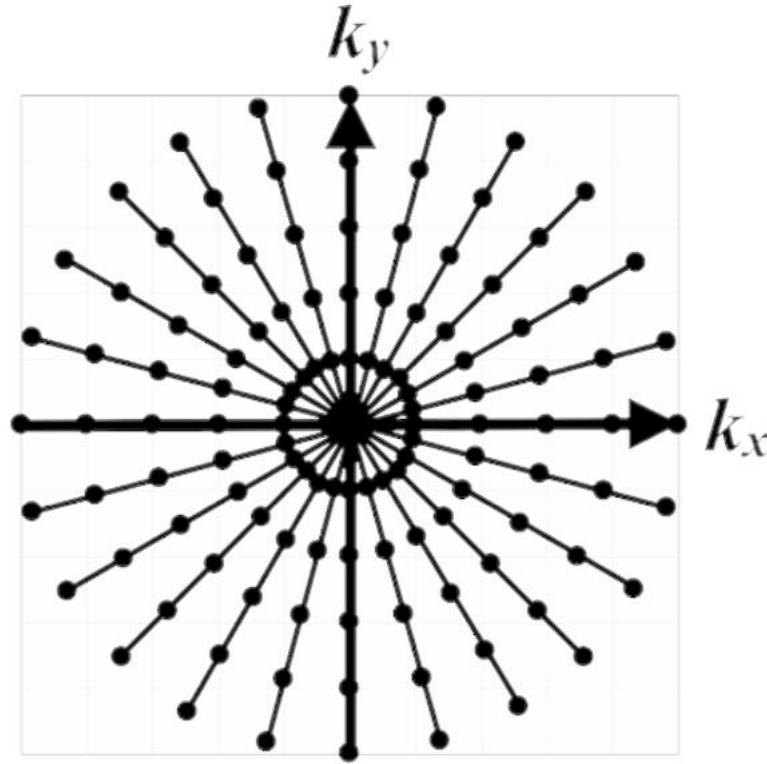
Echo times (TE) in the order of few milliseconds can be achieved via different approaches. One such approach is “two-dimensional radial imaging”, where k-space is acquired following radial projections during the frequency encoding step (**Figure 1.5**), by manipulating the gradients on the x and y planes. Such a pulse sequence only uses gradients for slice selection and frequency encoding – there is no phase encoding step, allowing for very short TE. Total imaging time, therefore, is the result of this formula (per single slice):

$$\text{Total imaging time} = N_{\text{SA}} * \text{TR} * N_{\text{RP}}$$

Where:  $N_{\text{SA}}$  = number of signal averages; TR = repetition time;  $N_{\text{RP}}$  = number of radial projections.

Figure 1.5: A representation of  $k$ -space as acquired by two-dimensional radial imaging.

$k$ -space is the location in which the MR signal is coded. Each point along the radial trajectories is defined by the spatial frequencies  $k_x$  and  $k_y$ , in terms of inverse distance (1/cm or cycles per cm).



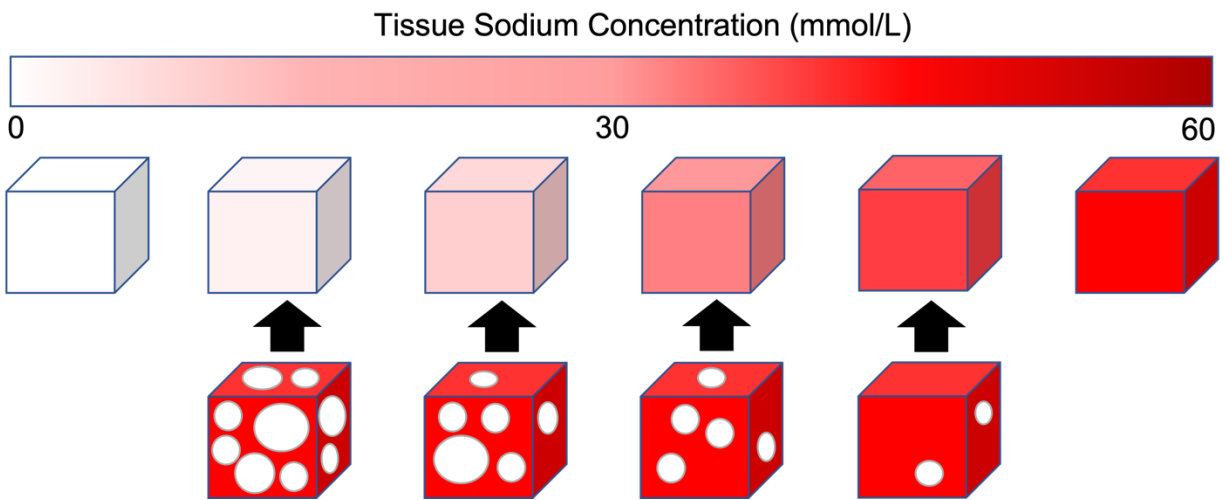
### *Sodium quantification*

To translate the sodium signal in images into  $[\text{Na}^+]$ , calibration vials (phantoms) containing known concentrations of sodium and relaxation times are included within the field-of-view. Solutions containing NaCl in either liquid or gel form (using agar) are commonly employed, with  $[\text{Na}^+]$  ranging from 10 mmol/L to 350 mmol/L, depending on the body location of interest. The signal generated by these phantoms is then calculated selecting a region of interest on the image, and used to measure tissue  $[\text{Na}^+]$  by linear regression, after correction for relaxation times.

### *Mechanisms Underlying Increased Tissue [Na<sup>+</sup>] and Potential Applications*

The interest surrounding <sup>23</sup>Na MRI is the ability to provide a different contrast parameter, compared with <sup>1</sup>H MRI. Indeed, several mechanisms underlie an increase in tissue [Na<sup>+</sup>]. First, as sodium is mainly an extracellular cation with an approximate concentration of 150 mmol/L, increased tissue [Na<sup>+</sup>] may indicate an increased ECV in the tissue of interest. This is likely the most significant mechanism of increased tissue [Na<sup>+</sup>], and this concept is closely connected, in <sup>23</sup>Na MRI, with the problem of “partial volume effect”.<sup>107</sup> At 3.0 T field, an approximate resolution of 3x3x30 mm<sup>3</sup> is usually achieved. Within its volume, each voxel includes different tissues in different proportions, such as fluid (e.g. fibrosis or edema), fat, cellular mass (e.g. muscle tissue): therefore, the extracellular to intracellular volume ratio within a voxel is a main determinant of signal intensity, as <sup>23</sup>Na signal in the image is an average of all sodium within this volume, with fat tissue acting as a confounder (acting as ECV but poor in sodium content) (**Figure 1.6**).

Figure 1.6:  $^{23}\text{Na}$  signal as a function of the extracellular to intracellular volume ratio, due to the partial volume effect. White circles stand for cell mass within the extracellular space.

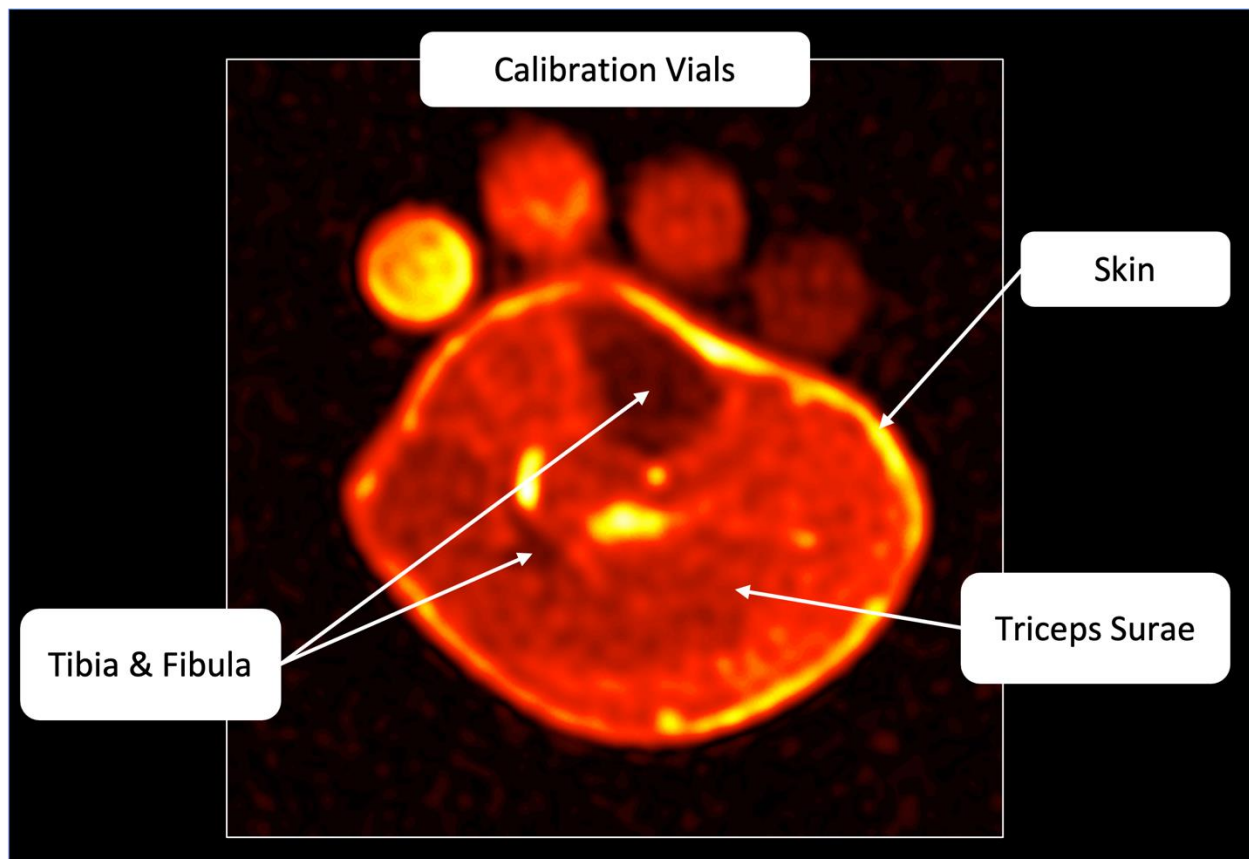


Secondly, tissue ischemia may result in dysfunction of the  $\text{Na}^+/\text{K}^+$  ATPase, resulting in increased intracellular  $[\text{Na}^+]$ .<sup>102</sup> This mechanism is relevant when evaluating image contrast in organs where ischemic damage is a possibility, such as cardiac tissue after myocardial infarction.<sup>108</sup> Other mechanisms are related to changes in tissue composition as a result of cancer growth (e.g. acidosis due to dysfunction of the  $\text{Na}^+/\text{H}^+$  exchanger, inflammation, fibrosis, neoangiogenesis), or ionic channel dysfunction, typical of some rare neuromuscular disorders.<sup>101,109</sup> Extracellular  $[\text{Na}^+]$  is also highly regulated at the kidney level, with the concentration gradient between the cortex and medulla being a promising biomarker of the kidneys' urine concentration ability.<sup>110</sup> The listed mechanisms of increased tissue  $[\text{Na}^+]$  suggest that  $^{23}\text{Na}$  MRI has numerous applications in clinical practice.

## Leg $^{23}\text{Na}$ MRI

For the purpose of this work, only the application of this  $^{23}\text{Na}$  MRI to the tissues of the leg will be treated, with particular attention to patients with CKD. As a peripheral limb, the human leg is convenient to image on an MRI scanner, with the several different anatomical structures for study, depending on the level: the knee cartilage, the tibia and fibula bones, the posterior (triceps surae), lateral (fibularis longus and brevis) and anterior skeletal muscles (tibialis and extensor digitorum muscles), fat and skin tissue (**Figure 1.7**).

Figure 1.7: Summary of the leg cross-section with  $^{23}\text{Na}$  MRI.



The triceps surae muscle and the skin are going to be the main object of interest in the studies mentioned below.

$^{23}\text{Na}$  MRI using a 3.0 T scanner to study the soft tissues of the leg in humans (skin, muscles) with hypertension was first applied by a German group, while studying the association between primary and secondary forms of hypertension with tissue sodium deposits.<sup>111,112</sup> The authors found older age and male sex, as well as a particular form of secondary hypertension (primary hyperaldosteronism, or Conn's disease) to be positively associated with skin and muscle  $[\text{Na}^+]$ . In light of the previous physiological studies by the same group,<sup>14,113</sup> the authors speculated whether the increased tissue  $[\text{Na}^+]$  would be due to osmotically inactive sodium accumulation. In addition, serum Vascular Endothelial Growth-Factor C (VEGF-C), a molecular mediator associated with interstitial lymphangiogenesis, was associated with increased tissue  $[\text{Na}^+]$ , suggesting that dysfunctional lymphatic drainage of the interstitium would lead to increased tissue sodium, likely due to local ECV expansion.

These findings were further confirmed in patients affected by CKD receiving dialysis, compared with healthy volunteers.<sup>114,115</sup> In the study published by Dahlmann et al,<sup>114</sup> age > 65 years was associated with greater tissue  $[\text{Na}^+]$ . In this study,  $^{23}\text{Na}$  MRI was performed immediately before and after a single HD session, showing a reduction in tissue  $[\text{Na}^+]$  after the procedure. Sodium removal by ultrafiltration, as well as the dialysate-to-plasma sodium gradient, were calculated for each HD session, but did not correlate with observed tissue sodium reduction, suggesting that tissue sodium clearance was not predictable given these variables alone. However, tissue sodium reduction after HD was greater in patients with higher serum VEGF-C level, suggesting improved lymphatic clearance during HD: it is therefore likely that interstitial lymphangiogenesis is an important determinant of sodium and water removal from peripheral tissues.

In addition, Schneider et al showed that skin  $[Na^+]$  was associated with hypertrophy of the heart, an important known predictor of hard clinical outcomes, in patients with CKD.<sup>116</sup> The authors went on to demonstrate that this relationship was independent of ECV status using bioimpedance spectroscopy, suggesting that osmotically inactive sodium might have been partially responsible of cardiac hypertrophy.

A later study in human healthy volunteers using  $^{23}Na$  MRI on a 7.0 T scanner showed sodium accumulation to occur specifically at the dermal layer of the skin,<sup>117</sup> which has been shown to contain large amounts of proteins containing negatively-charged sulfated carbohydrate chains (glycosaminoglycans), or proteoglycans, with the ability to bind and “store” sodium by osmotic inactivation, i.e. accumulation without water.<sup>15,17,118,119</sup> A recent study using  $^{23}Na$  MRI with triple quantum filtering in ex-vivo human skin samples later showed that large amounts of skin sodium to be bound to these proteins and likely undetectable by  $^{23}Na$  MRI using standard UTE pulse sequences, due to its extremely rapid T2 decay properties.<sup>120</sup>

## 1.5 Overarching Hypothesis and Rationale

In the material presented so far, we have summarized the available evidence supporting the potential clinical relevance of tissue  $[\text{Na}^+]$ , as well as the requirements and pitfalls for its quantification by  $^{23}\text{Na}$  MRI. At the time of this work's inception (2018), several knowledge gaps concerning tissue  $[\text{Na}^+]$  existed in the literature, despite sodium being recognized as a fundamental mediator of cardiovascular disease in the CKD and dialysis population. In particular:

- No formal comparison of tissue  $[\text{Na}^+]$  among healthy individuals, CKD patients and dialysis patients had been made.
- Similarly, no investigations were made in the pediatric CKD population, in spite of these patients generally having a smaller comorbidity burden (e.g. overt atherosclerosis and cardiovascular disease, complicated diabetes mellitus, hypertension) that may act as a confounder to tissue  $[\text{Na}^+]$ .
- Tissue  $[\text{Na}^+]$  had been shown to be positively associated with age and serum VEGF-C in patients receiving HD,<sup>114</sup> although no other clinical predictors, such as HD prescription or biochemical parameters, were investigated.
- Skin  $[\text{Na}^+]$  had been shown to be positively associated with cardiac mass in patients with CKD, but no data existed on HD patients.<sup>116</sup>
- No data concerning clinical outcomes, such as major cardiovascular adverse events (a composite outcome including several acute diseases such as myocardial infarction, stroke, pulmonary embolism and death resulting from these causes) or general mortality, had been published.

Therefore, as a premise to this work, we hypothesized that *tissue [Na<sup>+</sup>] is a relevant quantitative imaging biomarker in the CKD, HD and PD population, with significant consequences on the cardiovascular system and clinical outcomes.*

Four projects have been included in this work to verify this hypothesis, and the research aims for each individual project are summarized below:

**Chapter 2.** The aims of this project were to (1) explore the differences in tissue [Na<sup>+</sup>] between healthy controls, CKD, HD and PD patients, (2) explore the associations of tissue sodium with standard blood-based biomarkers and (3) assess the reproducibility of tissue [Na<sup>+</sup>] measurements by <sup>23</sup>Na MRI.

**Chapter 3.** This project aimed to compare (1) tissue [Na<sup>+</sup>] in children and adolescents with CKD against healthy controls and (2) investigate the associations of tissue [Na<sup>+</sup>] with clinical biomarkers of kidney function.

**Chapter 4.** In this project the aims were to investigate the associations of tissue [Na<sup>+</sup>] with left ventricular hypertrophy and other markers of left ventricular structure, such as end-diastolic volume and geometry.

**Chapter 5.** In this final project, the aims were to (1) investigate the association between skin [Na<sup>+</sup>] with mortality and MACE in a cohort of HD and PD patients, and (2) define the clinical predictors of skin [Na<sup>+</sup>].

## 1.6 Bibliography

1. Bhavé G, Neilson EG. Body fluid dynamics: Back to the future. *J Am Soc Nephrol.* 2011;22(12):2166-2181. doi:10.1681/ASN.2011080865
2. Levick JR, Michel CC. Microvascular fluid exchange and the revised Starling principle. *Cardiovasc Res.* 2010;87(2):198-210. doi:10.1093/cvr/cvq062
3. Edelman IS, Leibman J, O'Meara MP, Birkenfeld LW. Interrelations between serum sodium concentration, serum osmolality and total exchangeable sodium, total exchangeable potassium and total body water. *J Clin Invest.* 1958;37(9):1236-1256. doi:10.1172/JCI103712
4. FORBES GB, PERLEY A. Estimation of total body sodium by isotopic dilution. I. Studies on young adults. *J Clin Invest.* 1951;30(6):558-565. doi:10.1172/JCI102472
5. DEANE N, SMITH HW. The distribution of sodium and potassium in man. *J Clin Invest.* 1952;31(2):197-199. doi:10.1172/JCI102591
6. EDELMAN IS, JAMES AH, BADEN H, MOORE FD. Electrolyte composition of bone and the penetration of radiosodium and deuterium oxide into dog and human bone. *J Clin Invest.* 1954;33(2):122-131. doi:10.1172/JCI102878
7. JAGGER PI, HINE GJ, CARDARELLI JA, BURROWS BA. Influence of Sodium Intake on Exchangeable Sodium in Normal Human Subjects. *J Clin Invest.* 1963;42(9):1459-1470. doi:10.1172/JCI104830
8. Nguyen MK, Kurtz I. Quantitative interrelationship between Gibbs-Donnan equilibrium, osmolality of body fluid compartments, and plasma water sodium concentration. *J Appl Physiol.* 2006;100(4):1293-1300. doi:10.1152/jappphysiol.01274.2005
9. Rossitto G, Touyz RM, Petrie MC, Delles C. "Much ado about N . . . Atrium: Modelling

- tissue sodium as a highly sensitive marker of subclinical and localised oedema.” *Clin Sci.* 2018;132(24):2609-2613. doi:10.1042/CS20180575
10. Rossitto G, Delles C. Mechanisms of sodium-mediated injury in cardiovascular disease: old play, new scripts. *FEBS J.* Published online 2021:1-14. doi:10.1111/febs.16155
  11. Maroudas A. Balance between swelling pressure and collagen tension in normal and degenerate cartilage Growth of algal symbionts in regenerating hydra. *Nature.* 1976;260:808-809.
  12. Ivanova LN, Archibasova VK, Shterental’ IS. [Sodium-depositing function of the skin in white rats]. *Fiziol Zh SSSR Im IM Sechenova.* 1978;64(3):358-363.
  13. Zolotova VF, Priadeina TE, Archibasova VK, Shterental’ IS. [Distribution of sodium in the tissues in experimental salt hypertension]. *Kardiologiya.* 1975;15(8):32-36.
  14. Titze J, Lang R, Ilies C, et al. Osmotically inactive skin Na + storage in rats. *Am J Physiol Physiol.* 2003;285(6):F1108-F1117. doi:10.1152/ajprenal.00200.2003
  15. Titze J, Shakibaei M, Schafflhuber M, et al. Glycosaminoglycan polymerization may enable osmotically inactive Na + storage in the skin . *Am J Physiol Circ Physiol.* 2004;287(1):H203-H208. doi:10.1152/ajpheart.01237.2003
  16. Ziomber A, Machnik A, Dahlmann A, et al. Sodium-, potassium-, chloride-, and bicarbonate-related effects on blood pressure and electrolyte homeostasis in deoxycorticosterone acetate-treated rats. *Am J Physiol Physiol.* 2008;295(6):F1752-F1763. doi:10.1152/ajprenal.00531.2007
  17. Wenstedt EFE, Oppelaar JJ, Besseling S, et al. Distinct osmoregulatory responses to sodium loading in patients with altered glycosaminoglycan structure: a randomized cross-over trial. *J Transl Med.* 2021;19(1):1-16. doi:10.1186/s12967-021-02700-0

18. Hofmeister LH, Perisic S, Titze J. Tissue sodium storage: evidence for kidney-like extrarenal countercurrent systems? *Pflugers Arch.* 2015;467(3):551-558. doi:10.1007/s00424-014-1685-x
19. Nikpey E, Karlsen T V., Rakova N, Titze JM, Tenstad O, Wiig H. High-Salt Diet Causes Osmotic Gradients and Hyperosmolality in Skin Without Affecting Interstitial Fluid and Lymph. *Hypertension.* 2017;69(4):660-668. doi:10.1161/HYPERTENSIONAHA.116.08539
20. MacHnik A, Neuhofer W, Jantsch J, et al. Macrophages regulate salt-dependent volume and blood pressure by a vascular endothelial growth factor-C-dependent buffering mechanism. *Nat Med.* 2009;15(5):545-552. doi:10.1038/nm.1960
21. MacHnik A, Dahlmann A, Kopp C, et al. Mononuclear phagocyte system depletion blocks interstitial tonicity-responsive enhancer binding protein/vascular endothelial growth factor c expression and induces salt-sensitive hypertension in rats. *Hypertension.* 2010;55(3):755-761. doi:10.1161/HYPERTENSIONAHA.109.143339
22. Wiig H, Schröder A, Neuhofer W, et al. Immune cells control skin lymphatic electrolyte homeostasis and blood pressure. *J Clin Invest.* 2013;123(7):2803-2815. doi:10.1172/JCI60113
23. MacHnik A, Dahlmann A, Kopp C, et al. Mononuclear phagocyte system depletion blocks interstitial tonicity-responsive enhancer binding protein/vascular endothelial growth factor c expression and induces salt-sensitive hypertension in rats. *Hypertension.* 2010;55(3):755-761. doi:10.1161/HYPERTENSIONAHA.109.143339
24. Titze J, Maillet A, Lang R, et al. Long-term sodium balance in humans in a terrestrial space station simulation study. *Am J Kidney Dis.* 2002;40(3):508-516.

- doi:10.1053/ajkd.2002.34908
25. Lerchl K, Rakova N, Dahlmann A, et al. Agreement between 24-hour salt ingestion and sodium excretion in a controlled environment. *Hypertension*. 2015;66(4):850-857. doi:10.1161/HYPERTENSIONAHA.115.05851
  26. Rakova N, Juttner K, Dahlmann A, et al. Long-term space flight simulation reveals infradian rhythmicity in human Na(+) balance. *Cell Metab*. 2013;17(1):125-131. doi:10.1016/j.cmet.2012.11.013
  27. Titze J, Bauer K, Schafflhuber M, et al. Internal sodium balance in DOCA-salt rats: a body composition study. *Am J Physiol Physiol*. 2005;289(4):F793-F802. doi:10.1152/ajprenal.00096.2005
  28. Jantsch J, Schatz V, Friedrich D, et al. Cutaneous Na<sup>+</sup> storage strengthens the antimicrobial barrier function of the skin and boosts macrophage-driven host defense. *Cell Metab*. 2015;21(3):493-501. doi:10.1016/j.cmet.2015.02.003
  29. Olde Engberink RHG, Rorije NMG, Van Der Heide JJH, Van Den Born BJH, Vogt L. Role of the vascular wall in sodium homeostasis and salt sensitivity. *J Am Soc Nephrol*. 2015;26(4):777-783. doi:10.1681/ASN.2014050430
  30. Wenstedt EFE, Engberink RHGO, Vogt L. Sodium handling by the blood vessel wall critical for hypertension development. *Hypertension*. 2018;71(6):990-996. doi:10.1161/HYPERTENSIONAHA.118.10211
  31. Koch J, Idzerda NMA, Ettema EM, et al. An acute rise of plasma Na<sup>+</sup> concentration associates with syndecan-1 shedding during hemodialysis. *Am J Physiol - Ren Physiol*. 2020;319(2):F171-F177. doi:10.1152/ajprenal.00005.2020
  32. Koch J, Idzerda NMA, Dam W, Assa S, Franssen CFM, van den Born J. Plasma syndecan-

- 1 in hemodialysis patients associates with survival and lower markers of volume status. *Am J Physiol - Ren Physiol*. 2019;316(1):F121-F127. doi:10.1152/ajprenal.00252.2018
33. Oberleithner H, Peters W, Kusche-Vihrog K, et al. Salt overload damages the glycocalyx sodium barrier of vascular endothelium. *Pflugers Arch Eur J Physiol*. 2011;462(4):519-528. doi:10.1007/s00424-011-0999-1
34. Feehally J, Floege J, Tonelli M, Jonhson RJ. *Comprehensive Clinical Nephrology*. 6th Editio. Elsevier; 2019.
35. Salomonsson M, Gonzalez E, Westerlund P, Persson AE. Chloride concentration in macula densa and cortical thick ascending limb cells. *Kidney Int Suppl*. 1991;32:S51-4.
36. Levey AS, Coresh J, Greene T, et al. Using standardized serum creatinine values in the modification of diet in renal disease study equation for estimating glomerular filtration rate. *Ann Intern Med*. 2006;145(4):247-254. doi:10.7326/0003-4819-145-4-200608150-00004
37. Levey AS, Stevens LA, Schmid CH, et al. A New Equation to Estimate Glomerular Filtration Rate. *Ann Intern Med*. 2009;150(9):604-612. doi:10.1059/0003-4819-150-9-200905050-00006
38. Bovée DM, Cuevas CA, Zietse R, Danser AHJ, Mirabito Colafella KM, Hoorn EJ. Salt-sensitive hypertension in chronic kidney disease: Distal tubular mechanisms. *Am J Physiol - Ren Physiol*. 2020;319(5):F729-F745. doi:10.1152/ajprenal.00407.2020
39. Dubey AK, Sahoo J, Vairappan B, Haridasan S, Parameswaran S, Priyamvada PS. Correction of metabolic acidosis improves muscle mass and renal function in chronic kidney disease stages 3 and 4: A randomized controlled trial. *Nephrol Dial Transplant*. 2020;35(1):121-129. doi:10.1093/ndt/gfy214
40. Thakar S, Paller MS. *Sodium Metabolism in Chronic Kidney Disease*. Elsevier Inc.; 2020.

doi:10.1016/b978-0-12-815876-0.00039-5

41. Chamberlain RM, Shirley DG. Time course of the renal functional response to partial nephrectomy: Measurements in conscious rats. *Exp Physiol.* 2007;92(1):251-262. doi:10.1113/expphysiol.2006.034751
42. Layton AT, Edwards A, Vallon V. Adaptive changes in GFR, tubular morphology, and transport in subtotal nephrectomized kidneys: Modeling and analysis. *Am J Physiol - Ren Physiol.* 2017;313(2):F199-F209. doi:10.1152/ajprenal.00018.2017
43. Klein IHHT, Ligtenberg G, Neumann J, Oey PL, Koomans HA, Blankestijn PJ. Sympathetic Nerve Activity Is Inappropriately Increased in Chronic Renal Disease. *J Am Soc Nephrol.* 2003;14(12):3239-3244. doi:10.1097/01.ASN.0000098687.01005.A5
44. Kolff WJ, Nakamoto S, Poutasse EF, Straffon RA, Figueroa JE. Effect of Bilateral Nephrectomy and Kidney Transplantation on Hypertension in Man. *Circulation.* 1964;30(2s2):II-23-II-28. doi:10.1161/01.CIR.30.2S2.II-23
45. Moranne O, Froissart M, Rossert J, et al. Timing of onset of CKD-related metabolic complications. *J Am Soc Nephrol.* 2009;20(1):164-171. doi:10.1681/ASN.2008020159
46. Taylor AHM, Rankin AJ, McQuarrie EP, et al. Non-uniform relationship between salt status and aldosterone activity in patients with chronic kidney disease. *Clin Sci.* 2018;132(2):285-294. doi:10.1042/CS20171603
47. McQuarrie EP, Freel EM, Mark PB, Fraser R, Connell JMC, Jardine AG. Urinary sodium excretion is the main determinant of mineralocorticoid excretion rates in patients with chronic kidney disease. *Nephrol Dial Transplant.* 2013;28(6):1526-1532. doi:10.1093/ndt/gft007
48. Ramkumar N, Kohan DE. Proximal tubule angiotensinogen modulation of arterial pressure.

- Curr Opin Nephrol Hypertens.* 2013;22(1). [https://journals.lww.com/co-nephrolhypertens/Fulltext/2013/01000/Proximal\\_tubule\\_angiotensinogen\\_modulation\\_of.6.aspx](https://journals.lww.com/co-nephrolhypertens/Fulltext/2013/01000/Proximal_tubule_angiotensinogen_modulation_of.6.aspx)
49. Casarini DE, Boim MA, Stella RC, Krieger-Azzolini MH, Krieger JE, Schor N. Angiotensin I-converting enzyme activity in tubular fluid along the rat nephron. *Am J Physiol Physiol.* 1997;272(3):F405-F409. doi:10.1152/ajprenal.1997.272.3.F405
50. Wang T, Giebisch G. Effects of angiotensin II on electrolyte transport in the early and late distal tubule in rat kidney. *Am J Physiol Physiol.* 1996;271(1):F143-F149. doi:10.1152/ajprenal.1996.271.1.F143
51. Hollenberg NK, Fisher NDL, Nussberger J, Moukarbel G V, Barkoudah E, Danser AHJ. Renal responses to three types of renin–angiotensin system blockers in patients with diabetes mellitus on a high-salt diet: a need for higher doses in diabetic patients? *J Hypertens.* 2011;29(12). [https://journals.lww.com/jhypertension/Fulltext/2011/12000/Renal\\_responses\\_to\\_three\\_types\\_of.23.aspx](https://journals.lww.com/jhypertension/Fulltext/2011/12000/Renal_responses_to_three_types_of.23.aspx)
52. Tang J, Wysocki J, Ye M, et al. Urinary Renin in Patients and Mice with Diabetic Kidney Disease. *Hypertension.* 2019;74(1):83-94. doi:10.1161/HYPERTENSIONAHA.119.12873
53. Kawarazaki H, Ando K, Shibata S, et al. Mineralocorticoid receptor–Rac1 activation and oxidative stress play major roles in salt-induced hypertension and kidney injury in prepubertal rats. *J Hypertens.* 2012;30(10). [https://journals.lww.com/jhypertension/Fulltext/2012/10000/Mineralocorticoid\\_receptor\\_Rac1\\_activation\\_and.18.aspx](https://journals.lww.com/jhypertension/Fulltext/2012/10000/Mineralocorticoid_receptor_Rac1_activation_and.18.aspx)
54. Shibata S, Mu SY, Kawarazaki H, et al. Rac1 GTPase in rodent kidneys is essential for salt-

- sensitive hypertension via a mineralocorticoid receptor-dependent pathway. *J Clin Invest*. 2011;121(8):3233-3243. doi:10.1172/JCI43124
55. Wesson DE, Buysse JM, Bushinsky DA. Mechanisms of metabolic acidosis–induced kidney injury in chronic kidney disease. *J Am Soc Nephrol*. 2020;31(3):469-482. doi:10.1681/ASN.2019070677
56. Svenningsen P, Bistrup C, Friis UG, et al. Plasmin in nephrotic urine activates the epithelial sodium channel. *J Am Soc Nephrol*. 2009;20(2):299-310. doi:10.1681/ASN.2008040364
57. Buhl KB, Oxlund CS, Friis UG, et al. Plasmin in urine from patients with type 2 diabetes and treatment-resistant hypertension activates ENaC in vitro. *J Hypertens*. 2014;32(8):1672-1677. doi:10.1097/HJH.0000000000000216
58. Artunc F, Wörn M, Schork A, Bohnert BN. Proteasuria—The impact of active urinary proteases on sodium retention in nephrotic syndrome. *Acta Physiol*. 2019;225(4):1-10. doi:10.1111/apha.13249
59. Andersen H, Friis UG, Hansen PBL, Svenningsen P, Henriksen JE, Jensen BL. Diabetic nephropathy is associated with increased urine excretion of proteases plasmin, prostatic and urokinase and activation of amiloride-sensitive current in collecting duct cells. *Nephrol Dial Transplant*. 2015;30(5):781-789. doi:10.1093/ndt/gfu402
60. Olde Engberink RHG, Van Den Hoek TC, Van Noordenne ND, Van Den Born BJH, Peters-Sengers H, Vogt L. Use of a single baseline versus multiyear 24-hour urine collection for estimation of long-term sodium intake and associated cardiovascular and renal risk. *Circulation*. 2017;136(10):917-926. doi:10.1161/CIRCULATIONAHA.117.029028
61. Lunyera J, Mohottige D, von Isenburg M, Jeuland M, Patel UD, Stanifer JW. CKD of uncertain etiology: A systematic review. *Clin J Am Soc Nephrol*. 2016;11(3):379-385.

doi:10.2215/CJN.07500715

62. Ramdeen G, Tzamaloukas AH, Malhotra D, Leger A, Murata GH. Estimates of interdialytic sodium and water intake based on the balance principle: differences between nondiabetic and diabetic subjects on hemodialysis. *ASAIO J.* 1998;44(6):812-817.
63. Argent NB, Burrell LM, Goodship THJ, Wilkinson R, Baylis PH. Osmoregulation of thirst and vasopressin release in severe chronic renal failure. *Kidney Int.* 1991;39(2):295-300.  
doi:10.1038/ki.1991.36
64. Bossola M, Calvani R, Marzetti E, Picca A, Antocicco E. Thirst in patients on chronic hemodialysis: What do we know so far? *Int Urol Nephrol.* 2020;52(4):697-711.  
doi:10.1007/s11255-020-02401-5
65. Stachenfeld NS, Mack GW, Takamata A, DiPietro L, Nadel ER. Thirst and fluid regulatory responses to hypertonicity in older adults. *Am J Physiol Integr Comp Physiol.* 1996;271(3):R757-R765. doi:10.1152/ajpregu.1996.271.3.R757
66. Keen ML, Gotch FA. The association of the sodium “setpoint” to interdialytic weight gain and blood pressure in hemodialysis patients. *Int J Artif Organs.* 2007;30(11):971-979.  
doi:10.1177/039139880703001105
67. Thomson BKA, Huang SHS, Chan CT, House AA, Lindsay RM. Plasma sodium setpoint: Is it constant or changed by hemodialysis prescription? *ASAIO J.* 2013;59(5):497-504.  
doi:10.1097/MAT.0b013e31829ed829
68. Obi Y, Rhee CM, Mathew AT, et al. Residual Kidney Function Decline and Mortality in Incident Hemodialysis Patients. *J Am Soc Nephrol.* 2016;27(12):3758-3768.  
doi:10.1681/ASN.2015101142
69. Wang M, Obi Y, Streja E, et al. Impact of residual kidney function on hemodialysis

- adequacy and patient survival. *Nephrol Dial Transplant*. 2018;33(10):1823-1831. doi:10.1093/ndt/gfy060
70. McIntyre CW. Recurrent Circulatory Stress: The Dark Side of Dialysis. *Semin Dial*. 2010;23(5):449-451. doi:10.1111/j.1525-139X.2010.00782.x
  71. Huang SHS, Filler G, Lindsay R, McIntyre CW. Euvolemia in Hemodialysis Patients: A Potentially Dangerous Goal? *Semin Dial*. 2015;28(1):1-5. doi:10.1111/sdi.12317
  72. Flanigan MJ. Role of sodium in hemodialysis. *Kidney Int Suppl*. 2000;58(76):72-78. doi:10.1046/j.1523-1755.2000.07609.x
  73. De Paula FM, Peixoto AJ, Pinto L V., Dorigo D, Patricio PJM, Santos SFF. Clinical consequences of an individualized dialysate sodium prescription in hemodialysis patients. *Kidney Int*. 2004;66(3):1232-1238. doi:10.1111/j.1523-1755.2004.00876.x
  74. Peixoto AJ, Santos SFF. How should the predialysis plasma sodium level be interpreted in hemodialysis patients? *Semin Dial*. 2011;24(4):409-411. doi:10.1111/j.1525-139X.2011.00934.x
  75. Lopot F, Kotyk P, Blaha J, Valek A. Influence of the Dialyzer Membrane Material on Sodium Transport in Hemodialysis. 1995;19(11):1172-1175.
  76. Gotch FA, Evans MC, Keen ML. Measurement of the effective dialyzer Na diffusion gradient in vitro and in vivo. *Trans Am Soc Artif Intern Organs*. 1985;31:354-358.
  77. Locatelli F, Ponti R, Pedrini L, et al. Sodium kinetics across dialysis membranes. *Nephron*. 1984;38(3):174-177. doi:10.1159/000183303
  78. Locatelli F, Filippo S Di, Manzoni C. Sodium Kinetics During Dialysis. *Semin Dial*. 1999;12(Suppl 1):S41-S44.
  79. Santos SFF, Peixoto AJ. Sodium Balance in Maintenance Hemodialysis. *Semin Dial*.

- 2010;23(6):549-555. doi:10.1111/j.1525-139X.2010.00794.x
80. Flythe JE, Mc Causland FR. Dialysate Sodium: Rationale for Evolution over Time. *Semin Dial.* 2017;30(2):99-111. doi:10.1111/sdi.12570
81. Lambie SH, Taal MW, Fluck RJ, McIntyre CW. Online conductivity monitoring: Validation and usefulness in a clinical trial of reduced dialysate conductivity. *ASAIO J.* 2005;51(1):70-76. doi:10.1097/01.MAT.0000150525.96413.AW
82. Locatelli F, Covic A, Chazot C, Leunissen K, Luño J, Yaqoob M. Optimal composition of the dialysate, with emphasis on its influence on blood pressure. *Nephrol Dial Transplant.* 2004;19(4):785-796. doi:10.1093/ndt/gfh102
83. Dasselaar JJ, Slart RHJA, Knip M, et al. Haemodialysis is associated with a pronounced fall in myocardial perfusion. *Nephrol Dial Transplant.* 2009;24(2):604-610. doi:10.1093/ndt/gfn501
84. Marants R, Qirjazi E, Grant CJ, Lee TY, McIntyre CW. Renal Perfusion during Hemodialysis: Intradialytic Blood Flow Decline and Effects of Dialysate Cooling. *J Am Soc Nephrol.* 2019;30(6):1086-1095. doi:10.1681/ASN.2018121194
85. Sellars L, Robson V, Wilkinson R. Sodium retention and hypertension with short dialysis. *Br Med J.* 1979;1(6162):520-521. doi:10.1136/bmj.1.6162.520
86. Parfrey PS, Foley RN, Harnett JD, Kent GM, Murray DC, Barre PE. Outcome and risk factors for left ventricular disorders in chronic uraemia. *Nephrol Dial Transplant.* 1996;11(7):1277-1285. doi:10.1093/ndt/11.7.1277
87. Foley RN, Parfrey PS, Harnett JD, et al. Clinical and echocardiographic disease in patients starting end-stage renal disease therapy. *Kidney Int.* 1995;47(1):186-192. doi:10.1038/ki.1995.22

88. Zoccali C, Benedetto FA, Mallamaci F, et al. Left ventricular mass monitoring in the follow-up of dialysis patients: Prognostic value of left ventricular hypertrophy progression. *Kidney Int.* 2004;65(4):1492-1498. doi:10.1111/j.1523-1755.2004.00530.x
89. Charra B, Terrat JC, Vanel T, et al. Long thrice weekly hemodialysis: The Tassin experience. *Int J Artif Organs.* 2004;27(4):265-283. doi:10.1177/039139880402700403
90. Ozkahya M, Ok E, Toz H, et al. Long-term survival rates in haemodialysis patients treated with strict volume control. *Nephrol Dial Transplant.* 2006;21(12):3506-3513. doi:10.1093/ndt/gfl487
91. Zoccali C, Moissl U, Chazot C, et al. Chronic fluid overload and mortality in ESRD. *J Am Soc Nephrol.* 2017;28(8):2491-2497. doi:10.1681/ASN.2016121341
92. Kong YW, Baqar S, Jerums G, Ekinici EI. Sodium and its role in cardiovascular disease - The debate continues. *Front Endocrinol (Lausanne).* 2016;7(DEC):1-17. doi:10.3389/fendo.2016.00164
93. Titze J, Luft FC. Speculations on salt and the genesis of arterial hypertension. *Kidney Int.* 2017;91(6):1324-1335. doi:10.1016/j.kint.2017.02.034
94. Cozzolino M, Mangano M, Stucchi A, Ciceri P, Conte F, Galassi A. Cardiovascular disease in dialysis patients. *Nephrol Dial Transplant.* 2018;33:iii28-iii34. doi:10.1093/ndt/gfy174
95. Canaud B, Lertdumrongluk P. Probing “dry weight” in haemodialysis patients: “Back to the future.” *Nephrol Dial Transplant.* 2012;27(6):2140-2143. doi:10.1093/ndt/gfs094
96. Chazot C, Wabel P, Chamney P, Moissl U, Wieskotten S, Wizemann V. Importance of normohydration for the long-term survival of haemodialysis patients. *Nephrol Dial Transplant.* 2012;27(6):2404-2410. doi:10.1093/ndt/gfr678
97. McIntyre CW, Burton JO, Selby NM, et al. Hemodialysis-induced cardiac dysfunction is

- associated with an acute reduction in global and segmental myocardial blood flow. *Clin J Am Soc Nephrol*. 2008;3(1):19-26. doi:10.2215/CJN.03170707
98. Burton JO, Jefferies HJ, Selby NM, McIntyre CW. Hemodialysis-induced cardiac injury: Determinants and associated outcomes. *Clin J Am Soc Nephrol*. 2009;4(5):914-920. doi:10.2215/CJN.03900808
99. Flythe JE, Kimmel SE, Brunelli SM. Rapid fluid removal during dialysis is associated with cardiovascular morbidity and mortality. *Kidney Int*. 2011;79(2):250-257. doi:10.1038/ki.2010.383
100. Assimon MM, Flythe JE. Definitions of intradialytic hypotension. *Semin Dial*. 2017;30(6):464-472. doi:10.1111/sdi.12626
101. Madelin G, Regatte RR. Biomedical applications of sodium MRI in vivo. *J Magn Reson Imaging*. 2013;38(3):511-529. doi:10.1002/jmri.24168
102. Maudsley AA, Hilal SK. Biological aspects of sodium-23 imaging. *Br Med Bull*. 1984;40(2):165-166. doi:10.1093/oxfordjournals.bmb.a071964
103. Berendsen HJC, Edzes HT. THE OBSERVATION AND GENERAL INTERPRETATION OF SODIUM MAGNETIC RESONANCE IN BIOLOGICAL MATERIAL. *Ann N Y Acad Sci*. 1973;204(1):459-485. doi:https://doi.org/10.1111/j.1749-6632.1973.tb30799.x
104. Shporer M, Civan MM. Effects of temperature and field strength on the NMR relaxation times of <sup>23</sup>Na in frog striated muscle. *BBA - Gen Subj*. 1974;354(2):291-304. doi:10.1016/0304-4165(74)90014-2
105. Tyler DJ, Robson MD, Henkelman RM, Young IR, Bydder GM. Magnetic resonance imaging with ultrashort TE (UTE) PULSE sequences: Technical considerations. *J Magn Reson Imaging*. 2007;25(2):279-289. doi:10.1002/jmri.20851

106. Nagel AM, Laun FB, Weber MA, Matthies C, Semmler W, Schad LR. Sodium MRI using a density-adapted 3D radial acquisition technique. *Magn Reson Med*. 2009;62(6):1565-1573. doi:10.1002/mrm.22157
107. Rossitto G, Mary S, Chen JY, et al. Tissue sodium excess is not hypertonic and reflects extracellular volume expansion. *Nat Commun*. 2020;11(1):1-9. doi:10.1038/s41467-020-17820-2
108. Bottomley PA. Sodium MRI in human heart: a review. *NMR Biomed*. 2016;29(2):187-196. doi:10.1002/nbm.3265
109. Petracca M, Fleysher L, Oesingmann N, Inglese M. Sodium MRI of multiple sclerosis. *NMR Biomed*. 2016;29(2):153-161. doi:10.1002/nbm.3289
110. Maril N, Rosen Y, Reynolds GH, Ivanishev A, Ngo L, Lenkinski RE. Sodium MRI of the human kidney at 3 tesla. *Magn Reson Med*. 2006;56(6):1229-1234. doi:10.1002/mrm.21031
111. Kopp C, Linz P, Wachsmuth L, et al. <sup>23</sup>Na magnetic resonance imaging of tissue sodium. *Hypertension*. 2012;59(1):167-172. doi:10.1161/HYPERTENSIONAHA.111.183517
112. Kopp C, Linz P, Dahlmann A, et al. <sup>23</sup>Na magnetic resonance imaging-determined tissue sodium in healthy subjects and hypertensive patients. *Hypertension*. 2013;61(3):635-640. doi:10.1161/HYPERTENSIONAHA.111.00566
113. Titze J, Bauer K, Schafflhuber M, et al. Internal sodium balance in DOCA-salt rats: A body composition study. *Am J Physiol - Ren Physiol*. 2005;289(4 58-4):793-802. doi:10.1152/ajprenal.00096.2005
114. Dahlmann A, Dörfelt K, Eicher F, et al. Magnetic resonance-determined sodium removal from tissue stores in hemodialysis patients. *Kidney Int*. 2015;87(2):434-441. doi:10.1038/ki.2014.269

115. Sahinoz M, Tintara S, Deger SM, et al. Tissue sodium stores in peritoneal dialysis and hemodialysis patients determined by sodium-23 magnetic resonance imaging. *Nephrol Dial Transplant*. 2021;36(7):1307-1317. doi:10.1093/ndt/gfaa350
116. Schneider MP, Raff U, Kopp C, et al. Skin Sodium Concentration Correlates with Left Ventricular Hypertrophy in CKD. *J Am Soc Nephrol*. 2017;28(6):1867-1876. doi:10.1681/asn.2016060662
117. Linz P, Santoro D, Renz W, et al. Skin sodium measured with <sup>23</sup>Na MRI at 7.0 T. *NMR Biomed*. 2015;28(1):54-62. doi:10.1002/nbm.3224
118. Titze J, Machnik A. Sodium sensing in the interstitium and relationship to hypertension. *Curr Opin Nephrol Hypertens*. 2010;19(4):385-392. doi:10.1097/MNH.0b013e32833aeb3b
119. Fischereeder M, Michalke B, Schmöckel E, et al. Sodium storage in human tissues is mediated by glycosaminoglycan expression. *Am J Physiol Physiol*. 2017;313(2):F319-F325. doi:10.1152/ajprenal.00703.2016
120. Hanson P, Philp CJ, Randeva HS, et al. Sodium in the dermis collocates to glycosaminoglycan scaffold, with diminishment in type 2 diabetes mellitus. *JCI Insight*. 2021;6(12):1-16. doi:10.1172/jci.insight.145470

## Chapter 2

### **Leg Tissue Sodium Concentration in Chronic Kidney Disease and Dialysis Patients by Sodium-23 Magnetic Resonance Imaging**

*In this study, we compared  $[\text{Na}^+]$  of the leg tissues with  $^{23}\text{Na}$  MRI, in order to understand whether CKD, HD and PD were associated with tissue sodium accumulation compared with healthy controls. Furthermore, we explored the predictors of tissue  $[\text{Na}^+]$ .*

*A version of this chapter has been published in the journal “Nephrology, Dialysis, Transplantation” Qirjazi E, Salerno FR, Akbari A, Hur L, Penny J, Scholl T, McIntyre CW. Tissue sodium concentrations in chronic kidney disease and dialysis patients by lower leg sodium-23 magnetic resonance imaging. Nephrol Dial Transplant. 2020 Apr 6:gfaa036. doi: 10.1093/ndt/gfaa036. Epub ahead of print. PMID: 32252091. This article is available under the terms of the Creative Commons Attribution License.*

### **2.1 Introduction**

The toxic effects of sodium in CKD patients have been recognized since the 1940s, when Walter Kempner proposed the “Rice Diet” to manage hypertension by minimizing dietary sodium intake to 150 mg per day.<sup>1</sup> In the first clinical experiences with chronic HD, dietary sodium restriction and ultrafiltration were the mainstay of treatment, to manage BP and ECV overload.<sup>2</sup> Single center studies conducted in Tassin, France, demonstrated optimal BP control by a strict dietary sodium restriction regimen and an extended HD treatment duration.<sup>3</sup> Furthermore, high dietary sodium intake has been associated with greater mortality in prevalent HD patients.<sup>4</sup>

Our understanding of sodium metabolism has changed significantly over the past twenty years. Excess body sodium is stored in an osmotically inactive form in the skeleton and soft tissues.<sup>5</sup> The skin acts as a major extracellular sodium reservoir: sodium is bound to negatively-charged proteoglycans, inactivating the osmotic effects of excess sodium and preventing ECV expansion.<sup>6</sup> Local macrophages regulate skin sodium clearance by VEGF-C-mediated lymphangiogenesis, a significant extrarenal mechanism for the regulation of BP and ECV.<sup>7</sup>

Estimating dietary sodium intake remains a major challenge in clinical practice due to the limitations associated with a urinary sodium excretion-based approach.<sup>8</sup> In addition, quantification of sodium deposition within the body has not been possible with clinically available imaging techniques until recently.

Sodium-23 Magnetic Resonance Imaging (<sup>23</sup>Na MRI) allows direct visualization of sodium signal at the tissue level. Kopp and colleagues validated this technique and have shown its feasibility in humans by acquiring images of the lower leg by measuring directly tissue [Na<sup>+</sup>] in the skin and the muscles.<sup>9</sup>

At present, several basic clinical questions still remain unanswered. Firstly, tissue [Na<sup>+</sup>] across the CKD spectrum have never been systematically explored. Secondly, the skeleton has been identified as a significant sodium reservoir,<sup>10</sup> but this compartment has never been investigated with <sup>23</sup>Na MRI in CKD or dialysis patients- potentially particularly important given the well-recognized association between disturbances of skeletal metabolism and cardiovascular outcomes in CKD . Finally, no study has investigated the correlations between tissue [Na<sup>+</sup>] and standard clinical biomarkers in CKD patients.

The aims of this study were to explore the differences in tissue [Na<sup>+</sup>] between healthy controls, CKD stage 3-5, HD and PD patients, to explore the associations of tissue sodium with standard

blood-based biomarkers and to assess the reproducibility of tissue  $[\text{Na}^+]$  measurements by  $^{23}\text{Na}$  MRI.

## **2.2 Materials and Methods**

### *Study Design*

This was a pilot cross-sectional cohort study. Study participants belonged to four different cohorts: healthy controls, CKD stage 3 to 5 not on dialysis, chronic thrice-weekly HD, and PD. Each study participant underwent a study visit during which baseline clinical and demographic information, blood tests, and proton and  $^{23}\text{Na}$  MRI scan of the right or left lower leg were acquired. HD patients were scanned on a non-dialysis day, during either the long or short interdialytic interval.

This study was approved by the University of Western Ontario Health Sciences Research Ethics Board and was conducted in compliance with the approved protocol, Good Clinical Practice Guidelines and all applicable regulatory requirements.

### *Subjects*

Healthy subjects were recruited from London, Canada; study patients were recruited from the London Health Sciences Centre Regional Renal Program. All participants were 18 years or older and provided written informed consent. Healthy controls lacked any history of kidney disease, heart failure, liver cirrhosis or peripheral edema. CKD patients were stage 3-5 according to KDIGO guidelines,<sup>11</sup> and had no indications to start dialysis. Both HD and PD had been established on their respective dialysis modality for at least 3 months. Subjects were excluded if they were pregnant, breast-feeding, intending pregnancy, unable to provide consent, or if they had any contraindication to MRI studies.

### *Biochemical Measurements*

Plasma, serum and blood specimens from each subject were collected, processed and analyzed in a central laboratory (London Health Sciences Centre, London, Canada) for routine clinical

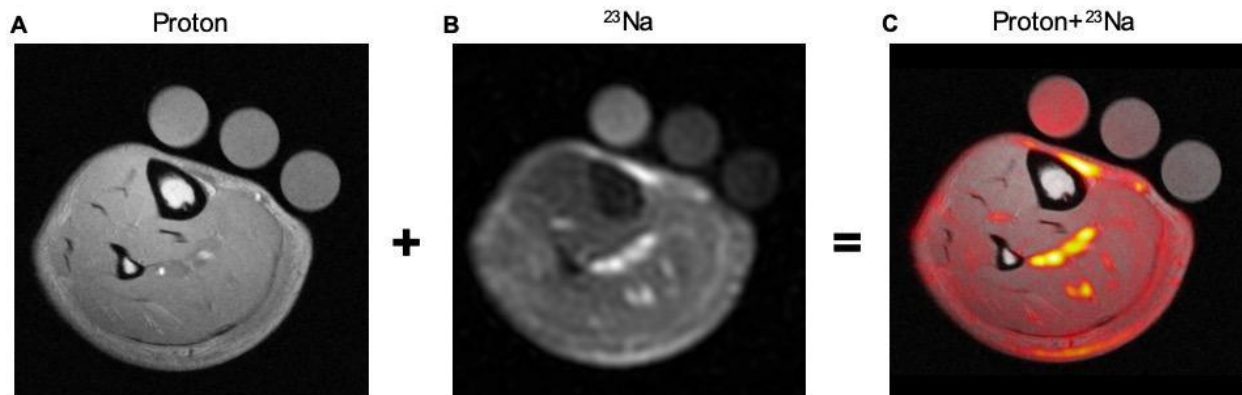
biochemistry. eGFR was estimated using the Chronic Kidney Disease Epidemiology Collaboration formula.<sup>12</sup>

### *<sup>23</sup>Na MRI Acquisition and Quantification of Tissue [Na<sup>+</sup>]*

To measure tissue [Na<sup>+</sup>] in the lower leg tissues non-invasively, a multinuclear-capable 3.0-T MRI (Discovery MR750, General Electric Healthcare, Milwaukee WI) was used to acquire proton and sodium images. Subjects were positioned supine in the magnet bore with the thickest part of their right, otherwise left, calf muscle at the center of a custom-made <sup>23</sup>Na birdcage radiofrequency (RF) coil. Calibration vials with 10, 20 and 40 mmol/L of saline were placed in the RF coil, over the subjects' shins. Axial proton T1-weighted Spoiled Gradient Recalled Echo (SPGR) sequences were acquired to delineate the anatomy of the lower leg. A single-slice <sup>23</sup>Na MR image was obtained with <sup>23</sup>Na-optimized pulse sequence, with the following parameters: slice-selective RF pulse with a 90° flip angle, TR/TE: 100/1.2ms, total acquisition time: 30min, number of signal averaging: 100, slice-thickness: 30mm, and isotropic field of view/resolution: 18/0.3cm<sup>2</sup>.

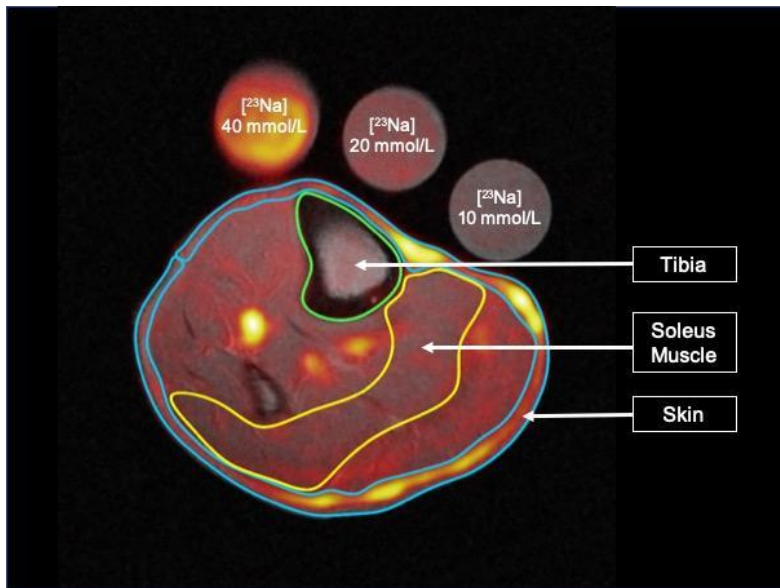
Maps of tissue [Na<sup>+</sup>] were generated using an in-house software developed within Matlab (Mathworks, Natick, USA, R2018a). [Na<sup>+</sup>] maps were superimposed with the proton-anatomy images to delineate the regions of interest (Figure 2.1).

Figure 2.1: Schematic summary of proton (Panel A) and  $^{23}\text{Na}$  MRI (Panel B) acquisition. Proton and  $^{23}\text{Na}$  images are acquired separately and superimposed (Panel C) after acquisition for software analysis.



Three regions of interest (ROIs) were drawn, using OsiriX Lite (Version 10.0.5) software, highlighting different tissues: 1) skin, 2) soleus muscle, and 3) tibial bone (Figure 2.2). Skin, soleus, and tibial  $[\text{Na}^+]$  in the ROIs were recorded for analysis.

Figure 2.2: Superimposed Proton and  $^{23}\text{Na}$  MRI of the leg for the anatomical selection of Regions of Interest (Tibia, Soleus Muscle, Skin). The different Regions of Interest are represented by different colored sections.



### Data Analysis

Statistical analysis was performed using GraphPad Prism version 8.0.0 for Windows/Mac OS X (GraphPad Software, San Diego, California USA, [www.graphpad.com](http://www.graphpad.com)) and SPSS version 23.0 (IBM Corp. Released 2015. IBM SPSS Statistics for Windows. Armonk, NY: IBM Corp). Normal distribution was assessed using the Shapiro-Wilk test. Continuous variables were presented as mean (standard deviation or range) if normally distributed and median (interquartile range) if non-normally distributed. Categorical variables were expressed as percentages. Comparisons between continuous variables were assessed with the appropriate parametric and nonparametric tests. Fisher's exact tests was used to compare categorical variables. Correlations were assessed by calculating Pearson correlation coefficient ( $r$ ) for normally distributed variables and Spearman correlation coefficient ( $\rho$ ) for non-normally distributed variables; 95% confidence intervals were computed and a p-value of  $<0.05$  was considered statistically significant. The Bonferroni

correction was performed to control for type 1 errors when performing repeated correlations for each given dependent variable.

Measures of effect size were also calculated. Cohen's  $d$  was calculated for power size calculation for all tissue  $[Na^+]$ ; Cliff's delta was calculated as a non-parametric effect size measure for skin  $[Na^+]$ . We performed sample size calculation for future studies; a power of 80%, with a two-sided level of significance equal to 0.05 was selected.

Interobserver variability was calculated between three independent raters (FRS, LH, JP). The intraclass correlation coefficient was computed for each region of interest (skin, soleus, and tibia) by using the two-way mixed model for single measures and absolute agreement.

## 2.3 Results

### *Baseline Characteristics and Medications*

The CKD group consisted of stage 3a (n=1), stage 3b (n=2), CKD stage 4 (n=5), CKD stage 5 (n=4). The HD group included n=13 subjects, with mean HD length 3.8 hours (range 3-4.5 hours) per session, mean dialysate sodium 139.5 mmol/L (range 136-145 mmol/L), mean dialysate potassium 2.1 mmol/L (range 1.5-3.0 mmol/L) and a dialysate calcium of 1.25 mmol/L. The PD group included n=10 subjects on: continuous ambulatory PD (n=2), automated PD (n=5), nocturnal intermittent PD (n=3), with mean total fluid dwell 9,475 ml/day (range 6,000-11,500 ml/day). Glucose-based solutions contained a  $[Na^+]$  of 132 mmol/L, while icodextrin-based solutions contained 133 mmol/L.

Table 2.1 shows baseline demographics, comorbidities, etiology of kidney disease, and medications in the four groups. Mean age and sex distribution were comparable across all groups. Body weight (p=0.02) and BMI (p=0.05) were significantly different. Mean dialysis vintage did not differ significantly between HD and PD (p=0.24). eGFR was significantly lower in CKD patients vs controls (CKD:  $23.1 \pm 11.8$  ml/min/1.73m<sup>2</sup>; Controls:  $88.1 \pm 16.1$  ml/min/1.73m<sup>2</sup>, p<0.0001) and PD patients had significantly higher residual urinary volume vs HD (HD: 100 ml/24h, IQR 0-285 ml/24h; PD: 1125 ml/24h, IQR 450-1,700 ml/24h, p=0.0002). The prevalence of hypertension was significantly different between groups (p<0.0001); no significant differences were observed in the prevalence of other reported comorbidities.

A significant difference in prescribed medications was observed between groups:  $\beta$ -blocker, calcium channel blocker and diuretics (p-values: 0.002, 0.03, and <0.0001, respectively). Of note, all PD patients were on loop diuretic therapy.

Table 2.1: Baseline characteristics in the four groups (Controls, CKD, HD, PD).

Characteristics	Control (n=10)	CKD (n=12)	HD (n=13)	PD (n=10)	p-value
<i>Demographics &amp; Anthropometrics</i>					
Age, years, mean (SD)	53.3 (19.5)	66.3 (6.7)	62.5 (9.1)	60.3 (10.2)	0.17
Sex (Male/Female)	4/6	8/4	9/4	5/5	0.45
Weight, kg, mean (SD)	70.5 (8.2)	88.5 (18.6)	83.9 (22.6)	83.1 (13.0)	0.02
Height, cm, mean (SD)	167.3 (7.0)	166.4 (8.9)	171.2 (7.5)	170.3 (8.4)	0.40
BMI, kg/m <sup>2</sup> , mean (SD)	25.2 (2.7)	31.7 (4.5)	28.4 (7.0)	28.8 (5.0)	0.05
eGFR, ml/min/1.73m <sup>2</sup> , mean (SD)	88.1 (16.1)	23.1 (11.8)	-	-	<0.0001
Residual Urinary Volume ml/24h, median (IQR)	-	-	100 (0, 285)	1125 (450, 1700)	0.0002
Dialysis Vintage, months, median (IQR)	-	-	37.0 (13.0, 63.0)	22.5 (15.6, 61.0)	0.24
spKt/V, median (IQR)	-	-	1.48 (1.45, 1.89)	-	-
Weekly Kt/V, median (IQR)	-	-	-	1.99 (1.60, 2.79)	-
<i>Comorbidities</i>					
Hypertension, %	10.0	91.7	100.0	70.0	<0.0001
Coronary Artery Disease, %	0	16.7	30.8	10.0	0.22
Cerebrovascular Disease, %	0	16.7	15.4	10.0	0.60
Peripheral Vascular Disease, %	0	8.3	15.4	10.0	0.64
Congestive Heart Failure, %	0	0	30.8	20.0	0.07
Diabetes Mellitus, %	10.0	58.3	46.2	40.0	0.13
COPD, %	0	0	23.1	10.0	0.17
<i>Etiology of Kidney Disease</i>					
Vascular Nephropathy, %	-	41.7	38.5	50.0	0.85
Diabetic Nephropathy, %	-	33.3	38.5	40.0	0.94
Glomerulonephritis, %	-	16.7	15.4	0	0.40
Other, %	-	41.7	30.8	30.0	0.80
<i>Medications</i>					
ACE-Inhibitor/ARB, %	10.0	58.3	30.8	30.0	0.12
α-blocker, %	0	16.7	23.1	20.0	0.46
β-blocker, %	0	66.7	76.9	50.0	0.002
Calcium Channel Blocker, %	0	41.7	46.2	60.0	0.03

Diuretic, %	10.0	66.7	23.1	100.0	<0.0001
ESA, %	-	25.0	69.2	50.0	0.17

*ACE: angiotensin-converting enzyme; ARB: angiotensin-receptor blocker; CKD: chronic kidney disease; COPD: chronic obstructive pulmonary disease; eGFR: estimated glomerular filtration rate; ESA: erythropoiesis-stimulating agent; HD: hemodialysis; spKt/V: single pool Kt/V; IQR: interquartile range; PD: peritoneal dialysis; SD: standard deviation.*

Table 2.2 shows biomarker levels in the different groups. 1,25-OH Vitamin D, Albumin and Hemoglobin levels were significantly lower in HD and PD patients relative to Controls ( $p < 0.0001$ ). Conversely, no significant difference was observed in 25-OH Vitamin D. A statistically significant increase in c-reactive protein and PTH was observed both in HD and PD groups relative to Controls.

*Table 2.2: Biomarker levels in the four groups (Controls, CKD, HD, PD).*

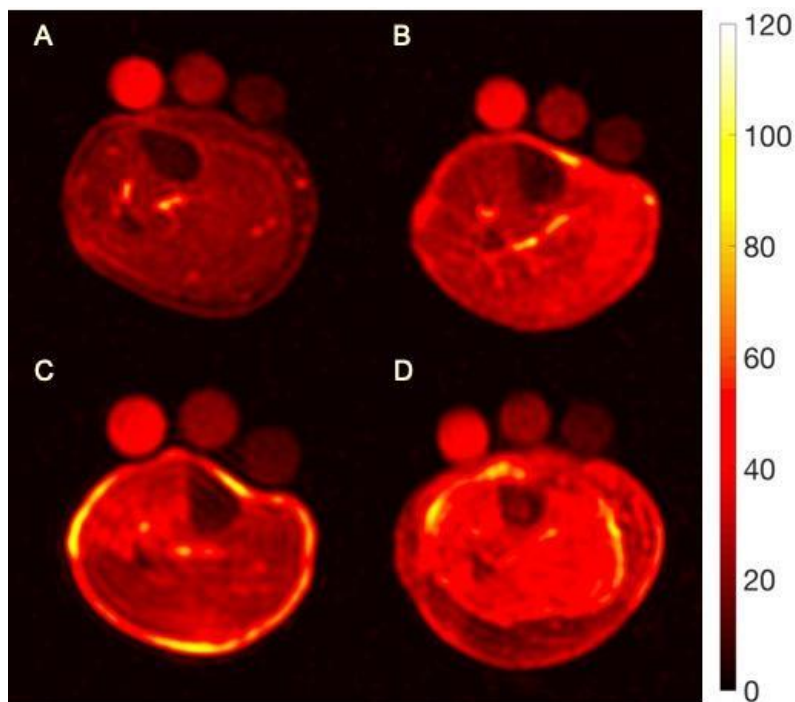
	<b>Control (n=10)</b>	<b>CKD (n=12)</b>	<b>HD (n=13)</b>	<b>PD (n=10)</b>	<b>p-value</b>
<b><i>Biomarkers</i></b>					
1,25 Vitamin D, pmol/L, mean (SD)	98.6 (28.4)	77.0 (32.5)	23.0 (9.8)	23.9 (14.3)	<0.0001
25 Vitamin D, nmol/L, mean (SD)	55.6 (36.3)	67.3 (27.5)	61.2 (34.4)	40.9 (28.7)	0.10
Albumin, g/L, mean (SD)	43.7 (2.5)	43.3 (2.4)	41.2 (3.6)	36.7 (4.0)	0.0008
C-Reactive Protein mg/L, median (IQR)	0.7 (0.6, 4.9)	2.1 (0.6, 5.2)	8.0 (2.4, 17.6)	8.7 (5.3, 12.9)	0.0007
Hemoglobin, g/L, mean (SD)	142.9 (12.8)	117.3 (22.7)	120.3 (15.2)	104.0 (12.6)	<0.0001
PTH, pmol/L, mean (SD)	4.5 (1.2)	18.8 (16.9)	44.8 (42.9)	35.9 (38.7)	0.001

*CKD: chronic kidney disease; HD: hemodialysis; IQR: interquartile range; PD: peritoneal dialysis; SD: standard deviation.*

## <sup>23</sup>Na MRI Analysis

Figure 2.3 shows sample <sup>23</sup>Na MR images of the leg from the four patient groups: a qualitative difference in sodium signal can be observed mainly in the skin and muscles, with HD and PD showing the most evident differences.

Figure 2.3: Sample <sup>23</sup>Na MR images of the leg in 4 sample subjects from each group. The color bar on the right represents [Na<sup>+</sup>] in mmol/L. Panel A: Healthy control. Panel B: CKD patient. Panel C: HD patient. Panel D: PD patient. The images show a progressive increase in the sodium signal eminently in the skin and in the muscle, especially evident in Panels C and D. A notable increase in tibial sodium can be observed in Panel D.



Tissue [Na<sup>+</sup>] in the four groups are listed in Table 2.3.

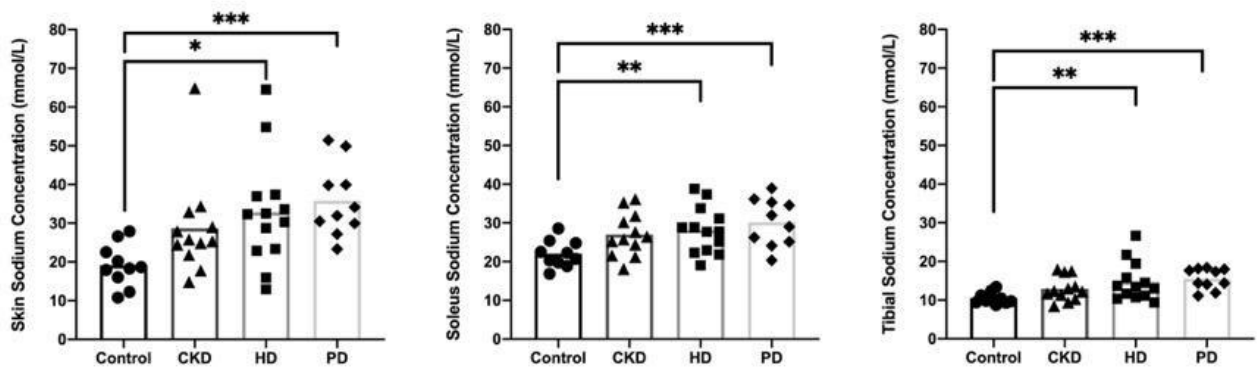
Table 2.3: Tissue [Na<sup>+</sup>] in the four groups (Controls, CKD, HD, PD). Data presented as mean (SD)

	Control (n=10)	CKD (n=12)	HD (n=13)	PD (n=10)
Skin [Na <sup>+</sup> ] (mmol/L)	19.1 (5.5)	28.7 (12.7)	32.8 (14.2)	35.8 (9.3)
Soleus [Na <sup>+</sup> ] (mmol/L)	22.0 (3.5)	27.0 (5.6)	28.1 (6.0)	30.2 (6.1)

<b>Tibial [Na<sup>+</sup>] (mmol/L)</b>	10.5 (1.5)	12.9 (3.2)	14.7 (5.1)	15.5 (2.7)
---	------------	------------	------------	------------

Figure 2.4 shows a statistically significant increase in skin, soleus and tibial [Na<sup>+</sup>] (Panel A, B, C respectively) in HD and PD vs controls. Multiple comparisons did not demonstrate statistically significant differences in the CKD vs other groups, nor in HD vs PD. However, a trend towards a progressive increase in [Na<sup>+</sup>] is evident in all compartments, with PD showing the highest [Na<sup>+</sup>].

Figure 2.4: Between group comparison in mean Tissue [Na<sup>+</sup>] (Skin, panel A; Soleus, panel B; Tibia, panel C).



\* $p < 0.01$  \*\* $p < 0.001$  \*\*\* $p < 0.0001$

## Correlation Analysis

Tables 2.4 to 2.7 show the correlations between tissue [Na<sup>+</sup>] with biomarker levels, demographics and anthropometrics in controls, CKD, HD and PD, respectively.

In healthy controls (Table 2.4), skin [Na<sup>+</sup>] was positively associated with age ( $r=0.67$ ,  $p=0.03$ ), BMI ( $r=0.83$ ,  $p<0.01$ ) and weight ( $r=0.69$ ,  $p=0.03$ ). Soleus [Na<sup>+</sup>] was also positively associated with age ( $r=0.84$ ,  $p<0.01$ ). Among the biomarkers, only a statistically significant negative association was observed between serum albumin and tibial [Na<sup>+</sup>] ( $r=-0.66$ ,  $p=0.04$ ).

Table 2.4: Correlation analysis between skin, soleus and tibial [Na<sup>+</sup>] with demographics, anthropometrics and biomarkers in the control group.

	Skin [Na <sup>+</sup> ] (mmol/L) <i>r</i> (95% CI)	<i>p</i> -value	Soleus [Na <sup>+</sup> ] (mmol/L) <i>r</i> (95% CI)	<i>p</i> -value	Tibial [Na <sup>+</sup> ] (mmol/L) <i>r</i> (95% CI)	<i>p</i> -value
<b>Demographics &amp; Anthropometrics</b>						
Age (years)	0.67 (0.07 to 0.91)	0.03	0.84 (0.43 to 0.96)	<0.01	0.56 (-0.11 to 0.88)	0.09
BMI (kg/m <sup>2</sup> )	0.83 (0.43 to 0.96)	<0.01	0.38 (-0.32 to 0.82)	0.27	0.34 (-0.37 to 0.80)	0.34
Height (cm)	-0.08 (-0.68 to 0.58)	0.82	-0.20 (-0.73 to 0.50)	0.59	-0.13 (-0.70 to 0.54)	0.72
Weight (kg)	0.69 (0.10 to 0.92)	0.03	0.20 (-0.49 to 0.74)	0.57	0.20 (-0.49 to 0.74)	0.58
<b>Biomarkers</b>						
1,25 Vitamin D (pmol/L)	-0.01 (-0.63 to 0.63)	0.98	-0.44 (-0.84 to 0.26)	0.20	-0.43 (-0.83 to 0.27)	0.21
25 Vitamin D (nmol/L)	-0.02 (-0.64 to 0.62)	0.96	0.14 (-0.53 to 0.71)	0.71	0.02 (-0.62 to 0.64)	0.96
Albumin (g/L)	-0.28 (-0.77 to 0.42)	0.43	-0.50 (-0.86 to 0.18)	0.14	-0.66 (-0.91 to -0.06)	0.04
C-Reactive Protein (mg/L)	0.67 (N/A) <sup>‡</sup>	0.08	0.70 (N/A) <sup>‡</sup>	0.07	0.13 (N/A) <sup>‡</sup>	0.76
eGFR (ml/min/1.73m <sup>2</sup> )	0.33 (-0.38 to 0.79)	0.36	-0.32 (-0.79 to 0.38)	0.36	-0.05 (-0.66 to 0.60)	0.89
Hemoglobin (g/L)	0.40 (-0.31 to 0.82)	0.26	-0.04 (-0.65 to 0.60)	0.90	-0.18 (-0.73 to 0.51)	0.63
PTH (pmol/L)	0.37 (-0.39 to 0.83)	0.33	0.01 (-0.66 to 0.67)	0.99	-0.21 (-0.77 to 0.53)	0.58

<sup>‡</sup> Spearman's correlation coefficient

In CKD patients (Table 2.5), height was negatively associated with soleus and tibial sodium concentration ( $r=-0.69$ ,  $p=0.01$  and  $r=-0.60$ ,  $p=0.04$ , respectively), whereas weight was negatively associated with soleus sodium concentration alone ( $r=-0.59$ ,  $p=0.04$ ). Among the biomarkers, serum albumin was negatively associated with skin sodium concentration ( $r=-0.60$ ,  $p=0.04$ ); hemoglobin was negatively associated with both soleus and tibial sodium concentration ( $r=-0.65$ ,  $p=0.02$  and  $r=-0.73$ ,  $p<0.01$ , respectively). In addition, a non-statistically significant negative correlation between eGFR with soleus and tibial sodium concentration was observed (Soleus:  $r=-0.45$ ,  $p=0.14$ ; tibia:  $r=-0.44$ ,  $p=0.15$ ).

Table 2.5: Correlation analysis between skin, soleus and tibial sodium concentration with demographics, anthropometrics and biomarkers in the CKD group.

	Skin [Na <sup>+</sup> ] (mmol/L) <i>r</i> (95% CI)	<i>p</i> - value	Soleus [Na <sup>+</sup> ] (mmol/L) <i>r</i> (95% CI)	<i>p</i> - value	Tibial [Na <sup>+</sup> ] (mmol/L) <i>r</i> (95% CI)	<i>p</i> -value
<b>Demographics &amp; Anthropometrics</b>						
Age (years)	0.16 (-0.47 to 0.68) <sup>‡</sup>	0.62	-0.02 (-0.59 to 0.56)	0.95	-0.42 (-0.80 to 0.20)	0.17
BMI (kg/m <sup>2</sup> )	0.20 (-0.44 to 0.71) <sup>‡</sup>	0.53	-0.39 (-0.79 to 0.24)	0.21	-0.28 (-0.74 to 0.35)	0.38
Height (cm)	-0.31 (-0.76 to 0.34) <sup>‡</sup>	0.32	-0.69 (-0.91 to -0.19)	0.01	-0.60 (-0.87 to -0.04)	0.04
Weight (kg)	0.00 (-0.59 to 0.59) <sup>‡</sup>	1.00	-0.59 (-0.87 to -0.03)	0.04	-0.48 (-0.82 to 0.13)	0.12
<b>Biomarkers</b>						
1,25 Vitamin D (pmol/L)	0.41 (-0.28 to 0.82) <sup>‡</sup>	0.22	-0.09 (-0.66 to 0.56) <sup>‡</sup>	0.80	-0.42 (-0.82 to 0.26) <sup>‡</sup>	0.19
25 Vitamin D (nmol/L)	0.01 (-0.58 to 0.60) <sup>‡</sup>	0.97	0.35 (-0.28 to 0.77)	0.26	0.19 (-0.43 to 0.69)	0.17
Albumin (g/L)	-0.60 (-0.88 to 0.02) <sup>‡</sup>	0.04	-0.47 (-0.83 to 0.16) <sup>‡</sup>	0.13	0.00 (-0.59 to 0.59) <sup>‡</sup>	1.00
C-Reactive Protein (mg/L)	0.28 (-0.37 to 0.75) <sup>‡</sup>	0.37	-0.04 (-0.61 to 0.56) <sup>‡</sup>	0.90	0.05 (-0.55 to 0.62) <sup>‡</sup>	0.89
eGFR (ml/min/1.73m <sup>2</sup> )	-0.06 (-0.62 to 0.55) <sup>‡</sup>	0.87	-0.45 (-0.81 to 0.17)	0.14	-0.44 (-0.81 to 0.18)	0.15
Hemoglobin (g/L)	-0.12 (-0.66 to 0.50) <sup>‡</sup>	0.48	-0.65 (-0.89 to -0.13)	0.02	-0.73 (-0.91 to -0.26)	<0.01
PTH (pmol/L)	-0.34 (-0.77 to 0.31) <sup>‡</sup>	0.29	0.29 (-0.36 to 0.74) <sup>‡</sup>	0.37	0.53 (-0.08 to 0.85) <sup>‡</sup>	0.08

<sup>‡</sup> Spearman's correlation coefficient

In HD patients (Table 2.6), age was positively correlated with skin [Na<sup>+</sup>], although the association did not quite reach statistical significance ( $r=0.53$ ,  $p=0.06$ ). Among the biomarkers, serum albumin was negatively associated with both soleus and tibial [Na<sup>+</sup>] ( $r=-0.81$ ,  $p<0.01$  and  $r=-0.78$ ,  $p<0.01$ , respectively); hemoglobin was negatively associated with [Na<sup>+</sup>] in all tissues, although it did not reach statistical significance in the soleus (skin  $r=-0.60$ ,  $p=0.04$ , soleus  $r=-0.55$ ,  $p=0.06$ , tibia  $r=-0.76$ ,  $p<0.01$ ).

Table 2.6: Correlation analysis between skin, soleus and tibial [Na<sup>+</sup>] with demographics, anthropometrics and biomarkers in the HD group.

	Skin [Na <sup>+</sup> ] (mmol/L) <i>r</i> (95% CI)	<i>p</i> - value	Soleus [Na <sup>+</sup> ] (mmol/L) <i>r</i> (95% CI)	<i>p</i> - value	Tibial [Na <sup>+</sup> ] (mmol/L) <i>r</i> (95% CI)	<i>p</i> - value
<b>Demographics &amp; Anthropometrics</b>						
Age (years)	0.53 (-0.02 to 0.84)	0.06	0.33 (-0.27 to 0.74)	0.27	0.24 (-0.37 to 0.71) <sup>‡</sup>	0.43
BMI (kg/m <sup>2</sup> )	0.23 (-0.36 to 0.70)	0.44	-0.01 (-0.56 to 0.54)	0.96	0.14 (-0.46 to 0.65) <sup>‡</sup>	0.66
Dialysis Vintage (months)	-0.09 (-0.61 to 0.48)	0.77	0.23 (-0.37 to 0.69)	0.46	0.17 (-0.43 to 0.67) <sup>‡</sup>	0.58
Height (cm)	-0.14 (-0.64 to 0.44)	0.64	-0.48 (-0.82 to 0.09)	0.09	-0.38 (-0.77 to 0.22) <sup>‡</sup>	0.20
Residual Urinary Volume (ml/24h)	0.01 (-0.56 to 0.57) <sup>‡</sup>	0.97	0.07 (-0.51 to 0.61) <sup>‡</sup>	0.82	0.52 (-0.06 to 0.84) <sup>‡</sup>	0.07
spKt/V	0.29 (-0.33 to 0.73) <sup>‡</sup>	0.33	0.00 (-0.56 to 0.57) <sup>‡</sup>	1.00	0.03 (-0.54 to 0.58) <sup>‡</sup>	0.92
Weight (kg)	0.13 (-0.46 to 0.63)	0.68	-0.19 (-0.67 to 0.41)	0.54	0.03 (-0.54 to 0.59) <sup>‡</sup>	0.92
<b>Biomarkers</b>						
1,25 Vitamin D (pmol/L)	-0.24 (-0.78 to 0.50)	0.53	0.24 (-0.50 to 0.78)	0.52	-0.25 (N/A) <sup>‡</sup>	0.51
25 Vitamin D (nmol/L)	-0.40 (-0.79 to 0.22)	0.19	0.02 (-0.56 to 0.59)	0.94	-0.02 (-0.60 to 0.57) <sup>‡</sup>	0.95
Albumin (g/L)	-0.07 (-0.64 to 0.55)	0.83	-0.81 (-0.95 to -0.40)	<0.01	-0.78 (-0.94 to -0.32) <sup>‡</sup>	<0.01
C-Reactive Protein (mg/L)	0.18 (-0.45 to 0.69) <sup>‡</sup>	0.57	-0.27 (-0.74 to 0.37) <sup>‡</sup>	0.39	0.28 (-0.37 to 0.74) <sup>‡</sup>	0.38
Hemoglobin (g/L)	-0.60 (-0.87 to -0.04)	0.04	-0.55 (-0.86 to 0.03)	0.06	-0.76 (-0.93 to -0.32) <sup>‡</sup>	<0.01
PTH (pmol/L)	0.27 (-0.37 to 0.74) <sup>‡</sup>	0.39	-0.49 (-0.14 to 0.84) <sup>‡</sup>	0.11	0.57 (-0.03 to 0.87) <sup>‡</sup>	0.06

‡ Spearman's correlation coefficient

In PD patients (Table 2.7), age was positively correlated with soleus [Na<sup>+</sup>] (r=0.66, p=0.05).

Among the biomarkers, albumin showed a negative correlation with soleus [Na<sup>+</sup>] (r=-0.65, p=0.04); PTH showed a positive correlation with tibial [Na<sup>+</sup>] (r=0.68, p=0.04).

Table 2.7: Correlation analysis between skin, soleus and tibial [Na<sup>+</sup>] with biomarkers and demographics in the PD group.

	Skin [Na <sup>+</sup> ] (mmol/L) r (95% CI)	p-value	Soleus [Na <sup>+</sup> ] (mmol/L) r (95% CI)	p-value	Tibial [Na <sup>+</sup> ] (mmol/L) r (95% CI)	p-value
<b>Demographics &amp; Anthropometrics</b>						
Age (years)	0.30 (N/A) ‡	0.40	0.66 (N/A) ‡	0.05	-0.08 (N/A) ‡	0.84
BMI (kg/m <sup>2</sup> )	-0.21 (-0.74 to 0.48)	0.56	0.36 (-0.35 to 0.80)	0.31	0.11 (-0.56 to 0.69)	0.77
Dialysis Vintage (months)	-0.61 (N/A) ‡	0.06	0.00 (N/A) ‡	1.00	0.25 (N/A) ‡	0.48
Height (cm)	-0.17 (-0.72 to 0.51)	0.63	-0.51 (-0.86 to 0.17)	0.13	-0.36 (-0.81 to 0.35)	0.30
Residual Urinary Volume (ml/24h)	-0.33 (-0.79 to 0.37)	0.35	-0.22 (-0.75 to 0.48)	0.55	0.06 (-0.59 to 0.66)	0.87
Weekly Kt/V	-0.19 (-0.73 to 0.50)	0.59	0.06 (-0.59 to 0.67)	0.86	0.17 (-0.52 to 0.72)	0.64
Weight (kg)	-0.34 (-0.80 to 0.36)	0.33	0.05 (-0.60 to 0.66)	0.90	-0.11 (-0.56 to 0.69)	0.74
<b>Biomarkers</b>						
1,25 Vitamin D (pmol/L)	-0.12 (N/A) ‡	0.77	0.39 (N/A) ‡	0.30	0.42 (N/A) ‡	0.26
25 Vitamin D (nmol/L)	0.35 (N/A) ‡	0.33	0.39 (N/A) ‡	0.27	0.29 (N/A) ‡	0.42
Albumin (g/L)	-0.49 (-0.85 to 0.20)	0.15	-0.65 (-0.91 to -0.04)	0.04	-0.45 (-0.84 to 0.26)	0.20
C-Reactive Protein (mg/L)	-0.35 (N/A) ‡	0.33	-0.15 (N/A) ‡	0.68	0.09 (N/A) ‡	0.81
Hemoglobin (g/L)	-0.33 (-0.80 to 0.38)	0.35	-0.34 (-0.80 to 0.37)	0.34	-0.14 (-0.71 to 0.54)	0.70
PTH (pmol/L)	0.07 (N/A) ‡	0.84	0.13 (N/A) ‡	0.71	0.68 (N/A) ‡	0.04

‡ Spearman's correlation coefficient

Table 2.8 shows the results of the statistically significant correlations from Tables 2.4-2.7 after Bonferroni correction. Only BMI vs Skin [Na<sup>+</sup>] (Control), Age vs Soleus [Na<sup>+</sup>] (Control) and Albumin vs Soleus [Na<sup>+</sup>] (HD) remained statistically significant after correction.

Table 2.8: Bonferroni correction for significant findings.

Group	Dependent variable	Independent variable	<i>r</i> (95% CI)	<i>p</i> -value	Bonferroni's $\alpha$	Significance
Controls	Skin [Na <sup>+</sup> ]	BMI	0.83 (0.43 to 0.96)	0.0027	0.0045	Yes
Controls	Skin [Na <sup>+</sup> ]	Age	0.67 (0.07 to 0.91)	0.0331	0.0045	No
Controls	Soleus [Na <sup>+</sup> ]	Age	0.84 (0.43 to 0.96)	0.0026	0.0045	Yes
CKD	Soleus [Na <sup>+</sup> ]	Hemoglobin	-0.65 (-0.89 to -0.13)	0.0211	0.0045	No
CKD	Tibial [Na <sup>+</sup> ]	Hemoglobin	-0.73 (-0.91 to -0.26)	0.0073	0.0045	No
HD	Skin [Na <sup>+</sup> ]	Hemoglobin	-0.60 (-0.87 to -0.04)	0.0379	0.0038	No
HD	Soleus [Na <sup>+</sup> ]	Albumin	-0.81 (-0.95 to -0.40)	0.0027	0.0038	Yes
HD	Tibial [Na <sup>+</sup> ]	Albumin	-0.78 (-0.94 to -0.32) ‡	0.0063	0.0038	No
HD	Tibial [Na <sup>+</sup> ]	Hemoglobin	-0.76 (-0.93 to -0.32) ‡	0.0052	0.0038	No
PD	Tibial [Na <sup>+</sup> ]	PTH	0.68 (N/A) ‡	0.0355	0.0038	No

Figures 2.5, 2.6 and 2.7 show the main correlations of tissue [Na<sup>+</sup>] with clinical biomarkers. Figure 2.5 shows a negative, statistically significant correlation between eGFR and soleus and tibial [Na<sup>+</sup>] after merging the Control and CKD groups.

Figure 2.5: Correlation analysis for the relationship between eGFR and Skin, Soleus and Tibial [Na<sup>+</sup>] (Panels A, B and C respectively) in both Control and CKD group.

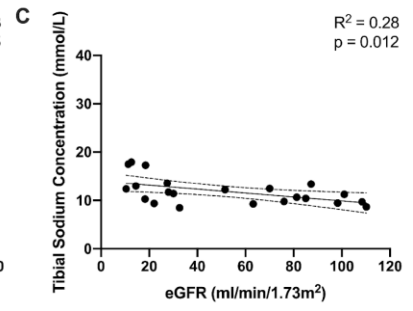
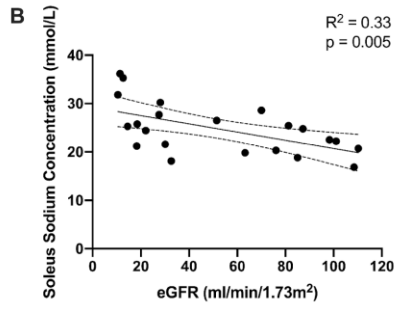
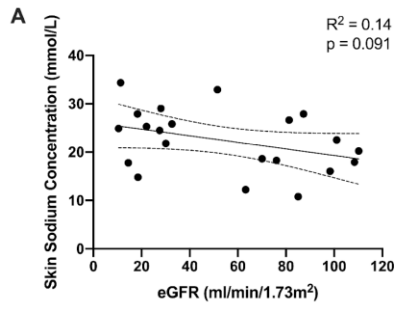


Figure 2.6 shows that hemoglobin had the strongest correlation with tibial  $[Na^+]$  in both CKD (Panel C) and HD group (Panel D).

Figure 2.6: Correlation analysis for the relationship between Hemoglobin and Soleus  $[Na^+]$  (Panels A, B), and Tibial  $[Na^+]$  (Panel C, D) in CKD and HD patients.

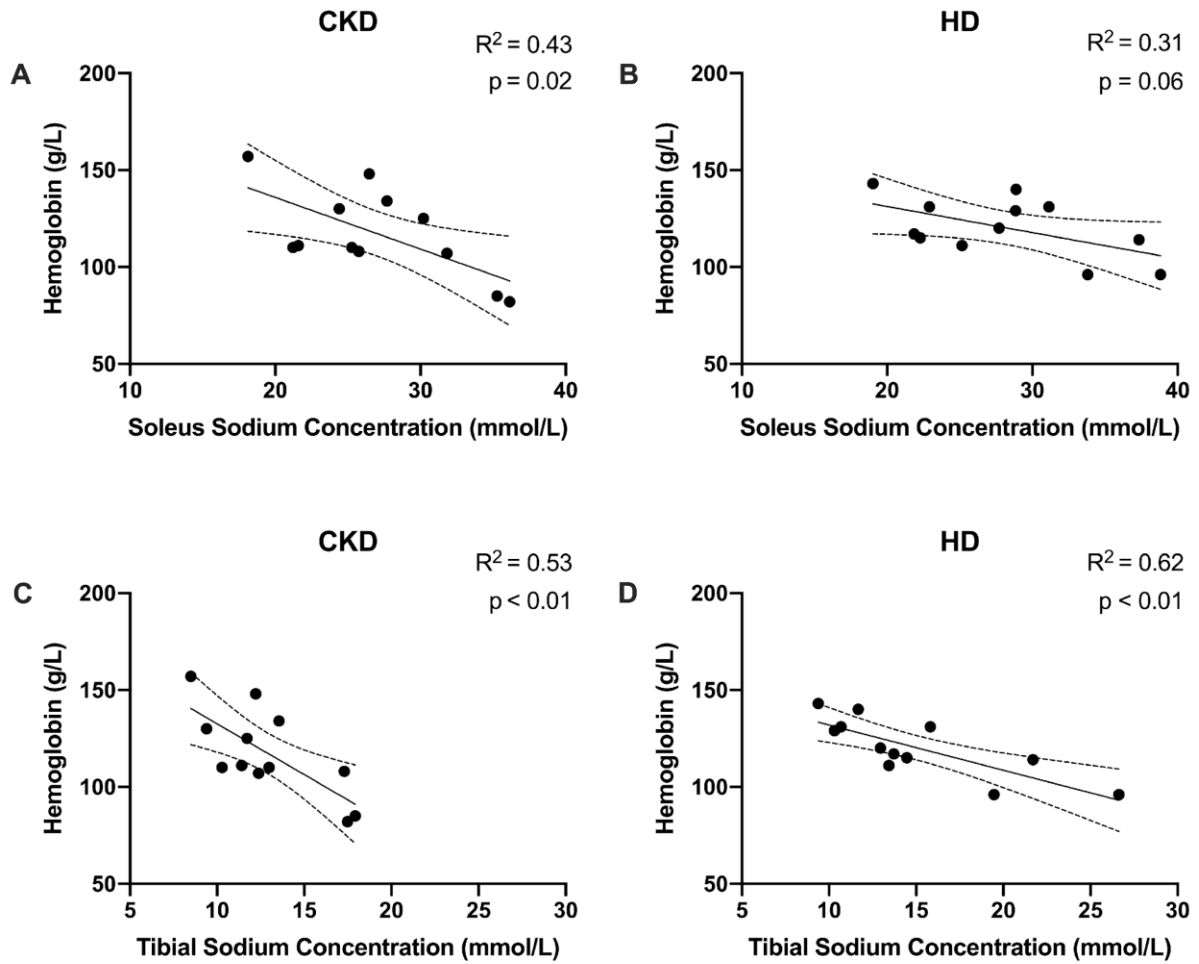
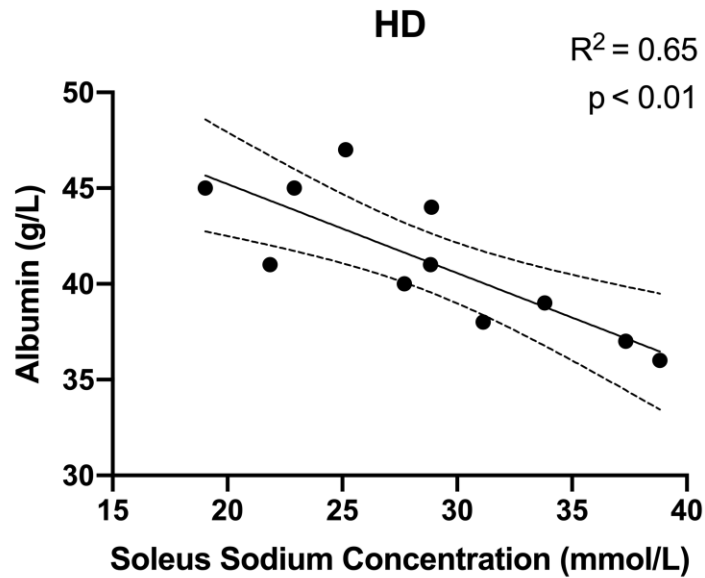


Figure 2.7 shows that albumin exhibits a strong, negative linear correlation with soleus [Na<sup>+</sup>] in the HD group.

Figure 2.7: Correlation analysis for the relationship between serum Albumin and Soleus [Na<sup>+</sup>] in HD patients.



### *Interobserver Variability*

The intraclass correlation coefficients for single measures were 0.98 ( $p < 0.0001$ ) for the skin [Na<sup>+</sup>], 0.96 ( $p < 0.0001$ ) for the soleus [Na<sup>+</sup>] and 0.88 ( $p < 0.0001$ ) for the tibial [Na<sup>+</sup>]. An intraclass correlation coefficient value of  $> 0.90$  was considered excellent, and a value between 0.75 and 0.90 was considered good.

## 2.4 Discussion

In this study, we report several novel aspects of tissue sodium deposition measured by  $^{23}\text{Na}$  MRI of the lower leg. Firstly, we systematically compared tissue  $[\text{Na}^+]$  between CKD, HD and PD patients, representing the broad clinical spectrum of CKD. Secondly, we described tissue  $[\text{Na}^+]$  in the tibial bone of CKD and dialysis patients. Finally, we showed preliminary correlations between tissue  $[\text{Na}^+]$ , demographics, anthropometrics and clinical biomarkers of renal function and inflammation.

We observed that tissue  $[\text{Na}^+]$  increases progressively in all measured compartments across the whole kidney disease spectrum, with HD and PD patients demonstrating the highest tissue  $[\text{Na}^+]$ . Although not statistically significant, healthy controls were younger when compared to CKD, HD and PD patients. This needs to be taken into account as a potential confounder, as age plays a major role in determining skin and muscle  $[\text{Na}^+]$ , as pointed out by several studies.<sup>13-15</sup>

Many other factors need to be taken into account when analyzing the differences between groups; we have shown a role of sex, diabetes and diuretic use (Table S2). In this respect, patients showing peripheral and subcutaneous edema were outliers and were excluded from the subgroup analysis. In healthy controls and CKD patients, we observed a negative correlation between eGFR and both soleus and tibial  $[\text{Na}^+]$ , suggesting that a progressive impairment in kidney function may result in increased tissue  $[\text{Na}^+]$ .

The current status of the clinical knowledge of sodium metabolism in CKD and renal replacement therapy has been recently reviewed in detail by Canaud et al.<sup>16</sup> Historically, Titze's experimental findings in rat models have clarified many of the mechanisms underlying sodium deposition in different tissues. The skin has been identified as a major site of extracellular, osmotically inactive

sodium storage in both rodents and humans.<sup>5,9</sup> In this compartment, the osmotic effects of sodium are inactivated by negatively charged proteoglycans.<sup>6</sup> Resident macrophages are able to sense local  $[Na^+]$ , and regulate skin sodium clearance by controlling lymphangiogenesis through VEGF-C secretion.<sup>17</sup> In the muscles, sodium is stored largely intracellularly via a mechanism mediated by mineralcorticoid receptors, and exchanged with intracellular potassium to maintain intracellular osmolarity.<sup>18</sup> The skeleton is another essential site of tissue sodium deposition, as suggested by Titze et al in 2002.<sup>19</sup> To our knowledge, however, the underlying mechanisms controlling this have not been elucidated.

Studies describing tissue sodium deposition and its effects in humans with CKD are limited and are dependent on direct sodium visualization with leg  $^{23}Na$  MRI. Schneider et al reported a positive correlation between skin  $[Na^+]$  and left ventricular mass, independent of BP and overhydration (by bioimpedance spectroscopy).<sup>20</sup> Dahlmann and co-workers reported higher skin and muscle  $[Na^+]$  in HD patients over 60 years, compared to age-matched healthy controls.<sup>15</sup> In addition, lower plasma levels of VEGF-C were observed in HD patients compared to controls, suggesting that HD patients have an impaired skin sodium clearance. Kopp et al also reported an increased skin and muscle  $[Na^+]$  in type 2 diabetes HD patients compared to non-diabetic HD patients, suggesting a role of insulin resistance in tissue sodium deposition.<sup>21</sup> Recent studies have also reported that skin and muscle sodium can be mobilized by clinical interventions, namely diuretic therapy in acute heart failure<sup>22</sup> and ultrafiltration in HD patients.<sup>15</sup>

A significant finding of this study is that increased muscle  $[Na^+]$  were associated with a significant reduction in serum albumin in HD patients. Serum albumin is a strong independent predictor of mortality in patients on renal replacement therapy.<sup>23,24</sup> Although the mechanisms of

hypoalbuminemia in these patients are still largely unclear,<sup>25</sup> we speculate whether elevated tissue [Na<sup>+</sup>] (directly or via inflammation) could impair albumin synthesis, in patients on renal replacement therapy.

A potential association between increased tissue [Na<sup>+</sup>] and anemia was also observed in CKD and HD patients. These associations may point out a role of sodium in regulating iron metabolism and/or erythropoiesis through inflammatory pathways, leading to erythropoiesis-stimulating agent resistance in patients on renal replacement therapy.<sup>26,27</sup> Although these findings failed to reach statistical significance after correcting for type 1 error, the novelty of this findings likely deserves further investigation in future studies.

In this study, we described several associations of tibial [Na<sup>+</sup>] with demographics, anthropometrics and other clinical biomarkers. These findings suggest that <sup>23</sup>Na MRI may expand our understanding of sodium metabolism in relationship to mineral bone disease associated with CKD. To our knowledge, however, <sup>23</sup>Na MRI-based bone [Na<sup>+</sup>] measurements currently lack a validation against gold standard techniques (such as ashing, as reported by Kopp et al).<sup>13</sup>

<sup>23</sup>Na MRI allows direct visualization and quantification of tissue sodium deposition, non-invasively and with high reproducibility. This makes it extremely interesting in the nephrology setting due to the lack of other reliable sodium quantification techniques,<sup>8,9</sup> and will likely spark new interest to monitor the effects of interventions on dietary sodium and sodium removal techniques.

In the wake of our results, we anticipate that future studies will expand in four different directions: [1] delineating the clinical associations of  $^{23}\text{Na}$  MRI-based tissue  $[\text{Na}^+]$  in CKD and renal replacement therapy patients with appropriately powered observational studies; [2] validating tissue  $[\text{Na}^+]$  with clinical outcomes; [3] perfecting and optimizing sodium removal strategies; [4] designing randomized controlled trials to test the efficacy of sodium removal.

Several limitations need to be acknowledged in this study:  $^{23}\text{Na}$  MRI remains at present confined to the research environment, and its clinical availability is limited by the cost and the technical expertise required for its development. This imaging technique is inherently burdened by low resolution (voxel size:  $3 \times 3 \times 30$  mm), resulting in partial volume effects and affecting the signal recorded from the regions of interest (e.g. skin, edema). The cross-sectional design of this study does not allow us to infer causality from correlations. Our subject sample was small; as shown by our sample size calculation, our study was underpowered to show differences in tissue  $[\text{Na}^+]$  between controls and CKD patients. Other subgroup analyses we performed likely require bigger sample sizes as well. At present the measurement of tibial  $[\text{Na}^+]$  with  $^{23}\text{Na}$  MRI lacks a clinical validation and its role remains highly speculative.

The relationship between tissue  $[\text{Na}^+]$  and BP has been the subject of several  $^{23}\text{Na}$  MRI studies. However, office BP and 24-hour ambulatory BP measurements were not consistently available in this study. Dietary sodium intake is likely a major determinant of tissue sodium deposition, detailed assessment of this though was beyond the scope of this initial study.

### *Conclusions*

This study further reinforces and expands the previously recognized role of sodium as a critical uremic toxin, accumulating in patients with reduced kidney function. Tissue  $[\text{Na}^+]$  by leg  $^{23}\text{Na}$

MRI increase progressively across the CKD spectrum, with patients on renal replacement therapy having significantly higher tissue  $[Na^+]$  compared to healthy controls. Tissue  $[Na^+]$  were correlated with well-established clinical biomarkers, suggesting several potential adverse metabolic effects of tissue sodium deposition in CKD, HD and PD patients, and deserve further investigation.  $^{23}Na$  MRI allows noninvasive, reproducible tissue sodium quantification: its application may help clinicians guide diagnostic and therapeutic decision-making in CKD and renal replacement therapy patients.

## 2.5 Bibliography

1. Kempner W. Treatment of heart and kidney disease and of hypertensive and arteriosclerotic vascular disease with the rice diet. *Ann Intern Med.* 1949;31(5):821-856. doi:10.7326/0003-4819-31-5-821
2. Scribner BH, Buri R, Caner JEZ, Hegstrom R, M BJ. The Treatment of Chronic Uremia by Means of Intermittent Hemodialysis: a Preliminary Report. *Trans Am Soc Artif Intern Organs.* 1960;6:114-122.
3. Charra B, Terrat JC, Vanel T, et al. Long thrice weekly hemodialysis: The Tassin experience. *Int J Artif Organs.* 2004;27(4):265-283.
4. Mc Causland FR, Waikar SS, Brunelli SM. Increased dietary sodium is independently associated with greater mortality among prevalent hemodialysis patients. *Kidney Int.* 2012;82(2):204-211. doi:10.1038/ki.2012.42
5. Titze J, Lang R, Ilies C, et al. Osmotically inactive skin Na<sup>+</sup> storage in rats. *Am J Physiol Physiol.* 2003;285(6):F1108-F1117. doi:10.1152/ajprenal.00200.2003
6. Titze J, Shakibaei M, Schafflhuber M, et al. Glycosaminoglycan polymerization may enable osmotically inactive Na<sup>+</sup> storage in the skin . *Am J Physiol Circ Physiol.* 2004;287(1):H203-H208. doi:10.1152/ajpheart.01237.2003
7. Titze J, Machnik A. Sodium sensing in the interstitium and relationship to hypertension. *Curr Opin Nephrol Hypertens.* 2010;19(4):385-392. doi:10.1097/MNH.0b013e32833aeb3b
8. Titze J. Estimating salt intake in humans: Not so easy! *Am J Clin Nutr.* 2017;105(6):1253-1254. doi:10.3945/ajcn.117.158147
9. Kopp C, Linz P, Wachsmuth L, et al. <sup>23</sup>Na magnetic resonance imaging of tissue sodium. *Hypertension.* 2012;59(1):167-172. doi:10.1161/HYPERTENSIONAHA.111.183517

10. Bergstrom WH. The Participation of Bone in Total Body Sodium Metabolism in the Rat. *J Clin Invest.* 1955;2(7, pt 1):997-1004. doi:10.1172/JCI103168
11. KDIGO 2012 Clinical Practice Guideline for the Evaluation and Management of Chronic Kidney Disease. *Kidney Int Suppl.* 2013;3(1):4-4. doi:10.1038/kisup.2012.76
12. Levey AS, Stevens LA, Schmid CH, et al. A New Equation to Estimate Glomerular Filtration Rate. *Ann Intern Med.* 2009;150(9):604-612. doi:10.1059/0003-4819-150-9-200905050-00006
13. Kopp C, Linz P, Wachsmuth L, et al. (23)Na magnetic resonance imaging of tissue sodium. *Hypertens (Dallas, Tex 1979).* 2012;59(1):167-172. doi:10.1161/HYPERTENSIONAHA.111.183517
14. Kopp C, Linz P, Dahlmann A, et al. <sup>23</sup>Na magnetic resonance imaging-determined tissue sodium in healthy subjects and hypertensive patients. *Hypertens (Dallas, Tex 1979).* 2013;61(3):635-640. doi:10.1161/HYPERTENSIONAHA.111.00566
15. Dahlmann A, Dörfelt K, Eicher F, et al. Magnetic resonance-determined sodium removal from tissue stores in hemodialysis patients. *Kidney Int.* 2015;87(2):434-441. doi:10.1038/ki.2014.269
16. Canaud B, Kooman J, Selby NM, et al. Sodium and water handling during hemodialysis: new pathophysiologic insights and management approaches for improving outcomes in end-stage kidney disease. *Kidney Int.* 2019;95(2):296-309. doi:10.1016/j.kint.2018.09.024
17. Machnik A, Neuhofer W, Jantsch J, et al. Macrophages regulate salt-dependent volume and blood pressure by a vascular endothelial growth factor-C-dependent buffering mechanism. *Nat Med.* 2009;15(5):545-552. doi:10.1038/nm.1960
18. Ziomber A, Machnik A, Dahlmann A, et al. Sodium-, potassium-, chloride-, and

- bicarbonate-related effects on blood pressure and electrolyte homeostasis in deoxycorticosterone acetate-treated rats. *Am J Physiol Physiol*. 2008;295(6):F1752-F1763. doi:10.1152/ajprenal.00531.2007
19. Titze J, Krause H, Hecht H, et al. Reduced osmotically inactive Na storage capacity and hypertension in the Dahl model. *Am J Physiol Physiol*. 2002;283(1):F134-F141. doi:10.1152/ajprenal.00323.2001
  20. Schneider MP, Raff U, Kopp C, et al. Skin Sodium Concentration Correlates with Left Ventricular Hypertrophy in CKD. *J Am Soc Nephrol*. 2017;28(6):1867-1876. doi:10.1681/asn.2016060662
  21. Kopp C, Linz P, Maier C, et al. Elevated tissue sodium deposition in patients with type 2 diabetes on hemodialysis detected by <sup>23</sup>Na magnetic resonance imaging. *Kidney Int*. 2018;93(5):1191-1197. doi:10.1016/j.kint.2017.11.021
  22. Hammon M, Grossmann S, Linz P, et al. <sup>23</sup>Na magnetic resonance imaging of the lower leg of acute heart failure patients during diuretic treatment. *PLoS One*. 2015;10(10):1-13. doi:10.1371/journal.pone.0141336
  23. Levitt DG, Levitt MD. Human serum albumin homeostasis: a new look at the roles of synthesis, catabolism, renal and gastrointestinal excretion, and the clinical value of serum albumin measurements. *Int J Gen Med*. 2016;9:229-255. doi:10.2147/IJGM.S102819
  24. Kalantar-Zadeh K, Kilpatrick RD, Kuwae N, et al. Revisiting mortality predictability of serum albumin in the dialysis population: Time dependency, longitudinal changes and population-attributable fraction. *Nephrol Dial Transplant*. 2005;20(9):1880-1888. doi:10.1093/ndt/gfh941
  25. Kaysen GA, Dubin JA, Müller HG, Rosales L, Levin NW, Mitch WE. Inflammation and

- reduced albumin synthesis associated with stable decline in serum albumin in hemodialysis patients. *Kidney Int.* 2004;65(4):1408-1415. doi:10.1111/j.1523-1755.2004.00520.x
26. Eleftheriadis T, Liakopoulos V, Antoniadi G, Kartsios C, Stefanidis I. The role of hepcidin in iron homeostasis and anemia in hemodialysis patients. *Semin Dial.* 2009;22(1):70-77. doi:10.1111/j.1525-139X.2008.00532.x
27. Suttorp MM, Hoekstra T, Rotmans JJ, et al. Erythropoiesis-stimulating agent resistance and mortality in hemodialysis and peritoneal dialysis patients. *BMC Nephrol.* 2013;14(1). doi:10.1186/1471-2369-14-200

## Chapter 3

### **Effects of pediatric chronic kidney disease and its etiology on leg tissue sodium concentration.**

*In this study, we moved from the adult to the pediatric CKD population. Taking advantage of the lower comorbidity burden in the pediatric population compared with adults, we hypothesized that different etiologies of pediatric kidney disease would be associated with different tissue  $[Na^+]$ .*

*A version of this chapter has been published in the journal “Pediatric Nephrology” Salerno FR, Akbari A, Lemoine S, Scholl TJ, McIntyre CW, Filler G. Effects of pediatric chronic kidney disease and its etiology on tissue  $[Na^+]$ : a pilot study. *Pediatr Nephrol.* 2022 Jun 2. doi: 10.1007/s00467-022-05600-7. Epub ahead of print. PMID: 35655040. This article is available under the terms of the Creative Commons Attribution License.*

### **3.1 Introduction**

The ECV compartment is closely associated with total body sodium ( $Na^+$ ) content in humans<sup>1,2</sup>, and its accurate assessment is notably difficult in clinical practice. Changes in ECV status, and ECV expansion in particular, are associated with significant morbidity and mortality in patients with CKD<sup>3,4</sup>. Sodium-23 magnetic resonance imaging (<sup>23</sup>Na MRI) allows the non-invasive assessment of tissue  $[Na^+]$  to estimate  $Na^+$  status and ECV status<sup>5</sup>. Furthermore, osmotically inactive  $Na^+$  deposits have been suggested to influence tissue  $[Na^+]$ , adding an additional level of complexity to the clinical estimate of total body  $Na^+$ <sup>6,7</sup>. The clinical relevance of tissue  $[Na^+]$  is becoming increasingly recognized in the CKD setting, as skin  $[Na^+]$  accumulation has been

associated with left ventricular hypertrophy in non-dialysis CKD<sup>8</sup>, potentially leading to adverse outcomes in patients on dialysis<sup>9</sup>. Although there is evidence for increased tissue [Na<sup>+</sup>] in CKD adult patients compared with healthy individuals<sup>10,11</sup>, actual tissue [Na<sup>+</sup>] based on CKD etiology has not been demonstrated in children and adolescents to date. Indeed, this measure is also of interest in the pediatric CKD population, where kidney Na<sup>+</sup> handling can be widely impaired due to both acquired and inherited disease mechanisms. In fact, inherited tubular disorders (e.g. Bartter, Gitelman and Fanconi syndrome) are associated with kidney Na<sup>+</sup> wasting, whereas proteinuric glomerular diseases and nephrotic syndrome (e.g. minimal change disease, focal segmental glomerulosclerosis) are associated with kidney Na<sup>+</sup> retention<sup>12,13</sup>. Furthermore, the pediatric setting offers an ideal opportunity to explore the impact of specific CKD disorders on tissue [Na<sup>+</sup>], due to the lower prevalence of metabolic and cardiovascular disease compared with the adult CKD population.

In this study, we hypothesized that CKD in children and adolescents is associated with altered tissue [Na<sup>+</sup>] in relation to healthy controls and to the etiology of CKD. In a cross-sectional, case-control study, we compared tissue [Na<sup>+</sup>] in children and adolescents with CKD against healthy controls and investigated the associations of tissue [Na<sup>+</sup>] with clinical biomarkers of kidney function.

## **3.2 Materials and Methods**

### *Study design*

We performed a cross-sectional, case-control exploratory study. Study participants underwent an investigational visit consisting of a research imaging session (<sup>1</sup>H and <sup>23</sup>Na MRI of either the right or left leg), demographic and clinical data were collected, and blood biochemistry was measured.

The study received approval from the Western University Human Research Ethics Board (number: 108765) and was conducted in compliance with the Declaration of Helsinki and all applicable regulatory requirements. This study was registered (ClinicalTrials.gov Identifier: NCT03004547) on December 29<sup>th</sup>, 2016.

### *Study participants*

Study patients were recruited from the London Health Sciences Centre, London, ON, Canada from March 2018 to June 2021. For consenting minors, a written assent was obtained in addition to a written informed consent signed by their legal guardians. Adult (age  $\geq 18$ ) study participants provided written informed consent. Healthy children and adolescents, as well as adults, had no history of kidney, heart and liver disease or edema. Pediatric CKD patients had a clinical diagnosis of CKD according to current clinical guidelines (augmented by histological assessment in some patients), were kidney allograft recipients, or were currently receiving kidney replacement therapy. Potential study candidates were excluded if they had contraindications to MRI or did not consent to the study.

### *Magnetic Resonance Imaging and Image Analysis*

All MRI data were acquired using a multinuclear-capable, 3.0-Tesla GE MRI scanner (Discovery MR750, General Electric Healthcare, Milwaukee, WI, USA). To acquire  $^{23}\text{Na}$  spin density images, subjects were positioned in the magnet bore in the supine position, with the thickest part of their right or left calf muscle at the center of a custom-made  $^{23}\text{Na}$  birdcage radiofrequency coil (~20 cm diameter by 21.5 cm long). Calibration vials with increasing saline concentrations were placed in the RF coil adjacent to the subjects' shins. A single-slice  $^{23}\text{Na}$  MR image was obtained with a

radial  $k$ -space acquisition pulse sequence (Density-Adapted 2D Projection Reconstruction)<sup>14</sup>, with the following parameters: slice-selective radiofrequency pulse; flip angle 90°; repetition time/echo time: 100/1.2 msec; number of signals averages: 100; slice thickness: 3 cm and isotropic field of view/resolution: 18 cm/0.3 cm<sup>2</sup>; total acquisition time: ~30 minutes.

During the same imaging session, additional axial <sup>1</sup>H MR images were acquired using a standard (Spoiled Gradient-Recalled Echo) pulse sequence to identify and delineate the relevant anatomical structures.

<sup>23</sup>Na concentration maps were generated using custom software developed within MATLAB, version 9.6.0 – R2019a (The MathWorks Inc., Natick, Massachusetts) with additional open-source code from the Michigan Image Reconstruction Toolbox (Jeffery A. Fessler, “Michigan Reconstruction Toolbox”, [web.eecs.umich.edu/~fessler/code/](http://web.eecs.umich.edu/~fessler/code/)). Regions of interest for the whole leg, the skin and the soleus muscle were manually segmented after superimposing <sup>1</sup>H and <sup>23</sup>Na images, as detailed previously<sup>15</sup>.

### *Laboratory Analysis*

Blood samples were collected from study participants, processed, and analyzed in a central tertiary care hospital laboratory (London Health Sciences Centre, London, Ontario, Canada) for routine clinical biomarkers. Estimated glomerular filtration rate (eGFR) was calculated using the creatinine-based bedside Schwartz formula<sup>16</sup> and the cystatin C-based equation<sup>17</sup>. The normalized urinary [Na<sup>+</sup>] to urinary creatinine concentration (uNa<sup>+</sup>/uCreat) from morning spot urine samples was used to evaluate potential kidney sodium wasting and 24-hour urinary sodium excretion. Urinary protein-to-creatinine ratio (uPCR) was used to estimate 24-hour urinary protein excretion

and was calculated according to the 2012 CKD Kidney Disease: Improving Global Outcomes (KDIGO) clinical guidelines<sup>18</sup>.

### *Statistical Analysis*

Statistical analysis was performed using GraphPad Prism version 9.0.0 (GraphPad Software, San Diego, CA, USA; [www.graphpad.com](http://www.graphpad.com)) and SPSS Version 27.0 (IBM Corp. Released 2020. IBM SPSS Statistics for MacIntosh, Armonk, NY: IBM Corp). Normality was assessed using the Shapiro–Wilk test. Continuous variables were tabled as mean  $\pm$  standard deviation (SD) if normally distributed and as median (25<sup>th</sup> percentile, 75<sup>th</sup> percentile), if highly skewed. Highly skewed data sets were transformed using their natural logarithm for analyses. Kruskal-Wallis one-way analysis of variance test was used to compare tissue [Na<sup>+</sup>] between healthy children and pediatric CKD patients; Dunn’s posthoc test was used to compare the individual groups. Tissue [Na<sup>+</sup>] values in pediatric CKD patients were then stratified by etiology and individually compared against healthy children’s by computing their Z-scores, based on the healthy children’s mean tissue [Na<sup>+</sup>] and SD. An absolute Z-score greater than 1.96 was deemed to deviate significantly from the healthy children’s mean. Univariate associations were computed between tissue [Na<sup>+</sup>], demographics, anthropometry and clinical biomarkers of kidney function using Pearson’s product-moment correlation. For each dependent variable, *p*-values were corrected for family-wise error using the Bonferroni-Holm correction. An  $\alpha < 0.05$  was considered statistically significant.

### 3.3 Results

Table 3.1 summarizes the demographics, anthropometry, and tissue [Na<sup>+</sup>] values relative to the study sample. No significant differences in demographics and anthropometrics were found between healthy controls and CKD patients.

Table 3.1: Demographics, anthropometry and tissue [Na<sup>+</sup>] according to study group.

Variable	Healthy Adults (n=19)	Healthy Children and Adolescents (n=17)	CKD Patients (n=19)
Age (years)	57.4 ± 15.8	11.5 ± 3.5	12.0 ± 3.6
Sex (M/F)	10/9	9/8	10/9
Weight (kg)	69.9 ± 11.5	41.1 ± 13.8	45.7 ± 25.1
Height (m)	1.67 ± 7.72	1.50 ± 0.16	1.46 ± 0.22
BMI (kg/m <sup>2</sup> )	24.9 ± 2.8	17.8 ± 2.5	20.0 ± 6.2
<i><sup>23</sup>Na MRI</i>			
Whole leg [Na <sup>+</sup> ]	20.1 ± 3.5	16.3 ± 1.6	17.9 ± 6.2
Skin [Na <sup>+</sup> ]	20.2 ± 6.3	12.8 ± 2.5	15.0 ± 6.4
Muscle [Na <sup>+</sup> ]	22.0 ± 2.9	18.5 ± 1.8	19.8 ± 6.5

Data are presented as Mean ± SD or ratios (Sex). BMI: body mass index; CKD: chronic kidney disease; MRI: magnetic resonance imaging; SD: standard deviation.

Table 3.2 summarizes the clinical and biochemistry features of the CKD sample. Six (31%) CKD patients qualified as CKD KDIGO stage 3a. Ten (53%) CKD cases were primarily due to glomerular disease, the rest to inherited tubulo-interstitial kidney disease (six, 31%), CAKUT (two, 11%) and primary calcineurin inhibitor (CNI) toxicity (one, 5%). Three patients (16%) were kidney transplant recipients receiving standard immune-suppressant regimens. One was receiving thrice-weekly HD and one was receiving continuous ambulatory PD.

Table 3.2: Clinical features, blood and urine biochemistry of the CKD patient group.

<b>CKD Stages</b>	<b>Statistics</b>
<b>1</b>	3 (16%)
<b>2</b>	3 (16%)
<b>3a</b>	6 (31%)
<b>3b</b>	1 (5%)
<b>4</b>	3 (16%)
<b>5</b>	1 (5%)
<b>5d</b>	2 (11%)
<b>Primary Kidney Disease Etiology</b>	
<b>Glomerular Disease</b>	10 (53%)
<b>Tubulo-Interstitial (Inherited)</b>	6 (32%)
<b>CAKUT/Reflux Nephropathy</b>	2 (11%)
<b>CNI Toxicity</b>	1 (5%)
<b>Heart Transplant</b>	1 (5%)
<b>Kidney Replacement Therapy</b>	
<b>HD</b>	1 (5%)
<b>Kidney Transplant</b>	3 (16%)
<b>PD</b>	1 (5%)
<b>Comorbidities</b>	
<b>Other Organ Transplants (heart, liver)</b>	2 (11%)
<b>Hypertension</b>	9 (47%)
<b>Diabetes Mellitus</b>	2 (11%)
<b>Medications</b>	
<b>ACEi-ARB</b>	10 (53%)
<b>Beta-Blocker</b>	1 (5%)
<b>Calcium Channel Blocker</b>	9 (47%)
<b>Loop Diuretic</b>	6 (32%)
<b>Immune Suppressant Medications</b>	
<b>Steroids</b>	5 (26%)
<b>CNI</b>	5 (26%)
<b>mTORi</b>	1 (5%)
<b>Antimetabolite</b>	5 (26%)

<b>eGFR Schwartz (ml/min/1.73m<sup>2</sup>)</b>	55 ± 42
<b>eGFR Cystatin (ml/min/1.73m<sup>2</sup>)</b>	43 ± 25
<b>Urine creatinine (mg/L)</b>	758 ± 382
<b>Proteinuria (mg/L) (median (IQR))</b>	300 (80-2,185)
<b>uPCR (mg/g) (median (IQR))</b>	422 (121-3,420)
<b>Urine [Na<sup>+</sup>]/uCreat (mmol/mmol)</b>	21.8 ± 17.2
<b>Serum creatinine (umol/L)</b>	198.6 ± 224.9
<b>Serum cystatin C (mg/L)</b>	2.55 ± 1.90
<b>Serum urea (mmol/L)</b>	11.3 ± 5.9
<b>Serum albumin (g/L)</b>	40.9 ± 8.4
<b>Serum glucose (mmol/L)</b>	6.5 ± 2.7
<b>Serum [Na<sup>+</sup>] (mmol/L)</b>	138.9 ± 2.5
<b>Serum [K<sup>+</sup>] (mmol/L)</b>	4.3 ± 0.7
<b>Serum [HCO<sub>3</sub><sup>-</sup>] (mmol/L)</b>	24.8 ± 2.9
<b>Blood hemoglobin (g/L)</b>	118.0 ± 14.4

Data are expressed as %, mean ± SD and median (IQR) as appropriate.

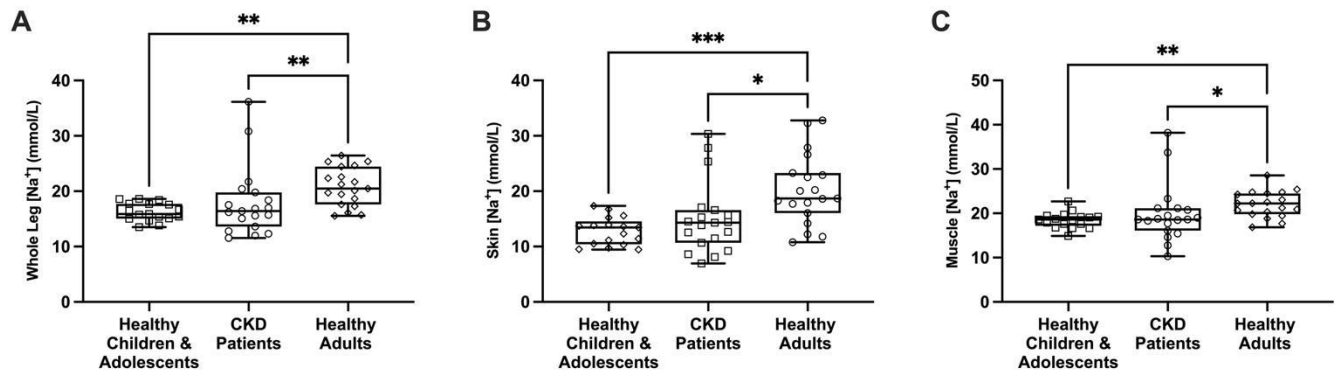
[HCO<sub>3</sub><sup>-</sup>]: bicarbonate concentration; [K<sup>+</sup>]: potassium concentration; [Na<sup>+</sup>]: Sodium concentration; ACEi/ARB: angiotensin-converting enzyme inhibitor/ angiotensin receptor blocker; CAKUT: congenital anomalies of kidney and urinary tract; CKD: chronic kidney disease; CNI: calcineurin inhibitor; eGFR: estimated glomerular filtration rate; HD: hemodialysis; IQR: interquartile range; mTORi: mammalian Target Of Rapamycin inhibitor; PD: peritoneal dialysis; SD: standard deviation; uCreat: urinary creatinine concentration; uPCR: urinary protein-to-creatinine ratio.

#### *Tissue [Na<sup>+</sup>] in Healthy Controls vs. CKD Patients*

Healthy adults had significantly higher tissue [Na<sup>+</sup>] compared with both healthy children and adolescents (Table 3.1).

After comparing the healthy children and adolescents with CKD patients, no statistically significant differences in whole leg, skin, and muscle  $[Na^+]$  were observed (Figure 3.1).

Figure 3.1: Tissue  $[Na^+]$  according to the three groups: in healthy children and adolescents vs CKD patients vs healthy adults. (A: Whole leg  $[Na^+]$ ; B: Skin  $[Na^+]$ ; C: Muscle  $[Na^+]$ )



\*:  $p < 0.05$ ; \*\*:  $p < 0.01$ ; \*\*\*:  $p < 0.001$

However, a large variability in tissue  $[Na^+]$  values was observed among the patients with CKD, suggesting a more detailed investigation on a case-by-case analysis was warranted. Tissue  $[Na^+]$  Z-scores were therefore computed for each CKD patient using the healthy children and adolescents group data to compare individual CKD patients to the reference healthy sample.

### Tissue [Na<sup>+</sup>] According to CKD Etiology

Table 3.3 summarizes individual CKD patient kidney function, tissue [Na<sup>+</sup>] raw values and Z-scores. Elevated whole-leg [Na<sup>+</sup>] Z-scores were found among patients with non-hemolytic uremic syndrome (HUS) glomerular disease and native kidneys (ID: 1, 3, 9, 18), and one kidney transplant recipient due to atypical HUS (ID: 5). Reduced whole-leg [Na<sup>+</sup>] Z-scores were found in patients with inherited tubular disorders (ID 12, idiopathic Fanconi syndrome, and ID 17, idiopathic combined proximal and distal renal tubular acidosis), and in patients with CNI toxicity (ID 11, heart transplant recipient, and ID 13, kidney transplant recipient due to atypical HUS).

Skin [Na<sup>+</sup>] and muscle [Na<sup>+</sup>] were similarly increased in three glomerular disease patients (ID: 1, 5, 18, and 1, 9, 18, respectively). Only 1/19 (5%) CKD patient had a skin [Na<sup>+</sup>] Z-score <-1.96 (ID 17), and 3/19 (16%) had muscle [Na<sup>+</sup>] Z-scores <-1.96 (ID 12, 13, 17), as detailed in Table 3.3.

Table 3.3: Individual demographics, clinical features and tissue [Na<sup>+</sup>] of the CKD patient group.

ID	Age	Sex	Kidney Disease Etiology	eGFR <sub>Schw</sub> (ml/min/1.73 m <sup>2</sup> )	eGFR <sub>Cyst</sub> (ml/min/1.73 m <sup>2</sup> )	uPCR (mg/g)	uNa <sup>+</sup> /uCreat (mmol/mmol)	Whole-leg [Na <sup>+</sup> ] mmol/L (Z-score)	Skin [Na <sup>+</sup> ] mmol/L (Z-score)	Muscle [Na <sup>+</sup> ] mmol/L (Z-score)
1	6	M	FSGS ( <i>NPHS1</i> mutation)	16	20	14,428	29	30.8 (8.93)	27.8 (5.96)	33.7 (8.52)
2	13	F	Typical HUS	51	46	503	16	15.1 (-0.71)	11.5 (-0.52)	18.8 (0.17)
3	13	M	FSGS	22	23	1,354	12	19.8 (2.16)	17.1 (1.70)	18.6 (0.08)
4	14	F	Recurrent UTI, neurogenic bladder (spina bifida)	16	23	396	10	17.0 (0.44)	14.5 (0.66)	17.7 (-0.42)
5	14	M	Kidney transplant (atypical HUS)	58	44	500	19	21.7 (3.35)	25.4 (4.98)	20.8 (1.28)
6	10	M	Tubulo-interstitial kidney disease due to methylmalonic acidemia, liver transplantation	63	37	65	7	16.2 (-0.04)	12.5 (-0.10)	18.6 (0.07)

7	16	M	Renal coloboma syndrome ( <i>PAX2</i> mutation)	28	28	6,661	20	15.6 (-0.42)	14.3 (0.60)	18.5 (0.01)
8	8	F	Atypical HUS	28	25	4,109	26	16.4 (0.09)	8.6 (-1.66)	19.5 (0.57)
9	17	F	Immune-complex MPGN	10	17	6,532	4	20.4 (2.55)	12.7 (-0.06)	23.3 (2.71)
10	6	F	Unilateral kidney agenesis, kidney infarction	57	50	118	35	13.6 (-1.63)	8.1 (-1.86)	19.0 (0.29)
11	9	M	CNI toxicity (heart transplantation)	79	68	88	21	12.3 (-2.43)	9.2 (-1.42)	16.1 (-1.33)
12	14	F	Idiopathic Fanconi Syndrome	68	55	449	16	12.0 (-2.62)	10.7 (-0.84)	14.6 (-2.16)
13	14	M	Kidney transplant (atypical HUS), Secondary CNI toxicity	116	40	245	25	12.8 (-2.14)	13.8 (0.41)	10.3 (-4.56)
14	14	M	Kidney transplant (Alport Syndrome)	56	46	61	6	17.5 (0.78)	15.6 (1.13)	21.1 (1.49)
15	17	F	Autosomal dominant tubulointerstitial kidney disease ( <i>UMOD</i> mutation)	40	47	38	7	16.8 (0.36)	15.3 (0.99)	18.3 (-0.08)
16	11	M	Hypophosphatemic Rickets with Hypercalciuria ( <i>SLC34A3</i> mutation)	156	38	131	21	18.4 (1.31)	14.5 (0.68)	21.2 (1.50)
17	6	M	Idiopathic Combined Proximal and Distal Renal Tubular Acidosis (type 3)	128	131	157	78	11.6 (-2.89)	6.9 (-2.33)	12.8 (-3.20)
18	14	F	FSGS (currently on HD, with residual urinary volume)	-	-	-	-	36.2 (12.21)	30.4 (6.97)	38.2 (11.00)
19	12	F	FSGS (currently on PD, without residual urinary volume)	-	-	-	-	15.7 (-0.33)	16.6 (1.50)	15.4 (-1.69)

*Tissue [Na<sup>+</sup>] and Z-scores calculated from healthy children and adolescents are reported in parenthesis.*

CNI: calcineurin inhibitor; eGFR: estimated glomerular filtration rate; FSGS: focal segmental glomerulosclerosis; HD: hemodialysis; HUS: hemolytic-uremic syndrome; *NPHS1*: nephrin gene;

*PAX2*: paired box gene 2; *PD*: peritoneal dialysis; *SLC34A3*: sodium-phosphate cotransporter gene; *UMOD*: uromodulin;  $\text{uNa}^+/\text{uCreat}$ : urinary  $[\text{Na}^+]$  to urinary creatinine ratio; *uPCR*: urinary protein-to-creatinine ratio; *UTI*: urinary tract infection.

## Correlations

Correlations between variables are represented in Table 3.4.

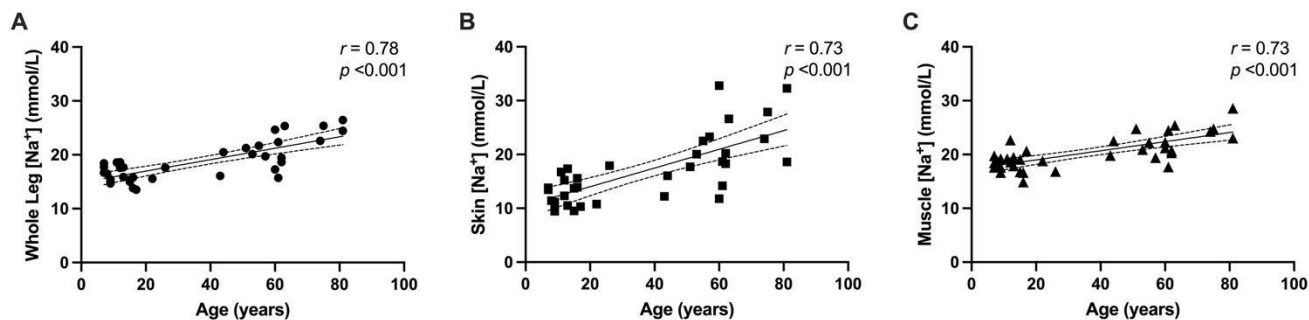
Table 3.4: Associations between demographics, anthropometry and clinical variables with tissue  $[\text{Na}^+]$  in healthy children and adolescents and CKD patients.

Variable	Whole leg $[\text{Na}^+]$		Skin $[\text{Na}^+]$		Muscle $[\text{Na}^+]$	
	<i>r</i> (95% CI)	Adjusted <i>p</i>	<i>r</i> (95% CI)	Adjusted <i>p</i>	<i>r</i> (95% CI)	Adjusted <i>p</i>
<b>Healthy Children, Adolescents and Adults</b>						
<b>Age</b>	0.776 (0.600; 0.880)	<0.001	0.734 (0.534; 0.856)	<0.001	0.727 (0.524; 0.852)	<0.001
<b>Healthy Children and Adolescents</b>						
<b>Age</b>	-0.479 (-0.780; 0.003)	0.10	0.084 (-0.414; 0.542)	0.78	-0.118 (-0.567; 0.384)	>0.99
<b>BMI</b>	-0.073 (-0.535; 0.422)	0.78	0.224 (-0.288; 0.636)	0.78	-0.006 (-0.485; 0.476)	>0.99
<b>CKD Patients</b>						
<b>Age</b>	0.071 (-0.396; 0.509)	>0.99	0.211 (-0.269; 0.607)	>0.99	-0.030 (-0.478; 0.430)	>0.99
<b>BMI</b>	-0.088 (-0.521; 0.382)	>0.99	0.030 (-0.430; 0.478)	>0.99	0.001 (-0.453; 0.455)	>0.99
<b>eGFR Cystatin</b>	-0.432 (-0.741; 0.028)	0.33	-0.431 (-0.740; 0.028)	0.33	-0.356 (-0.697; 0.117)	0.68
<b>eGFR Schwartz</b>	-0.323 (-0.678; 0.153)	0.71	-0.282 (-0.653; 0.197)	0.96	-0.324 (-0.678; 0.153)	0.71
<b>Serum Albumin</b>	-0.658 (-0.856; -0.291)	<0.05	-0.596 (-0.826; -0.194)	<0.05	-0.613 (-0.835; -0.220)	<0.05
<b><math>\text{uNa}^+/\text{UCreat}</math></b>	-0.249 (-0.652; 0.263)	0.34	-0.281 (-0.671; 0.231)	0.28	-0.237 (-0.645; 0.275)	0.36
<b><i>uPCR</i></b>	0.736 (0.394; 0.899)	<0.001	0.509 (0.037; 0.795)	<0.05	0.764 (0.448; 0.910)	<0.001

Pearson correlation was used to compute the relationship. BMI: body mass index; CKD: chronic kidney disease; eGFR: estimated glomerular filtration rate;  $\text{uNa}^+/\text{uCreat}$ : urinary sodium-to-creatinine ratio; *uPCR*: urinary protein-to-creatinine ratio.

Among healthy children, adolescents and adults, age was strongly and positively associated with all tissue  $[Na^+]$  (Figure 3.2).

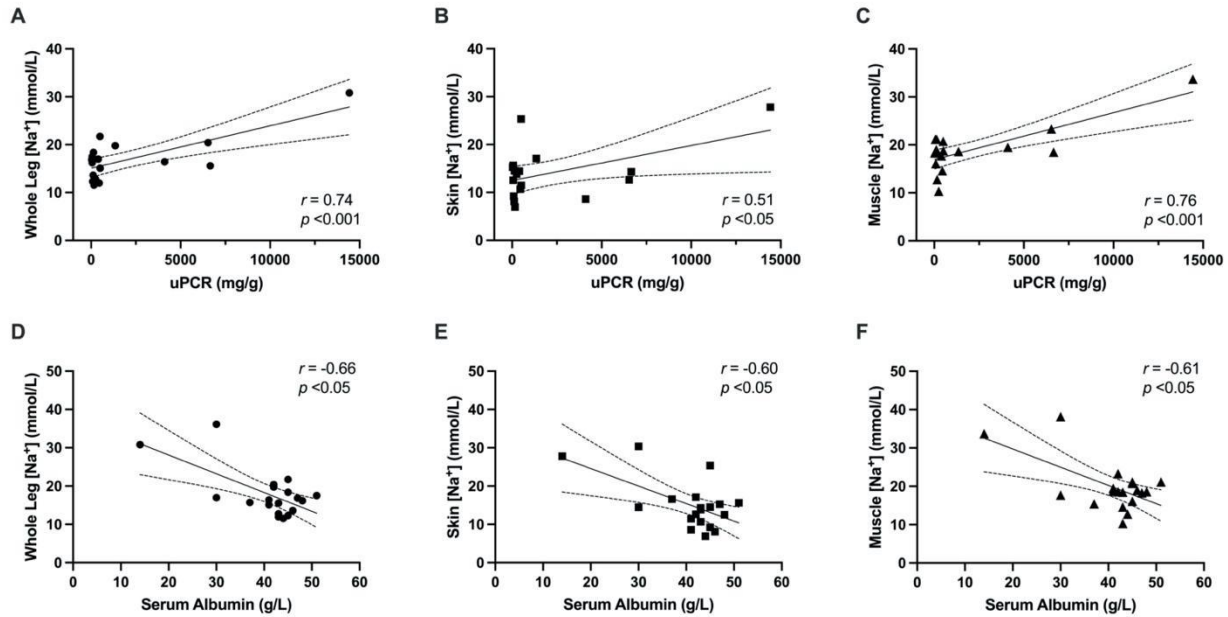
Figure 3.2: Scatterplots showing the relationship between age with whole leg  $[Na^+]$  (Panel A), skin  $[Na^+]$  (Panel B) and muscle  $[Na^+]$  (Panel C) in healthy children, adolescents and adults ( $n=36$ ).



Among CKD patients, serum albumin was negatively associated with all tissue  $[Na^+]$  measures (whole leg  $[Na^+]$   $r=-0.658$ ,  $p<0.01$ ; skin  $[Na^+]$   $r=-0.596$ ,  $p<0.01$ ; muscle  $[Na^+]$   $r=-0.613$ ,  $p<0.01$ ) (Figure 3.3, panels A, B and C).

Likewise, uPCR was positively associated with all tissue  $[Na^+]$  measures (whole leg  $[Na^+]$ ,  $r=0.736$ ,  $p<0.001$ , skin  $[Na^+]$ ,  $r=0.501$ ,  $p<0.05$ , muscle  $[Na^+]$ ,  $r=0.764$ ,  $p<0.001$ ) (Figure 3.3, panels D, E and F). No other significant associations were observed.

Figure 3.3: Scatterplots showing the relationship between serum albumin (Panels A-C) and uPCR (Panels D-F) with tissue  $[Na^+]$  in pediatric CKD patients ( $n=19$ ).



### 3.4 Discussion

This study provides early evidence that tissue [Na<sup>+</sup>] status in children and adolescents with CKD does not follow a uniform pattern of increased tissue [Na<sup>+</sup>]. Healthy children and adolescents had lower tissue [Na<sup>+</sup>] than healthy adults, and tissue [Na<sup>+</sup>] was positively correlated with age. Furthermore, some patients with tubular disease demonstrated reduced tissue [Na<sup>+</sup>], while others demonstrated tissue [Na<sup>+</sup>] retention when the underlying etiology was nephrotic syndrome. The main findings of this study may be summarized as follows:

- No significant differences in tissue [Na<sup>+</sup>] were observed between healthy children and adolescents and CKD patients, owing to the spectrum of [Na<sup>+</sup>] retention and wasting.
- All cases of nephrotic syndrome were associated with increased whole leg [Na<sup>+</sup>] compared with healthy controls.

- The severity of tissue  $[\text{Na}^+]$  among CKD patients correlated with the degree of proteinuria and hypoalbuminemia.

Tissue  $[\text{Na}^+]$  is an emerging quantitative imaging biomarker in clinical nephrology.  $^{23}\text{Na}$  MRI offers the possibility of quantifying total body sodium and estimating the clinical ECV status, due to the prevalent location of sodium in the extracellular space<sup>1,5,19</sup>,

CKD as a function of eGFR reduction was not associated with abnormal tissue  $[\text{Na}^+]$  per se. Indeed, we observed that non-tubular and non-proteinuric forms of CKD were not associated with abnormal tissue  $[\text{Na}^+]$ . This suggests that measures of glomerular filtration are of small relevance in relation to  $\text{Na}^+$  metabolism and highlights the challenges of a correct assessment of  $[\text{Na}^+]$  balance in CKD. Recent evidence points out that sodium retention in CKD is mainly associated with altered distal tubular function, as the final regulator of urinary sodium excretion<sup>20,21</sup>.

$^{23}\text{Na}$  MRI measures the sodium signal within a unit of tissue volume including extracellular matrix (high in sodium content), cellular mass and fat tissue (low in sodium content)<sup>5,19,22</sup>. Recently, ultra-high field (9.4T) coupled with triple quantum filtering  $^{23}\text{Na}$  MRI pulse sequence was able to visualize and differentiate free (dissolved in water) from bound sodium at the dermal skin level<sup>23</sup>. The authors found that ~40% of skin sodium in healthy volunteers to be bound to glycosaminoglycans, whereas this fraction significantly decreases in type 2 diabetes mellitus. Furthermore, the authors found that  $^{23}\text{Na}$  MRI using ultrashort echo-time pulse sequences, such as the one used in the present study, is unable to visualize the bound sodium fraction due to its faster transverse signal decay properties, compared with free sodium. Therefore,  $^{23}\text{Na}$  MRI technology we employed in this study likely underestimated tissue  $[\text{Na}^+]$ , measured only as free tissue  $[\text{Na}^+]$ , primarily relating to the ECV.

These findings may be useful to interpret current and recent findings. At present, little is known of tissue  $[Na^+]$  in healthy children and adolescents. In one report, muscle  $[Na^+]$  was found to be lower in obese, hypertensive adolescents, compared with obese normotensive and healthy adolescents. No differences in skin  $[Na^+]$  were found<sup>24</sup>. We did not observe a significant association between age and tissue  $[Na^+]$  among healthy children and adolescents, therefore we cannot comment on the changes in tissue composition and  $[Na^+]$  with physiological growth. Rather, the increase in tissue  $[Na^+]$  we observed occurred across the whole life cycle, possibly as a function of declining cellular mass with aging: it has been reported that the progressive increase in tissue  $[Na^+]$  observed in aging adults reflects a change in tissue composition over time.<sup>5</sup> Speculatively, an age-dependent decline in osmotically inactive tissue  $[Na^+]$  binding capacity may also result in increased tissue  $[Na^+]$ , due to the increased free tissue  $[Na^+]$  over bound tissue  $[Na^+]$ , as observed in patients with type 2 diabetes mellitus<sup>23</sup>. Importantly, we found that pediatric patients with nephrotic syndrome were likely to display higher tissue  $[Na^+]$  compared with healthy children and adolescents, and that tissue  $[Na^+]$  was significantly associated with the degree of proteinuria and hypoalbuminemia. This agrees with recent studies showing that distal tubular sodium reabsorption is a key mechanism for sodium retention in CKD. The main mechanism for sodium retention in proteinuric kidney disorders has been associated with urinary plasminogen excretion: plasminogen is converted to plasmin in the tubular lumen, which activates the epithelial  $Na^+$  channel (ENaC) located in the connecting tubules<sup>12</sup>. In the present study, this is supported by the positive association between all measures of tissue  $[Na^+]$  with uPCR.

On the other hand, salt-wasting syndrome is caused by a variety of inherited and acquired tubular disorders generally of childhood onset, and is associated with ECV contraction<sup>25</sup>. We have shown evidence of tissue  $[Na^+]$  depletion in two cases of inherited tubular disorders – Fanconi syndrome

and mixed (type 3) renal tubular acidosis<sup>26</sup>. Other more commonly known salt wasting tubular disorders, such as Bartter and Gitelman syndromes, may conceivably show similar results but were not included in the current study.

Furthermore, we found evidence of tissue  $[\text{Na}^+]$  depletion in two solid organ transplant recipients (heart and kidney, respectively) with CNI toxicity. This observation conflicts with published evidence showing that the CNI tacrolimus is associated with sodium-chloride cotransporter (NCC) upregulation and salt-sensitive hypertension in rats<sup>27</sup>. The nephrotoxicity of CNI is multifaceted and dose-dependent; tubular dysfunction is a recognized component of CNI toxicity, as proximal tubular vacuolization as well as impaired tubular electrolyte handling have been observed<sup>28</sup>. Because we cannot exclude the influence of tubulointerstitial damage related to chronic allograft rejection on tubular dysfunction, as suggested by previous authors<sup>29</sup>, as well as  $\text{Na}^+$  restriction and other supportive therapies, the observed findings are of anecdotal value and should be interpreted with caution.

Assessment of  $\text{Na}^+$  balance with <sup>23</sup>Na MRI in CKD patients is relevant, as ECV expansion, regardless of the methodology used to assess it in adults with CKD, is associated with adverse clinical outcomes<sup>3,4</sup>. In a recent publication from our group, skin  $[\text{Na}^+]$  was associated with increased mortality and major adverse cardiovascular events in adult patients on dialysis, highlighting the toxic effects of ECV expansion<sup>30</sup>. Although direct evidence of adverse outcomes is lacking in children, it is recognized that ECV expansion leads to progressive adverse cardiovascular remodeling which may translate into a negative prognostic impact in early and late adulthood<sup>31</sup>. It has been recently acknowledged that the toxicity of tissue  $\text{Na}^+$  may also be associated to osmotically inactive deposits, particularly at the skin level<sup>8,32</sup>. Importantly, the existence of such deposits was directly visualized in human skin using ultra-high field triple

quantum filtering  $^{23}\text{Na}$  MRI<sup>23</sup>. Sodium balance studies have shown potentially extremely large increases in total body sodium as a result of increased dietary salt intake, without concomitant ECV expansion<sup>33,34</sup>.

However,  $^{23}\text{Na}$  MRI technology is unable to differentiate water-free from water-bound tissue sodium. Future studies should compare  $^{23}\text{Na}$  MRI-based tissue  $[\text{Na}^+]$  against validated measures of ECV (e.g. bromide dilution, bioimpedance spectroscopy) and exchangeable sodium (e.g.  $^{24}\text{Na}$  radioisotope dilution).

## *Limitations*

Several limitations must be acknowledged when interpreting the results from this study. This was a pilot study, with a small and heterogeneous sample, as patient availability was limited due to the single-center nature of this study. The reported findings are of anecdotal value and should be interpreted with caution.

The effect of supportive (e.g., Na<sup>+</sup> restriction, antihypertensive, or diuretic therapy) and immune suppressant regimens (e.g., corticosteroids, CNI) might have affected kidney Na<sup>+</sup> handling and due to the cross-sectional nature of this study, may act as potential confounders when evaluating the results. Urinary Na<sup>+</sup> excretion was based on spot urine collection and indexed to urinary creatinine excretion; this biomarker has been shown to be an unreliable estimator of sodium intake, as sodium excretion varies throughout the day<sup>35</sup>. Additionally, it has been shown that 24-hour urinary sodium excretion fluctuates around daily dietary Na<sup>+</sup> intake in healthy individuals, following weekly (circaseptan) aldosterone and cortisol excretion cycles<sup>36,37</sup>. The mechanisms of urinary sodium excretion in CKD are less explored and likely differ from healthy individuals<sup>21</sup>, and are also likely to differ between different kidney disease etiologies. Urinary proteinase (plasminogen/plasmin) levels were not measured in the present study; although albuminuria severity has been shown to be positively associated with urinary protease levels in diabetic kidney disease and other kidney disorders<sup>38</sup>. Urinary protease may conceivably provide additional information on the relationship between tissue [Na<sup>+</sup>] and primary kidney Na<sup>+</sup> retention in proteinuric kidney disorders. Limitations linked to <sup>23</sup>Na MRI must be acknowledged: <sup>23</sup>Na signal is the weighted average of Na<sup>+</sup> contained in all tissues within a voxel (partial volume effect). This is relevant as fat tissue, low in Na<sup>+</sup>, may act as a potential confounder. Furthermore, it has been suggested that <sup>23</sup>Na MRI technology such as the one used in this study may be able to detect signal

from “free” sodium, dissolved in water. Therefore, osmotically inactive “bound” sodium, due to its spin properties would not be detected<sup>23</sup>.

### *Conclusions*

Children and adolescents with reduced GFR do not universally have increased tissue  $[\text{Na}^+]$ . Depending on etiology, pediatric CKD may be associated with either normal, increased, or reduced tissue  $[\text{Na}^+]$ , compared with healthy controls. Nephrotic syndrome may be associated with increased tissue  $[\text{Na}^+]$  due to kidney sodium retention and ECV expansion, whereas tubular disorders may be associated with reduced tissue  $[\text{Na}^+]$ , suggesting ECV depletion due to kidney  $\text{Na}^+$  wasting. These findings require confirmation in larger studies, focused on specific etiologies in the pediatric CKD population.

### 3.5 Bibliography

1. Bhawe G, Neilson EG. Body fluid dynamics: Back to the future. *J Am Soc Nephrol.* 2011;22(12):2166-2181. doi:10.1681/ASN.2011080865
2. Edelman IS, Leibman J, O'Meara MP, Birkenfeld LW. Interrelations between serum sodium concentration, serum osmolarity and total exchangeable sodium, total exchangeable potassium and total body water. *J Clin Invest.* 1958;37(9):1236-1256. doi:10.1172/JCI103712
3. Zoccali C, Moissl U, Chazot C, et al. Chronic fluid overload and mortality in ESRD. *J Am Soc Nephrol.* 2017;28(8):2491-2497. doi:10.1681/ASN.2016121341
4. Zoccali C, Torino C, Tripepi R, et al. Pulmonary congestion predicts cardiac events and mortality in ESRD. *J Am Soc Nephrol.* 2013;24(4):639-646. doi:10.1681/ASN.2012100990
5. Rossitto G, Touyz RM, Petrie MC, Delles C. "Much ado about N . . . Atrium: Modelling tissue sodium as a highly sensitive marker of subclinical and localised oedema." *Clin Sci.* 2018;132(24):2609-2613. doi:10.1042/CS20180575
6. Kopp C, Linz P, Dahlmann A, et al. <sup>23</sup>Na magnetic resonance imaging-determined tissue sodium in healthy subjects and hypertensive patients. *Hypertension.* 2013;61(3):635-640. doi:10.1161/HYPERTENSIONAHA.111.00566
7. Linz P, Santoro D, Renz W, et al. Skin sodium measured with <sup>23</sup>Na MRI at 7.0 T. *NMR Biomed.* 2015;28(1):54-62. doi:10.1002/nbm.3224
8. Schneider MP, Raff U, Kopp C, et al. Skin Sodium Concentration Correlates with Left Ventricular Hypertrophy in CKD. *J Am Soc Nephrol.* 2017;28(6):1867-1876. doi:10.1681/asn.2016060662
9. Salerno FR, Akbari A, Lemoine S, Filler G, Scholl TJ, McIntyre CW. Outcomes and

- predictors of skin sodium concentration in dialysis patients. *Clin Kidney J*. Published online January 28, 2022:sfac021. doi:10.1093/ckj/sfac021
10. Mitsides N, Alsehli FMS, Mc Hough D, et al. Salt and Water Retention Is Associated with Microinflammation and Endothelial Injury in Chronic Kidney Disease. *Nephron*. 2019;143(4):234-242. doi:10.1159/000502011
  11. Dahlmann A, Linz P, Zucker I, et al. Reduction of Tissue Na<sup>+</sup> Accumulation After Renal Transplantation. *Kidney Int Reports*. 2021;6(9):2338-2347. doi:10.1016/j.ekir.2021.06.022
  12. Svenningsen P, Bistrup C, Friis UG, et al. Plasmin in nephrotic urine activates the epithelial sodium channel. *J Am Soc Nephrol*. 2009;20(2):299-310. doi:10.1681/ASN.2008040364
  13. Artunc F, Wörn M, Schork A, Bohnert BN. Proteasuria—The impact of active urinary proteases on sodium retention in nephrotic syndrome. *Acta Physiol*. 2019;225(4):1-10. doi:10.1111/apha.13249
  14. Nagel AM, Laun FB, Weber MA, Matthies C, Semmler W, Schad LR. Sodium MRI using a density-adapted 3D radial acquisition technique. *Magn Reson Med*. 2009;62(6):1565-1573. doi:10.1002/mrm.22157
  15. Qirjazi E, Salerno FR, Akbari A, et al. Tissue sodium concentrations in chronic kidney disease and dialysis patients by lower leg sodium-23 magnetic resonance imaging. *Nephrol Dial Transplant*. 2020;Apr 6. doi:10.1093/ndt/gfaa036
  16. Schwartz GJ, Work DF. Measurement and estimation of GFR in children and adolescents. *Clin J Am Soc Nephrol*. 2009;4(11):1832-1843. doi:10.2215/CJN.01640309
  17. Schwartz GJ, Schneider MF, Maier PS, et al. Improved equations estimating GFR in children with chronic kidney disease using an immunonephelometric determination of cystatin C. *Kidney Int*. 2012;82(4):445-453. doi:10.1038/ki.2012.169

18. KDIGO 2012 Clinical Practice Guideline for the Evaluation and Management of Chronic Kidney Disease. *Kidney Int Suppl.* 2013;3(1):4-4. doi:10.1038/kisup.2012.76
19. Rossitto G, Mary S, Chen JY, et al. Tissue sodium excess is not hypertonic and reflects extracellular volume expansion. *Nat Commun.* 2020;11(1):1-9. doi:10.1038/s41467-020-17820-2
20. Palmer LG, Schnermann J. Integrated control of na transport along the nephron. *Clin J Am Soc Nephrol.* 2015;10(4):676-687. doi:10.2215/CJN.12391213
21. Bovée DM, Cuevas CA, Zietse R, Danser AHJ, Mirabito Colafella KM, Hoorn EJ. Salt-sensitive hypertension in chronic kidney disease: Distal tubular mechanisms. *Am J Physiol - Ren Physiol.* 2020;319(5):F729-F745. doi:10.1152/ajprenal.00407.2020
22. Rossitto G, Delles C. Mechanisms of sodium-mediated injury in cardiovascular disease: old play, new scripts. *FEBS J.* Published online 2021:1-14. doi:10.1111/febs.16155
23. Hanson P, Philp CJ, Randeva HS, et al. Sodium in the dermis collocates to glycosaminoglycan scaffold, with diminishment in type 2 diabetes mellitus. *JCI Insight.* 2021;6(12):1-16. doi:10.1172/jci.insight.145470
24. Roth S, Markó L, Birukov A, et al. Tissue Sodium Content and Arterial Hypertension in Obese Adolescents. *J Clin Med.* 2019;8(12):2036. doi:10.3390/jcm8122036
25. Zelikovic I. Hypokalaemic salt-losing tubulopathies: An evolving story. *Nephrol Dial Transplant.* 2003;18(9):1696-1700. doi:10.1093/ndt/gfg249
26. Filler G, Geda R, Salerno F, Zhang YC, de Ferris MEDG, McIntyre CW. Management of severe polyuria in idiopathic Fanconi syndrome. *Pediatr Nephrol.* 2021;36(11):3621-3626. doi:10.1007/s00467-021-05213-6
27. Hoorn EJ, Walsh SB, McCormick JA, et al. The calcineurin inhibitor tacrolimus activates

- the renal sodium chloride cotransporter to cause hypertension. *Nat Med.* 2011;17(10):1304-1309. doi:10.1038/nm.2497
28. Naesens M, Kuypers DRJ, Sarwal M. Calcineurin inhibitor nephrotoxicity. *Clin J Am Soc Nephrol.* 2009;4(2):481-508. doi:10.2215/CJN.04800908
29. Dagan A, Eisenstein B, Bar-Nathan N, et al. Tubular and glomerular function in children after renal transplantation. *Pediatr Transplant.* 2005;9(4):440-444. doi:10.1111/j.1399-3046.2005.00302.x
30. Kopp C, Linz P, Wachsmuth L, et al. <sup>23</sup>Na magnetic resonance imaging of tissue sodium. *Hypertension.* 2012;59(1):167-172. doi:10.1161/HYPERTENSIONAHA.111.183517
31. Shroff R, Weaver DJ, Mitsnefes MM. Cardiovascular complications in children with chronic kidney disease. *Nat Rev Nephrol.* 2011;7(11):642-649. doi:10.1038/nrneph.2011.116
32. MacHnik A, Neuhofer W, Jantsch J, et al. Macrophages regulate salt-dependent volume and blood pressure by a vascular endothelial growth factor-C-dependent buffering mechanism. *Nat Med.* 2009;15(5):545-552. doi:10.1038/nm.1960
33. Titze J, Maillet A, Lang R, et al. Long-term sodium balance in humans in a terrestrial space station simulation study. *Am J Kidney Dis.* 2002;40(3):508-516. doi:10.1053/ajkd.2002.34908
34. Birukov A, Rakova N, Lerchl K, et al. Ultra-long-term human salt balance studies reveal interrelations between sodium, potassium, and chloride intake and excretion. *Am J Clin Nutr.* 2016;104(1):49-57. doi:http://dx.doi.org/10.3945/ajcn.116.132951
35. Wang CY, Cogswell MM, Loria CC, et al. Urinary excretion of sodium, Potassium, and Chloride, but not Iodine, varies by timing of collection in a 24-hour calibration study. *J*

- Nutr.* 2013;143(8):1276-1282. doi:10.3945/jn.113.175927
36. Rakova N, Jüttner K, Dahlmann A, et al. Long-term space flight simulation reveals infradian rhythmicity in human Na<sup>+</sup>balance. *Cell Metab.* 2013;17(1):125-131. doi:10.1016/j.cmet.2012.11.013
37. Olde Engberink RHG, Van Den Hoek TC, Van Noordenne ND, Van Den Born BJH, Peters-Sengers H, Vogt L. Use of a single baseline versus multiyear 24-hour urine collection for estimation of long-term sodium intake and associated cardiovascular and renal risk. *Circulation.* 2017;136(10):917-926. doi:10.1161/CIRCULATIONAHA.117.029028
38. Unruh ML, Pankratz VS, Demko JE, Ray EC, Hughey RP, Kleyman TR. Trial of Amiloride in Type 2 Diabetes With Proteinuria. *Kidney Int Reports.* 2017;2(5):893-904. doi:10.1016/j.ekir.2017.05.008

## Chapter 4

### Tissue Sodium and Cardiac Structure in Chronic Hemodialysis Patients

*In this study, we investigated the relationship between tissue  $[Na^+]$  and cardiac structure, in patients receiving HD.*

*A version of this chapter has been submitted to the journal “Hemodialysis International” and is currently under peer review (ID: HDI-22-0128).*

#### 4.1 Introduction

Patients requiring long term HD commonly display left ventricular hypertrophy (LVH) and abnormal left ventricular (LV) geometry.<sup>1</sup> LVH itself is common in the HD population, with a prevalence from 44% to 64% within cardiac magnetic resonance imaging-based studies.<sup>2,3</sup> Furthermore, aberrant LV morphology is well-recognized as an independent prognostic factor for cardiovascular morbidity and mortality.<sup>4</sup> LVH can be further characterized into concentric hypertrophy (CH) or eccentric hypertrophy (EH), and each category has been associated with differing severity of effect on cardiovascular outcomes.<sup>5</sup>

ECV expansion is associated with increased total body sodium, and this is reflected by increased tissue  $[Na^+]$  measured with sodium-23 magnetic resonance imaging (<sup>23</sup>Na MRI).<sup>6,7</sup> ECV expansion is considered a fundamental driver of left ventricular mass (LVM) in CKD and dialysis patients.<sup>8</sup> In addition, Schneider et al recently showed that skin  $[Na^+]$ , as measured with <sup>23</sup>Na MRI of the leg, is a strong predictor of left LVM in CKD patients, suggesting that skin  $[Na^+]$  may have adverse effects on the cardiovascular system.<sup>9</sup> This may also be related to the effects of osmotically inactive

sodium deposits at the skin dermis level.<sup>9</sup> We have recently shown that HD patients exhibit greater tissue  $[\text{Na}^+]$  compared with healthy individuals, and that skin  $[\text{Na}^+]$  is associated with adverse outcomes in these patients.<sup>10,11</sup> At present, however, no data is currently available on the relationship between tissue  $[\text{Na}^+]$  and LV structure in HD patients: we hypothesized that whole-leg and skin  $[\text{Na}^+]$  were associated with LVH and other markers of LV structure, such as end-diastolic volume and geometry.

## **4.2 Materials and Methods**

Study participants underwent a single research visit on a non-HD day (during the short interdialytic interval). This consisted of an imaging session, clinical data collection and collection of blood for laboratory analysis. All study participants signed informed consent prior to study enrollment. The study received approval from the Western University Human Research Ethics board and was conducted in compliance with the Declaration of Helsinki and all applicable regulatory requirements (ClinicalTrials.gov: NCT03004547).

Study patients were recruited between March 2018 to March 2020 from the London Health Sciences Centre, London, ON, Canada, from a maintenance HD population established on a stable HD prescription for at least three months. Potential study candidates were excluded if pregnant, breastfeeding or intending pregnancy, unable to provide consent or had contraindications to MRI. Participant information were extracted from digital chart and HD treatment chart review. HD treatment information were collected relative to the HD session immediately prior and after the study visit and averaged. Office BP was measured with a clinically validated oscillometric automatic sphygmomanometer after five minutes of rest in a quiet room; three consecutive measurements were collected and the average was recorded for analysis.

Study participants underwent  $^{23}\text{Na}$  MRI of the leg as previously described by our group.<sup>10</sup>  $^{23}\text{Na}$  concentration maps were computed using saline calibration phantoms containing increasing sodium chloride concentrations. Two regions of interest, delineating the whole leg and the whole skin were delineated manually using Horos software v4.0.0 (Horosproject.org, Nimble Co LLC d/b/a Purview, Annapolis, MD, USA), and the average signal intensity were reported as whole-leg  $[\text{Na}^+]$  and skin  $[\text{Na}^+]$ .

Echocardiography was performed by an experienced member of the research team on the day of the visit, using a Vivid Q (GE Healthcare) ultrasound machine. All measurements were performed offline on the EchoPAC Software (GE Healthcare), were repeated three times in consecutive heart cycles and average measurements were reported for each individual participant. LVM was calculated using the linear method from 2D parasternal long axis images and indexed to height<sup>2,7</sup> (LVMI) due to the high prevalence of obesity in the study population, as according to the current American Society of Echocardiography (ASE) guidelines.<sup>12</sup> LVH was defined as LVMI above  $51.0 \text{ g/m}^{2,7}$  regardless of sex, according to previously published literature.<sup>4</sup> Relative wall thickness (RWT) was calculated according to the formula:  $\text{RWT} = (2 * \text{posterior wall thickness at end-diastole}) / (\text{LV internal diameter at end-diastole})$ . A cut-off RWT value  $>0.42$  was considered abnormal. LV geometry was classified into normal geometry (normal LVMI and RWT), concentric remodeling (normal LVMI, increased RWT), eccentric hypertrophy (increased LVMI, normal RWT) and concentric hypertrophy (increased LVMI and RWT), as defined by the ASE guidelines.<sup>12</sup> Left ventricular end-diastolic volume (LVEDV) and ejection fraction (LVEF) were measured from standard apical four and two-chamber views, according to the Simpson biplane method. LVEDV was indexed to body surface area (LVEDV/BSA).

### *Sample Size Justification and Statistical Methods*

To our knowledge, only one study has reported on correlation between LVM (using cardiac MRI) and skin  $[Na^+]$  in patients with CKD, with an  $r=0.56$ .<sup>9</sup> Utilizing data from this study, we calculated a minimum of 26 participants were required to detect an  $r=0.5$  with  $\alpha=0.05$  and 80% power. The analysis plan was primarily focused at detecting a statistically significant correlation between LVMI and whole-leg and skin  $[Na^+]$ ; secondary analyses aimed at the exploring the correlation between whole-leg and skin  $[Na^+]$  with LVEDV and LVEF, and differences in whole-leg and skin  $[Na^+]$  according to LV geometry.

We presented data stratifying participants according to LVH status. Continuous variables were presented as mean  $\pm$  standard deviation (SD) or median (interquartile range, IQR) depending on data distribution. Categorical variables are presented as ratio and percentages. Pearson correlation was used to investigate the association between whole-leg and skin  $[Na^+]$  and echocardiography parameters of interest. Student's  $t$  test for independent samples was used to compare continuous variables between non-LVH and LVH groups. Kruskal-Wallis one-way analysis of variance (ANOVA) with Dunn's post hoc test was used to compare Skin  $[Na^+]$  between LV geometry groups. Statistical analysis was performed with GraphPad Prism v9.0.0 for Mac, GraphPad Software, San Diego, CA USA ([www.graphpad.com](http://www.graphpad.com)) and R v3.6.2, R Foundation for Statistical Computing, Vienna, Austria. (<https://www.R-project.org/>).

### **4.3 Results**

31 participants underwent the study procedures. One patient was excluded from analysis due to significant motion artifacts during MRI that made it impossible to compute  $^{23}Na$  concentration maps.

Table 4.1 summarizes the clinical information of the overall sample and after LVH stratification.

Table 4.1: Characteristics of the study sample, stratified by left ventricular hypertrophy.

	<b>Overall (n=30)</b>	<b>No LVH (n=12)</b>	<b>LVH (n=18)</b>
<b><i>Demographics &amp; Anthropometrics</i></b>			
<b>Sex (M/F)</b>	17/13	6/6	11/7
<b>Age (years)</b>	66 ± 11	64 ± 12	66 ± 10
<b>BMI (kg/m<sup>2</sup>)</b>	31.8 ± 6.4	29.3 ± 5.9	33.5 ± 6.3
<b>Residual Renal Volume (ml/24h)</b>	273 ± 352	316 ± 378	244 ± 342
<b><i>HD Treatment Details</i></b>			
<b>HD Vintage (months)</b>	22.0 (11.3-32.5)	22.0 (16.5-30.3)	20.0 (11.3-32.5)
<b>HD Treatment Time (h/week)</b>	12.0 (10.5-12.0)	12.0 (10.5-12.0)	11.6 (10.5-12.0)
<b>Vascular Access (AVF/Catheter)</b>	13/17	4/8	9/9
<b>Average Weight Gain (%)</b>	2.1 ± 0.9	2.1 ± 1.2	2.2 ± 0.8
<b>[Na<sup>+</sup>]<sub>D</sub> (mmol/L)</b>	137 (137-140)	137 (137-139)	139 (137-140)
<b>Office SBP (mmHg)</b>	132 ± 26	118 ± 23	142 ± 26
<b>Office DBP (mmHg)</b>	75 ± 13	73 ± 15	73 ± 15
<b><i>Comorbidities</i></b>			
<b>Hypertension (%)</b>	77%	58%	89%
<b>Diabetes Mellitus (%)</b>	67%	58%	72%
<b>Ischemic Heart Disease (%)</b>	40%	25%	50%
<b>Congestive Heart Failure (%)</b>	23%	8%	33%
<b><i>Medications</i></b>			

<b>ACEi-ARB (%)</b>	23%	8%	33%
<b>Beta Blocker (%)</b>	47%	33%	56%
<b>Calcium Channel Blocker (%)</b>	43%	8%	67%
<b>Diuretic (%)</b>	40%	42%	39%
<i>Laboratory</i>			
<b>Hemoglobin (g/L)</b>	111 ± 12	113 ± 13	111 ± 13
<b>Serum Albumin (g/L)</b>	40.6 ± 3.4	42.5 ± 3.5	39.4 ± 2.9
<b>Serum CRP (mg/L)</b>	11.1 ± 17.7	8.2 ± 6.7	13.0 ± 22.2
<b>Serum PTH (pmol/L)</b>	58.7 ± 36.3	59.5 ± 45.6	58.1 ± 30.0
<b>Serum Sodium (mmol/L)</b>	137 ± 3	136 ± 3	137 ± 3

[Na<sup>+</sup>]<sub>D</sub>: dialysate sodium concentration; ACEi: angiotensin converting enzyme inhibitor; ARB: angiotensin receptor blocker; AVF: arterio-venous fistula; BMI: body mass index; BSA: body surface area; CRP: c-reactive protein; DBP: diastolic BP; HD: hemodialysis; LVH: left ventricular hypertrophy; PTH: parathyroid hormone; SBP: systolic BP.

Overall, 60% (n=18) of the study sample had LVH. Obesity was common in the study sample. Patients with LVH had higher whole-leg [Na<sup>+</sup>] and skin [Na<sup>+</sup>] compared with patients without LVH (whole-leg [Na<sup>+</sup>]:  $t(28)=2.53$ ,  $p<0.05$ ); skin [Na<sup>+</sup>]:  $t(28)=3.30$ ,  $p<0.01$ ). Of note, whole-leg [Na<sup>+</sup>] and skin [Na<sup>+</sup>] were strongly correlated with one another ( $r=0.85$ ). No significant differences in other demographics, anthropometrics and biomarkers were observed.

Skin [Na<sup>+</sup>], whole-leg [Na<sup>+</sup>] and echocardiography measurements are detailed in Table 4.2.

*Table 4.2: Imaging data, stratified by left ventricular hypertrophy.*

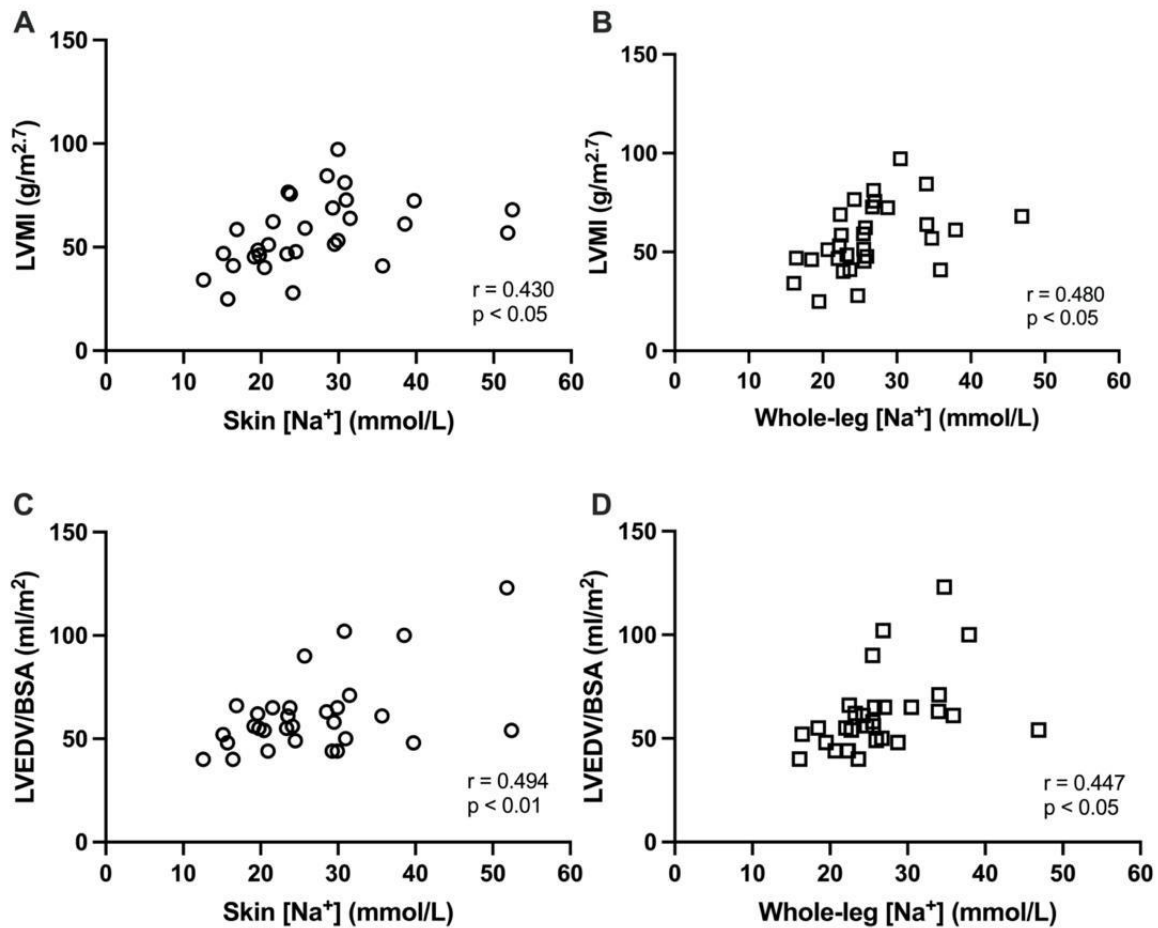
	<b>Overall (n=30)</b>	<b>No LVH (n=12)</b>	<b>LVH (n=18)</b>
<i><sup>23</sup>Na MRI</i>			
Skin [Na <sup>+</sup> ] (mmol/L)	26.7 ± 9.7	20.5 ± 7.5	30.9 ± 9.6
Whole-leg [Na <sup>+</sup> ] (mmol/L)	26.3 ± 6.7	23.3 ± 5.0	28.7 ± 6.7
<i>Echocardiography</i>			
IVSd (cm)	1.3 ± 0.2	1.1 ± 0.2	1.4 ± 0.2
LVEDd (cm)	5.0 ± 0.7	4.7 ± 0.6	5.2 ± 0.8
PWd (cm)	1.1 ± 0.2	1.0 ± 0.2	1.2 ± 0.2
LVEF (%)	55 ± 12	60 ± 6	52 ± 13
LVEDV (ml)	124 ± 41	102 ± 21	138 ± 45
LVEDV/BSA (ml/m <sup>2</sup> )	61.3 ± 19.2	52.3 ± 7.1	67.3 ± 22.5
LVM (g)	237 ± 71	173 ± 46	281 ± 47
LVMi (g/m <sup>2.7</sup> )	56.8 ± 16.7	40.9 ± 7.9	67.5 ± 12.4
RWT	0.46 ± 0.12	0.42 ± 0.10	0.49 ± 0.14

BSA: body surface area; IVSd: end-diastolic interventricular septum thickness; LVEDd: left ventricular end-diastolic diameter; LVEDV: left ventricular end-diastolic volume; LVEF: left ventricular ejection fraction; LVESV: left ventricular end-systolic volume; LVM: left ventricular mass; LVMi: left ventricular mass index (height<sup>2.7</sup>); MRI: magnetic resonance imaging; PWd: end-diastolic posterior wall thickness; RWT: relative wall thickness; Skin [Na<sup>+</sup>]: skin sodium-23 concentration; Whole-leg [Na<sup>+</sup>]: whole-leg sodium-23 concentration.

LVEF was largely preserved in the study sample, regardless of LVH status. Eight participants were classified as having a normal geometry (NG), five concentric remodeling (CR), eleven concentric hypertrophy (CH), six eccentric hypertrophy (EH), according to LVH status and RWT.

Figure 4.1 shows the correlations between tissue  $[\text{Na}^+]$  (skin and whole-leg), LVMI and LVEDV/BSA; both skin  $[\text{Na}^+]$  and whole-leg  $[\text{Na}^+]$  were positively associated with greater LVMI (Skin  $[\text{Na}^+]$ :  $r=0.425$ ,  $p<0.05$ ; whole-leg  $[\text{Na}^+]$ :  $r=0.480$ ,  $p<0.05$ ) and LVEDV/BSA (skin  $[\text{Na}^+]$ :  $r=0.494$ ,  $p<0.01$ ; whole-leg  $[\text{Na}^+]$ :  $r=0.447$ ,  $p<0.05$ ).

Figure 4.1: Correlation between tissue  $[Na^+]$  (skin, whole-leg  $[Na^+]$ ) with LVMI (A, B) and LVEDV/BSA (C, D), respectively.

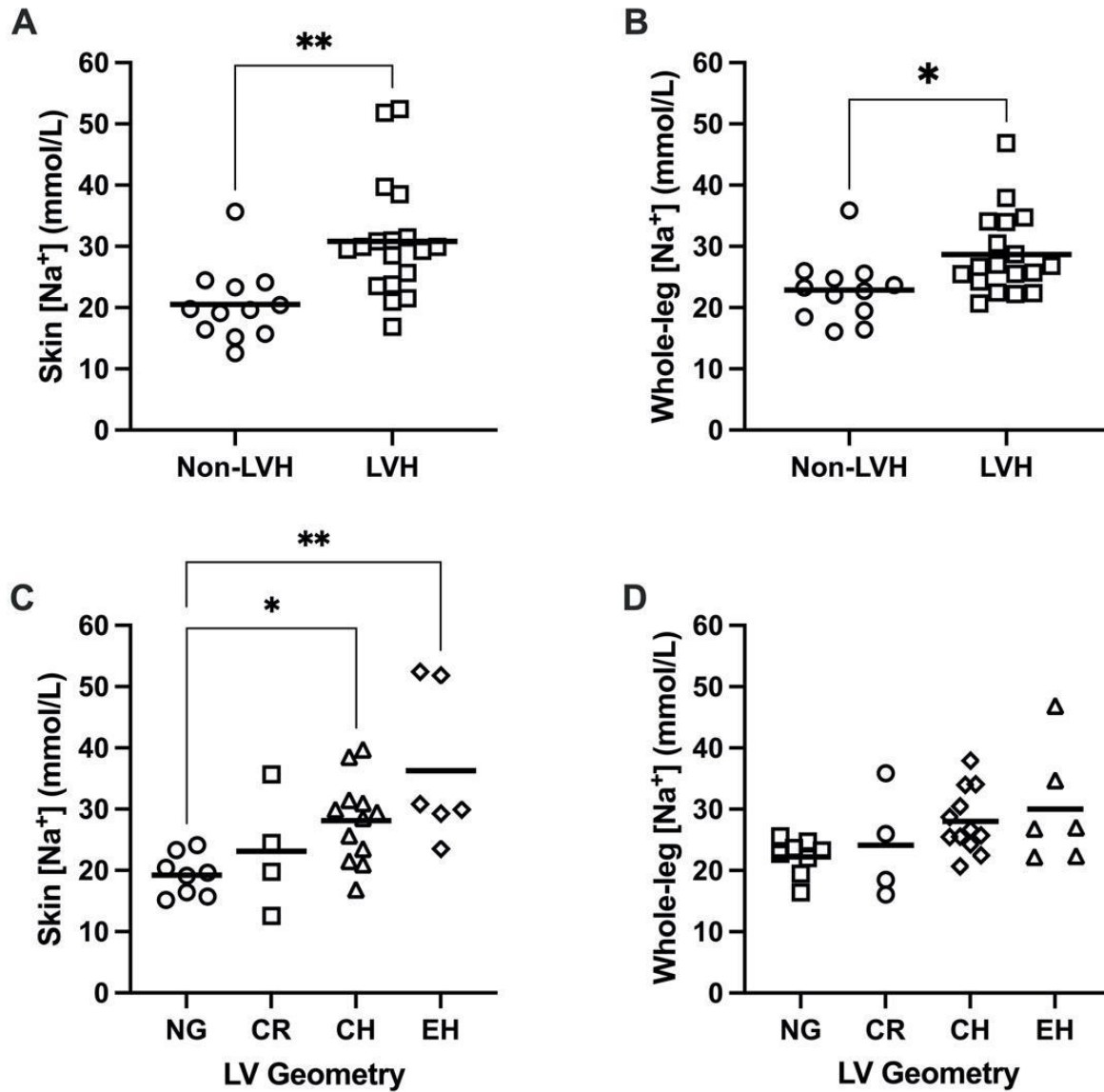


LVEDV/BSA: left ventricular end-diastolic volume / body surface area; LVMI: left ventricular mass index (height in m<sup>2.7</sup>).

Figure 4.2 shows the differences in skin and whole-leg  $[Na^+]$  according to LVH status (panels A,B) and LV geometry (panels C, D). Both skin and whole-leg  $[Na^+]$  were significantly higher in patients with LVH (skin  $[Na^+]$ :  $20.5 \pm 6.0$  mmol/L vs  $30.9 \pm 9.6$  mmol/L,  $p < 0.01$ ; whole-leg  $[Na^+]$ :  $22.9 \pm 5.3$  mmol/L vs  $28.7 \pm 6.7$  mmol/L,  $p < 0.05$ ). Conversely, only skin  $[Na^+]$  was significantly different across LV geometry categories (Kruskal-Wallis statistic=12.6,  $p < 0.01$ ; NG vs CH:  $19.2 \pm 3.4$  mmol/L vs  $28.1 \pm 6.9$  mmol/L,  $p < 0.05$ ; NG vs EH:  $19.2 \pm 3.4$  mmol/L vs  $36.3 \pm 12.5$

mmol/L,  $p < 0.01$ ). A trend for increasing whole-leg  $[Na^+]$  across LV geometry categories was observed, although it failed to reach statistical significance (Kruskal-Wallis statistic=6.6,  $p=0.09$ ).

Figure 4.2: Tissue  $[Na^+]$  (skin, whole-leg  $[Na^+]$ ) according to LVH (A, B) and to LV geometry category (C, D), ordered by known escalating influence on negative cardiovascular outcomes.



CH: concentric hypertrophy; CR: concentric remodeling; EH: eccentric hypertrophy; LVH: left ventricular hypertrophy; NG: normal geometry. \* =  $p < 0.05$ ; \*\* =  $p < 0.01$

## 4.4 Discussion

The main finding of this study is that quantitative  $^{23}\text{Na}$  MRI measures of tissue  $[\text{Na}^+]$ , namely whole-leg and skin  $[\text{Na}^+]$ , are associated with greater LVMI, LVEDV/BSA and LVH in patients receiving long-term HD.

ECV expansion is an increasingly recognized problem in the HD population and has been shown to correlate with LVH as well as clinical outcomes.<sup>13</sup> According to traditional Edelman physiology, sodium is the main extracellular cation and an increase in total body sodium is a hallmark of ECV expansion.<sup>14</sup> Indeed, tissue  $[\text{Na}^+]$  measured with  $^{23}\text{Na}$  MRI reflects tissue sodium content per unit of volume, as a function of both extracellular and intracellular volume.<sup>6,7</sup> Therefore, an increase in tissue  $[\text{Na}^+]$  will primarily reflect ECV expansion in the tissue volume of interest.

Furthermore, recent evidence suggests that humans are able to accumulate sodium independently of water mainly at the dermal skin level, bound to negatively-charged glycosaminoglycans and regulated by immune-mediated pathways.<sup>15,16</sup> These findings have been recently confirmed visually using ultra-high field triple quantum filtering  $^{23}\text{Na}$  MRI in ex vivo human skin samples from healthy volunteers and patients with type 2 diabetes mellitus.<sup>17</sup> In addition, the referenced study suggested that  $^{23}\text{Na}$  MRI using ultra-short echo time (UTE) pulse sequences (such as the one used in the present study) is incapable of detecting the signal from bound tissue sodium as a result of rapid signal decay due to its interactions with the glycosaminoglycan matrix, and that tissue  $[\text{Na}^+]$  would essentially be a function of sodium dissolved in water.

The present findings are in line with the results reported by Schneider and co-workers: the authors found a relationship between skin  $[\text{Na}^+]$  and LVM in 99 non-dialysis CKD patients as measured with cardiac MRI; in multiple regression modeling the relationship was independent of SBP and

bioimpedance spectroscopy measures of fluid overload, which the authors attributed to water-free skin sodium accumulation.<sup>9</sup>

The relationship between tissue  $[\text{Na}^+]$  and LV dilation has not been reported before. We also report for the first time that abnormal LV geometry, specifically CH and EH, traditionally associated with poorer cardiovascular outcomes, is significantly associated with higher skin  $[\text{Na}^+]$ . EH in particular is associated with previous cardiac events, ECV expansion and increased risk of sudden cardiac death, compared with CH.<sup>5</sup>

Hence, we suggest that increased tissue  $[\text{Na}^+]$  as detected by  $^{23}\text{Na}$  MRI in HD patients reflects ECV expansion, as previously mentioned,<sup>6,7,17</sup> and plays a significant role in determining LV dilation and abnormal LV geometry.

Several therapeutic options have been shown to reduce skin  $[\text{Na}^+]$ , such as ultrafiltration and diuretic therapies in several clinical settings.<sup>18-20</sup> A recent publication from our group also suggests that reducing the dialysate  $[\text{Na}^+]$  was associated with lower skin  $[\text{Na}^+]$ , although it was not possible to discriminate the underlying mechanisms.<sup>21</sup> Recent trial findings may provide additional support on the causal relationship between total body sodium and cardiac structure: indeed, improved ECV management may explain the findings of the Frequent Hemodialysis Network Daily Trial, where frequent daily HD was associated with improvements in LVM and LVEDV.<sup>22,23</sup>

From an imaging biomarker perspective, whole-leg  $[\text{Na}^+]$  reflects  $[\text{Na}^+]$  from all anatomical structures in the leg (skin, muscles, blood vessels, skeletal bones), and its delineation does not require high image resolution; conversely, skin  $[\text{Na}^+]$  requires sufficient image resolution for the region of interest to be delineated and avoid significant partial voluming effects. We show here that both biomarkers are similarly related to structural echocardiography measures. This is likely

due to both biomarkers measuring the signal from sodium dissolved in extracellular water, as previously mentioned.<sup>17</sup>

Study limitations include a cross-sectional design, single-center experience and the use of echocardiography, which is known to overestimate LVM compared to MRI;<sup>2</sup> in addition, no assessment of volume status was performed with bioimpedance spectroscopy – therefore it was not possible to relate tissue  $[\text{Na}^+]$  with other measures of ECV. The association between tissue  $[\text{Na}^+]$  and echocardiography measurements was not corrected for potential confounders. The association between tissue  $[\text{Na}^+]$  and LV geometry was exploratory, and its significance limited by the small and uneven number of cases per group.

We conclude that tissue  $[\text{Na}^+]$  is associated with worse cardiac structure and may be an important mediator of cardiovascular outcomes in the HD population: this highlights the central role of ECV expansion and sodium balance in HD. In this respect,  $^{23}\text{Na}$  MRI offers a quantifiable target to test the effects of optimized sodium removal strategies on cardiovascular outcomes for future clinical trials.

## 4.5 Bibliography

1. Foley N, Harnett D, Barr E, Robert, N. Foley Patrick and Paul E. Barr, S. Parfrey, John D. Harnett, Gloria M. Kent DCM and PEB. The Prognostic Importance Uremic Cardiomyopathy. *J Am Soc Nephrol*. 1995;5(12):2024-2031.
2. Grebe SJ, Malzahn U, Donhauser J, et al. Quantification of left ventricular mass by echocardiography compared to cardiac magnet resonance imaging in hemodialysis patients. *Cardiovasc Ultrasound*. 2020;18(1):1-9. doi:10.1186/s12947-020-00217-y
3. Patel RK, Oliver S, Mark PB, et al. Determinants of left ventricular mass and hypertrophy in hemodialysis patients assessed by cardiac magnetic resonance imaging. *Clin J Am Soc Nephrol*. 2009;4(9):1477-1483. doi:10.2215/CJN.03350509
4. Zoccali C, Benedetto FA, Mallamaci F, et al. Prognostic impact of the indexation of left ventricular mass in patients undergoing dialysis. *J Am Soc Nephrol*. 2001;12(12):2768-2774.
5. De Roij Van Zuijdewijn CLM, Hansildaar R, Bots ML, et al. Eccentric Left Ventricular Hypertrophy and Sudden Death in Patients with End-Stage Kidney Disease. *Am J Nephrol*. 2015;42(2):126-133. doi:10.1159/000439447
6. Rossitto G, Touyz RM, Petrie MC, Delles C. “Much ado about N . . . Atrium: Modelling tissue sodium as a highly sensitive marker of subclinical and localised oedema.” *Clin Sci*. 2018;132(24):2609-2613. doi:10.1042/CS20180575
7. Rossitto G, Mary S, Chen JY, et al. Tissue sodium excess is not hypertonic and reflects extracellular volume expansion. *Nat Commun*. 2020;11(1):1-9. doi:10.1038/s41467-020-17820-2
8. Hur E, Usta M, Toz H, et al. Effect of fluid management guided by bioimpedance

- spectroscopy on cardiovascular parameters in hemodialysis patients: A randomized controlled trial. *Am J Kidney Dis.* 2013;61(6):957-965. doi:10.1053/j.ajkd.2012.12.017
9. Schneider MP, Raff U, Kopp C, et al. Skin Sodium Concentration Correlates with Left Ventricular Hypertrophy in CKD. *J Am Soc Nephrol.* 2017;28(6):1867-1876. doi:10.1681/asn.2016060662
  10. Qirjazi E, Salerno FR, Akbari A, et al. Tissue sodium concentrations in chronic kidney disease and dialysis patients by lower leg sodium-23 magnetic resonance imaging. *Nephrol Dial Transplant.* 2020;Apr 6. doi:10.1093/ndt/gfaa036
  11. Salerno FR, Akbari A, Lemoine S, Filler G, Scholl TJ, McIntyre CW. Outcomes and predictors of skin sodium concentration in dialysis patients. *Clin Kidney J.* Published online January 28, 2022:sfac021. doi:10.1093/ckj/sfac021
  12. Lang RM, Badano LP, Mor-Avi V, et al. Recommendations for cardiac chamber quantification by echocardiography in adults: An update from the American society of echocardiography and the European association of cardiovascular imaging. *Eur Heart J Cardiovasc Imaging.* 2015;16(3):233-271. doi:10.1093/ehjci/jev014
  13. Zoccali C, Moissl U, Chazot C, et al. Chronic fluid overload and mortality in ESRD. *J Am Soc Nephrol.* 2017;28(8):2491-2497. doi:10.1681/ASN.2016121341
  14. EDELMAN IS, LEIBMAN J, O'MEARA MP, BIRKENFELD LW. Interrelations between serum sodium concentration, serum osmolarity and total exchangeable sodium, total exchangeable potassium and total body water. *J Clin Invest.* 1958;37(9):1236-1256. doi:10.1172/JCI103712
  15. Titze J, Lang R, Ilies C, et al. Osmotically inactive skin Na + storage in rats. *Am J Physiol Physiol.* 2003;285(6):F1108-F1117. doi:10.1152/ajprenal.00200.2003

16. Titze J, Shakibaei M, Schafflhuber M, et al. Glycosaminoglycan polymerization may enable osmotically inactive Na<sup>+</sup> storage in the skin. *Am J Physiol Circ Physiol*. 2004;287(1):H203-H208. doi:10.1152/ajpheart.01237.2003
17. Hanson P, Philp CJ, Randevara HS, et al. Sodium in the dermis colocalizes to glycosaminoglycan scaffold, with diminishment in type 2 diabetes mellitus. *JCI Insight*. 2021;6(12):1-16. doi:10.1172/jci.insight.145470
18. Dahlmann A, Dörfelt K, Eicher F, et al. Magnetic resonance-determined sodium removal from tissue stores in hemodialysis patients. *Kidney Int*. 2015;87(2):434-441. doi:10.1038/ki.2014.269
19. Hammon M, Grossmann S, Linz P, et al. <sup>23</sup>Na magnetic resonance imaging of the lower leg of acute heart failure patients during diuretic treatment. *PLoS One*. 2015;10(10):1-13. doi:10.1371/journal.pone.0141336
20. Karg M V., Bosch A, Kannenkeril D, et al. SGLT-2-inhibition with dapagliflozin reduces tissue sodium content: A randomised controlled trial. *Cardiovasc Diabetol*. 2018;17(1):1-8. doi:10.1186/s12933-017-0654-z
21. Lemoine S, Salerno FR, Akbari A, Mcintyre CW. Influence of Dialysate Sodium Prescription on Skin and Muscle Sodium Concentration. *Am J Kidney Dis*. 2021;Jan 8:S0272-6386(21)00005-6. doi:10.1053/j.ajkd.2020.11.025
22. Chan CT, Greene T, Chertow GM, et al. Determinants of left ventricular mass in patients on hemodialysis: Frequent hemodialysis network (FHN) trials. *Circ Cardiovasc Imaging*. 2012;5(2):251-261. doi:10.1161/CIRCIMAGING.111.969923
23. Chan CT, Greene T, Chertow GM, et al. Effects of frequent hemodialysis on ventricular volumes and left ventricular remodeling. *Clin J Am Soc Nephrol*. 2013;8(12):2106-2116.

doi:10.2215/CJN.03280313

## Chapter 5

### Outcomes and Predictors Associated with Skin Sodium Concentration in Dialysis Patients

*In this study, we investigated the clinical predictors of skin  $[Na^+]$  as well as the relationship between skin  $[Na^+]$  with clinical outcomes in patients receiving HD and PD.*

*A version of this chapter has been published in the “Clinical Kidney Journal” Salerno FR, Akbari A, Lemoine S, Filler G, Scholl TJ, McIntyre CW. Outcomes and predictors of skin  $[Na^+]$  in dialysis patients. Clin Kidney J. 2022 Jan 28;15(6):1129-1136. doi: 10.1093/ckj/sfac021. PMID: 35664280. This article is available under the terms of the Creative Commons Attribution License.*

#### 5.1 Introduction

Sodium-23 magnetic resonance imaging ( $^{23}Na$  MRI) is an emerging imaging technique in clinical nephrology.<sup>1</sup> The potential of  $^{23}Na$  MRI lies in the ability to visualize and quantify  $[Na^+]$  directly at the tissue level – of special interest in CKD and dialysis population where sodium excretion is impaired as a consequence of kidney failure. Methods to quantify skin  $[Na^+]$  are attracting increasing interest to study peripheral edema and water-independent sodium accumulation;<sup>2</sup> however, clear evidence linking skin  $[Na^+]$  with clinical outcomes is currently lacking. At present, ECV overload is a well-described predictor of clinical outcomes in the kidney failure population receiving dialysis.<sup>3,4</sup> Skin water-independent sodium accumulation likely plays an additional clinically significant role: this has been linked with increased left ventricular mass in non-dialysis CKD patients, independently of ECV overload.<sup>5</sup> Furthermore, skin  $[Na^+]$  has been shown to be

modifiable by interventions such as loop diuretics, SGLT2 inhibitors and ultrafiltration with HD.<sup>6-</sup>

<sup>8</sup> Skin [Na<sup>+</sup>] may be an attractive and modifiable biomarker to assess volume status to be directly addressed therapeutically.

In the present study, we explored the hypothesis that skin [Na<sup>+</sup>] is associated with mortality and major adverse cardiovascular events (MACE) in a cohort of HD and PD patients who underwent interdialytic <sup>23</sup>Na MRI of the leg. Furthermore, we aimed to define the determinants associated with increased skin [Na<sup>+</sup>].

## 5.2 Materials and Methods

### *Study design*

This was an observational, exploratory study. Study participants underwent a visit consisting of a research imaging session ( $^1\text{H}$  and  $^{23}\text{Na}$  MRI of either the right or left leg), demographic and clinical data collection and blood biochemistry. HD patients were scanned on the day following their last HD treatment, whenever feasible. Outcomes were assessed retrospectively by clinical chart review.

The study received approval from the Western University Human Research Ethics board and was conducted in compliance with the Declaration of Helsinki and all applicable regulatory requirements. This study was prospectively registered (ClinicalTrials.gov Identifier: NCT03004547).

### *Study participants*

Study patients were recruited between March 2018 to March 2020 from the London Health Sciences Centre (LHSC), London, ON, Canada. All study participants provided written informed consent. Study participants were recruited from the prevalent LHSC outpatient dialysis population and were on their established treatment modality (thrice-weekly HD or PD) for at least three months before recruitment. Potential study candidates were excluded if pregnant, breastfeeding or intending pregnancy, unable to provide consent or had contraindications to MRI.

### *Dialysate $[\text{Na}^+]$ prescription*

Dialysate  $[\text{Na}^+]$  was prescribed either according to dialysis unit protocol – within the LHSC organization, one unit used 137 mmol/L and the other 140 mmol/L – or individualized following

clinical indications (e.g. to match low serum  $[\text{Na}^+]$  or improve intradialytic hemodynamic stability) in selected patients. HD standard-of-care did not differ between units, except for dialysate  $[\text{Na}^+]$  prescription.

### *Magnetic Resonance Imaging and Image Analysis*

All magnetic resonance images were acquired using a multinuclear 3.0 Tesla GE MRI scanner (Discovery MR750, General Electric Healthcare, Milwaukee, WI, USA). To acquire  $^{23}\text{Na}$  spin density images, subjects were positioned in the magnet bore in the supine position, with the thickest part of their right or left calf muscle at the center of a custom-made  $^{23}\text{Na}$  birdcage radiofrequency coil. Calibration vials with increasing saline concentrations were placed in the RF coil over the subjects' shins. A single-slice  $^{23}\text{Na}$  MR image was obtained with a radial k-space acquisition pulse sequence (Density-Adapted 2D Projection Reconstruction),<sup>9</sup> with the following parameters: slice-selective radiofrequency pulse; flip angle  $90^\circ$ ; repetition time/echo time: 100/1.2 msec; number of signals averages: 100; slice thickness: 30 mm and isotropic field of view/resolution: 18/0.3  $\text{cm}^2$ ; total acquisition time: ~30 minutes. During the same imaging session, additional axial  $^1\text{H}$  MR images were acquired using a standard (Spoiled Gradient-Recalled Echo) pulse sequence to identify and delineate the relevant anatomical structures.

$^{23}\text{Na}$  concentration maps were generated using custom software developed within MATLAB, version 9.6.0 – R2019a (The MathWorks Inc., Natick, Massachusetts). A region of interest encompassing the whole skin (Skin  $[\text{Na}^+]$ ) was manually segmented after superimposing  $^1\text{H}$  and  $^{23}\text{Na}$  images, as detailed previously.<sup>10</sup>

### *Laboratory Analysis*

Blood samples collected from each participant were processed and analyzed in a central laboratory (London Health Sciences Centre, London, Ontario, Canada) for routine clinical biomarkers. Due to the high prevalence of diabetes mellitus in the study sample, serum sodium was corrected for serum glucose concentration as according to Katz.<sup>11</sup>

### *Outcomes and Statistical Analysis*

Statistical analysis was performed using GraphPad Prism version 9.0.0 (GraphPad Software, San Diego, CA, USA; [www.graphpad.com](http://www.graphpad.com)) and SPSS Version 27.0 (IBM Corp. Released 2020. IBM SPSS Statistics for MacIntosh, Armonk, NY: IBM Corp). Normality was assessed both graphically and with the Shapiro–Wilk test. Continuous variables were presented as mean (standard deviation, SD) if normally distributed and median (minimum, interquartile range (IQR), maximum) if highly skewed. Categorical variables were expressed as ratios or percentages. The study sample was stratified into four groups according to skin  $[\text{Na}^+]$  quartiles. Comparisons between two subgroups were performed with the Mann-Whitney U test; differences between quartiles were computed using one-way analysis of variance (ANOVA). The following outcomes were of interest for this study: all-cause mortality and a composite of all-cause mortality and MACE, the latter defined as: acute coronary syndrome, congestive heart failure, stroke, pulmonary embolism. Outcomes were determined by clinical chart review and adjudicated by FRS and CWM. Participants who received kidney transplantation were right censored at the transplant date. Survival or event-free survival curves for each group were compared using the Kaplan-Meier function, and the log-rank test was used to analyze survival trends, assuming an incremental risk with increasing skin  $[\text{Na}^+]$  quartiles. This analysis was performed for all-cause mortality and the composite endpoint of mortality and

MACE. For both endpoints, univariate Cox proportional hazards regression was used to model the hazard ratios associated with skin  $[Na^+]$ , either as a continuous or as a categorical variable; multivariate models were created using the enter method to adjust skin  $[Na^+]$  hazard ratios for confounder variables commonly associated with mortality and MACE (age, sex, serum  $[Na^+]$ , serum albumin), with the idea that skin  $[Na^+]$  would be associated with clinical outcomes, even after adjustment for basic demographics and traditional predictors of cardiovascular morbidity and all-cause mortality (serum albumin and serum  $[Na^+]$ ).

Univariate linear regression was used to analyze the relationship between skin  $[Na^+]$  and main variables of interest (dialysate  $[Na^+]$ , corrected serum  $[Na^+]$ , serum albumin and age). Multiple linear regression analysis with the enter method was used to model the variables associated with skin  $[Na^+]$ ; the models were assembled to describe the dependence of skin  $[Na^+]$  from variables associated with volume overload (hypoalbuminemia, congestive heart failure), traditional measures of sodium status (serum  $[Na^+]$ ), dialysis-based factors (dialysate  $[Na^+]$ ) and demographics (age). Independent variables were selected according to the following criteria: (1) previous published evidence (age, serum albumin, dialysate  $[Na^+]$ ),<sup>8,10,12</sup> (2) pathophysiological rationale (congestive heart failure, serum  $[Na^+]$ ), (3) statistically significant difference across the skin  $[Na^+]$  quartiles (serum albumin, dialysate  $[Na^+]$ , serum  $[Na^+]$ ). To avoid model overfitting, no more than one predictor or confounder variable every ten cases was used in the models. Missing data was handled by list-wise deletion. Unstandardized  $\beta$  coefficients, R-squared and adjusted R-squared values for goodness-of-fit were reported. An  $\alpha < 0.05$  was considered statistically significant.

### 5.3 Results

A total of 52 patients (42 HD and 10 PD) completed the study. Table 5.1 shows the main characteristics of the study sample, as overall and after quartile stratification according to skin [Na<sup>+</sup>].

Table 5.1: Demographics, anthropometrics, clinical information and medications of the overall study sample and after Skin [Na<sup>+</sup>] quartile stratification.

Variable	Overall	Skin [Na <sup>+</sup> ] Q <sub>1</sub>	Skin [Na <sup>+</sup> ] Q <sub>2</sub>	Skin [Na <sup>+</sup> ] Q <sub>3</sub>	Skin [Na <sup>+</sup> ] Q <sub>4</sub>	<i>p</i>
<b>n</b>	52	11	13	15	13	
<b>Age (years)</b>	63.9 ± 10.2	59.0 ± 9.8	64.4 ± 13.9	64.2 ± 8.2	67.1 ± 7.8	0.288
<b>Sex (M/F)</b>	30/22	7/4	6/7	8/7	9/4	0.638
<b>BMI (kg/m<sup>2</sup>)</b>	30.1 ± 6.4	29.6 ± 7.2	30.3 ± 5.4	30.1 ± 5.5	30.4 ± 8.1	0.991
<b>HD/PD</b>	42/10	11/0	11/2	11/4	9/4	
<b>Dialysis Vintage (months) (Median (IQR))</b>	22.0 (11.8-33.5)	22.0 (19.0-29.5)	23.0 (14.0-37.0)	21.0 (12.5-32.0)	16.0 (4.0-24.0)	0.859
<b>Residual Urine Output (ml/24h) (Median (IQR))</b>	250.0 (0.0-750)	0.0 (0.0-150.0)	250.0 (0.0-400.0)	400.0 (200.0-1000.0)	300.0 (100.0-900.0)	0.219
<b>CCI (Median (IQR))</b>	6.0 (5.0-8.0)	5.0 (4.0-7.0)	7.0 (5.0-8.0)	6.0 (4.0-8.5)	7.0 (6.0-9.0)	0.284
<b>CKD Etiology</b>						
<b>Hypertensive Nephrosclerosis (%)</b>	15%	18%	31%	13%	0%	0.184
<b>Diabetic Kidney Disease (%)</b>	44%	27%	54%	27%	69%	0.074
<b>Glomerular Disease (%)</b>	10%	0%	0%	20%	15%	0.178
<b>Other (%)</b>	25%	55%	8%	33%	8%	<0.05
<b>Unknown (%)</b>	6%	0%	8%	7%	8%	0.832
<b>Comorbidities</b>						
<b>Hypertension (%)</b>	79%	82%	77%	67%	92%	0.418
<b>Coronary Artery Disease (%)</b>	35%	18%	38%	33%	46%	0.537
<b>Congestive Heart Failure (%)</b>	27%	18%	23%	27%	38%	0.704

<b>Diabetes Mellitus (%)</b>	60%	36%	69%	53%	77%	0.184
<i>Medications</i>						
<b>ACEi-ARB (%)</b>	29%	27%	38%	7%	46%	0.107
<b>Beta Blockers (%)</b>	52%	45%	69%	33%	62%	0.231
<b>Calcium Channel Blockers (%)</b>	52%	45%	38%	53%	69%	0.44
<b>Diuretic (%)</b>	50%	36%	54%	53%	54%	0.792
<i>Hemodialysis Information (n=42)</i>						
<b>Time Elapsed from Last HD to MRI (hours) (Median (IQR))</b>	22.5 (20.2-24.7)	22.5 (20.1-23.2)	23.9 (22.6-25.2)	21.0 (20.3-33.3)	22.8 (18.5-23.6)	0.523
<b>spKt/V</b>	1.30 ± 0.23	1.26 ± 0.28	1.34 ± 0.23	1.32 ± 0.19	1.26 ± 0.26	0.856
<b>Dialysate [Na<sup>+</sup>] (mmol/L) (Median (IQR))</b>	138.0 (137.0-140.0)	137.0 (137.0-137.0)	138.0 (137.0-140.0)	140.0 (137.5-140.0)	140.0 (140.0-140.0)	<0.001
<b>IDWG (%body weight)</b>	2.1 ± 1.2	2.1 ± 1.0	2.1 ± 1.0	1.8 ± 1.3	2.3 ± 1.5	0.88
<b>UFR (ml/kg/h)</b>	7.6 ± 3.7	8.3 ± 4.7	8.2 ± 3.3	7.1 ± 3.5	6.7 ± 3.5	0.713
<b>PreHD SBP (mmHg)</b>	142.5 ± 22.8	137.3 ± 25.7	153.5 ± 21.5	142.1 ± 14.0	135.9 ± 27.4	0.279
<b>PreHD DBP (mmHg)</b>	62.8 ± 15.3	68.0 ± 19.4	59.5 ± 15.1	67.0 ± 8.4	55.1 ± 14.6	0.18
<i><sup>23</sup>Na MRI</i>						
<b>Skin [Na<sup>+</sup>] (mmol/L)</b>	30.8 ± 11.3	17.4 ± 3.2	25.7 ± 2.5	31.7 ± 1.7	46.1 ± 8.6	<0.001
<i>Laboratory Analyses</i>						
<b>Corrected Serum [Na<sup>+</sup>] (mmol/L)</b>	137.9 ± 3.3	136.2 ± 5.1	136.3 ± 2.1	139.2 ± 2.1	139.3 ± 2.6	<0.05
<b>Serum [K<sup>+</sup>] (mmol/L)</b>	4.4 ± 0.7	4.6 ± 0.9	4.2 ± 0.7	4.4 ± 0.7	4.4 ± 0.6	0.59
<b>Serum [HCO<sub>3</sub><sup>-</sup>] (mmol/L)</b>	24.9 ± 4.0	22.9 ± 3.3	26.5 ± 3.9	26.4 ± 3.2	23.3 ± 4.6	<0.05
<b>Serum Creatinine (umol/L)</b>	630.5 ± 231.8	735.7 ± 271.2	614.0 ± 192.3	603.4 ± 240.9	589.3 ± 221.8	0.409
<b>Serum Urea (mmol/L)</b>	19.1 ± 6.8	24.1 ± 6.3	17.0 ± 4.6	17.0 ± 6.8	19.2 ± 7.2	<0.05
<b>Serum Glucose (mmol/L)</b>	8.5 ± 3.9	8.0 ± 3.5	7.7 ± 2.3	9.0 ± 5.4	9.0 ± 3.5	0.759
<b>Serum Albumin (g/L)</b>	39.9 ± 3.9	42.8 ± 3.8	41.1 ± 2.2	39.1 ± 3.6	37.2 ± 3.9	<0.01
<b>Hemoglobin (g/L)</b>	112.4 ± 14.2	116.8 ± 16.8	113.2 ± 13.9	113.5 ± 13.2	106.5 ± 13.1	0.339

Data are expressed as mean  $\pm$  SD unless otherwise noted. ACEi: angiotensin converting enzyme inhibitors; ADKPD: autosomal dominant polycystic kidney disease; APD: automated peritoneal dialysis; ARB: angiotensin II receptor blocker; BMI: body mass index; CAPD: continuous ambulatory peritoneal dialysis; CCI: Charlson comorbidity index; CKD: chronic kidney disease; DBP: diastolic BP; HD: hemodialysis; IDWG: interdialytic weight gain; IQR: interquartile range; PD: peritoneal dialysis; preHD: pre-dialysis; SBP: systolic BP; spKt/V: single-pool Kt/V; UFR: ultrafiltration rate.

Study participants tended to be older as skin  $[\text{Na}^+]$  quartiles increased. Participants in Q<sub>4</sub> tended to have a shorter dialysis vintage, larger comorbidity burden and more anti-hypertensive medications compared with Q<sub>1</sub>-Q<sub>3</sub>. Participants in Q<sub>3</sub> and Q<sub>4</sub> also tended to higher dialysate  $[\text{Na}^+]$ , corrected serum  $[\text{Na}^+]$  and lower serum albumin compared with Q<sub>1</sub> and Q<sub>2</sub>. Eight out of 42 HD patients were receiving an individualized dialysate  $[\text{Na}^+]$  prescription (median, range: 138 mmol/L, 135-145); 17 patients were receiving a dialysate  $[\text{Na}^+]$  prescription of 137 mmol/L; 17 patients were receiving a dialysate  $[\text{Na}^+]$  prescription of 140 mmol/L. Dialysate  $[\text{Na}^+]$  distribution according to skin  $[\text{Na}^+]$  quartiles is shown in Figure 5.1.



hours from the previous HD session. No significant differences in time were observed among skin  $[\text{Na}^+]$  quartiles.

### *Linear Regression Models*

Univariate linear regression yielded the following results (Table 5.2): Dialysate  $[\text{Na}^+]$  was significantly and positively associated with skin  $[\text{Na}^+]$  ( $F(1,40)= 26.79, R^2=0.40$ , unstandardized  $\beta = 3.79, p<0.001$ ); serum albumin was significantly and negatively associated with skin  $[\text{Na}^+]$  ( $F(1,50)= 12.62, R^2=0.20$ , unstandardized  $\beta = -1.30, p<0.001$ ); corrected serum  $[\text{Na}^+]$  was significantly and positively associated with skin  $[\text{Na}^+]$  ( $F(1,50)= 10.214, R^2=0.17$ , unstandardized  $\beta = 1.39, p<0.01$ ). The relationship between skin  $[\text{Na}^+]$  and age did not reach statistical significance ( $F(1,50)= 3.443, R^2=0.06$ , unstandardized  $\beta = 0.28, p=0.07$ ).

The results of the multiple linear regression analysis are summarized in Table 5.2. Using the enter method, Model 1 explained a significant amount of the variance in skin  $[\text{Na}^+]$  in HD patients ( $F(4,37)= 17.82, p<0.001, R^2=0.66, R^2_{adj}=0.62$ ). In particular, the following predictors were statistically significant: dialysate  $[\text{Na}^+]$  (unstandardized  $\beta = 3.33, p<0.001$ ), Serum albumin (unstandardized  $\beta = -1.18, p<0.001$ ), comorbid congestive heart failure (unstandardized  $\beta = 7.07, p<0.01$ ).

Model 2 included variables from both HD and PD patients, and was significant as well ( $F(3,48)= 7.35, p<0.001, R^2=0.32, R^2_{adj}=0.27$ ). Compared with Model 1, after the removal of dialysate  $[\text{Na}^+]$ , corrected serum  $[\text{Na}^+]$ , serum albumin (unstandardized  $\beta = -1.11, p<0.01$ ) and comorbid congestive heart failure (unstandardized  $\beta = 7.76, p<0.05$ ) were statistically significant explanatory variables of skin  $[\text{Na}^+]$ .

Table 5.2: Multiple Linear Regression models to explain Skin [Na<sup>+</sup>].

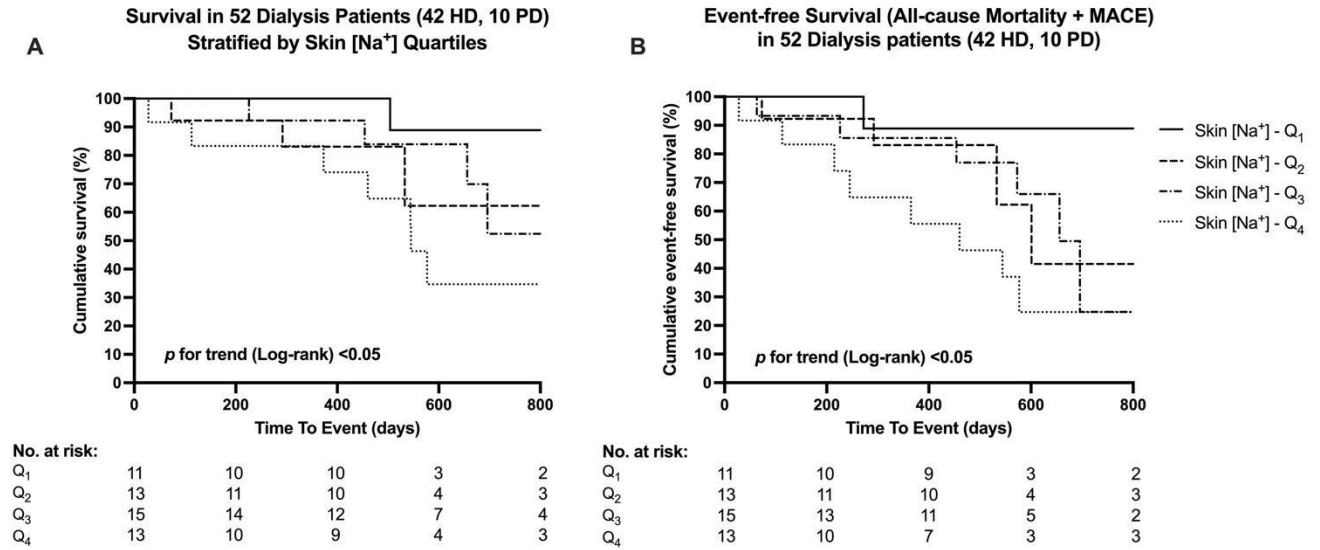
<b>Model 1: Dependent Variable: Skin [Na<sup>+</sup>] (HD)</b> <i>F</i> (4,37)= 17.82, <i>R</i> <sup>2</sup> =0.66, <i>R</i> <sup>2</sup> <sub>Adj</sub> =0.62, <i>p</i> <0.001		
<b>Independent Variable</b>	<b>Unstandardized β</b>	<b><i>p</i></b>
(Intercept)	-453.62	<0.001
Dialysate [Na <sup>+</sup> ]	3.33	<0.001
Serum Albumin	-1.18	<0.001
Congestive Heart Failure	7.07	<0.01
Corrected Serum [Na <sup>+</sup> ]	0.50	0.18
<b>Model 2: Dependent Variable: Skin [Na<sup>+</sup>] (HD &amp; PD)</b> <i>F</i> (4,47)= 9.573, <i>R</i> <sup>2</sup> =0.45, <i>R</i> <sup>2</sup> <sub>Adj</sub> =0.40, <i>p</i> <0.001		
<b>Independent Variable</b>	<b>Unstandardized β</b>	<b><i>p</i></b>
(Intercept)	-124.83	<0.05
Corrected Serum [Na <sup>+</sup> ]	1.29	<0.01
Serum Albumin	-0.89	<0.05
Congestive Heart Failure	9.33	<0.01
Age	0.17	0.17

### Outcomes

Follow-up and survival times, censoring, clinical events are summarized in Table 5.3. Of note, median follow-up time for the overall sample was 529 days (IQR: 353-602). 15 deaths and seven MACE were observed during the follow-up period. 11 participants were right-censored after a median of 215 days (IQR: 99-289) due to kidney transplantation.

For the endpoint of all-cause mortality, survival distributions for the skin [Na<sup>+</sup>] quartiles significantly differed (log-rank  $\chi^2(1) = 3.926$ , *p* for trend <0.05) (Figure 5.2A), as well as event-free survival distributions for the composite endpoint of death and MACE (log-rank  $\chi^2(1) = 5.685$ , *p* for trend <0.05) (Figure 5.2B).

Figure 5.2: Kaplan-Meier curves for overall survival (A) and event-free survival as a composite of all-cause mortality and major adverse cardiovascular events (B), after skin  $[Na^+]$  quartile stratification.



Mean survival and event-free survival times for each skin  $[Na^+]$  quartile group are summarized in Table 5.3.

Table 5.3: Summary of follow-up times, survival and clinical events, in the overall study sample and after Skin  $[Na^+]$  quartile stratification.

	<b>Overall</b>	<b>Q<sub>1</sub></b>	<b>Q<sub>2</sub></b>	<b>Q<sub>3</sub></b>	<b>Q<sub>4</sub></b>
Follow-up time (median (IQR))	529 (353-602)	546 (515-592)	505 (292-533)	588 (421-685)	544 (133-577)
Mean Est. Survival (mean (95% CI))	847 (716-975)	1020 (901-1140)	873 (587-1159)	875 (663-1087)	657 (420-895)
Mean Est. Composite Event-free Survival (mean (95% CI))	741 (602-880)	994 (827-1160)	754 (468-1041)	667 (473-861)	537 (301-774)
<b>Clinical Events</b>					
Kidney Transplant (n)	11	3	2	3	3
MACE (n)	7	1	1	2	3
Death (n)	15	1	3	4	7

CI: 95% confidence interval; IQR: interquartile range; MACE: major adverse cardiovascular events

According to univariate Cox proportional hazards regression (Table 5.4), skin [Na<sup>+</sup>] was significantly associated with all-cause mortality as a continuous variable (HR per 10 mmol/L skin [Na<sup>+</sup>] increments: 1.832, 95% CI: 1.234-2.720) and with composite events, both as a continuous variable and as a categorical variable (HR per 10 mmol/L skin [Na<sup>+</sup>] increments: 1.722, 95% CI: 1.226-2.418; HR per skin [Na<sup>+</sup>] quartile increment: 1.767, 95% CI: 1.089-2.866). In multivariate models, skin [Na<sup>+</sup>] was associated with all-cause mortality after adjusting for age, sex, corrected serum [Na<sup>+</sup>] and serum albumin (HR per 10 mmol/L skin [Na<sup>+</sup>] increments: 4.013, 95% CI: 1.988-8.101,  $p < 0.001$ ; HR per skin [Na<sup>+</sup>] quartile increment: 3.180, 95% CI: 1.314-7.700,  $p < 0.05$ ). Similarly, skin [Na<sup>+</sup>] was also associated with composite all-cause mortality and MACE (HR per 10 mmol/L skin [Na<sup>+</sup>] increments: 2.332, 95% CI: 1.378-3.945,  $p < 0.01$ ; HR per skin [Na<sup>+</sup>] quartile increment: 2.038, 95% CI: 1.058-3.925,  $p < 0.05$ )

Table 5.4: Cox proportional hazard regression to model the association between Skin [Na<sup>+</sup>] and clinical outcomes, before and after confounder adjustment.

<b>Endpoint: All-cause mortality</b>	<b>Univariate</b>		<b>Model 1</b>		<b>Model 2</b>	
<b>Variables</b>	<b>HR (95% CI)</b>	<b>p</b>	<b>HR (95% CI)</b>	<b>p</b>	<b>HR (95% CI)</b>	<b>p</b>
Skin [Na <sup>+</sup> ] (per 10 mmol/L)	1.832 (1.234-2.720)	<0.01	4.013 (1.988-8.101)	<0.001	-	-
Skin [Na <sup>+</sup> ] (per quartile)	1.709 (0.989-2.954)	0.055	-	-	3.180 (1.314-7.700)	<0.05
Age	1.014 (0.965-1.065)	0.584	0.996 (0.934-1.063)	0.912	1.002 (0.941-1.067)	0.949
Sex (female vs male)	0.225 (0.063-0.805)	<0.05	0.156 (0.039-0.630)	<0.01	0.217 (0.059-0.796)	<0.05
Corrected Serum [Na <sup>+</sup> ]	0.975 (0.854-1.113)	0.708	0.711 (0.559-0.904)	<0.01	0.786 (0.621-0.995)	<0.05
Serum Albumin	0.971 (0.838-1.124)	0.692	1.031 (0.883-1.202)	0.702	1.099 (0.919-1.313)	0.302
<b>Endpoint: All-cause mortality + MACE</b>	<b>Univariate</b>		<b>Model 1</b>		<b>Model 2</b>	
<b>Variables</b>	<b>HR (95% CI)</b>	<b>p</b>	<b>HR (95% CI)</b>	<b>p</b>	<b>HR (95% CI)</b>	<b>p</b>
Skin [Na <sup>+</sup> ] (per 10 mmol/L)	1.722 (1.226-2.418)	<0.01	2.332 (1.378-3.945)	<0.01	-	-

Skin [Na <sup>+</sup> ] (per quartile)	1.767 (1.089-2.866)	<0.05	-	-	2.038 (1.058-3.925)	<0.05
Age	1.023 (0.979-1.068)	0.309	0.996 (0.946-1.050)	0.894	1.001 (0.950-1.055)	0.959
Sex (female vs male)	0.315 (0.112-0.885)	<0.05	0.291 (0.099-0.859)	<0.05	0.314 (0.110-0.898)	<0.05
Corrected Serum [Na <sup>+</sup> ]	1.046 (0.912-1.201)	0.518	0.849 (0.695-1.036)	0.107	0.921 (0.759-1.117)	0.404
Serum Albumin	0.926 (0.808-1.062)	0.273	0.979 (0.846-1.133)	0.775	1.012 (0.862-1.189)	0.880

[Na<sup>+</sup>]: sodium concentration; 95% CI: 95% confidence interval; HR: hazard ratio; MACE: major

adverse cardiovascular events

## 5.4 Discussion

We report for the first time that increasing skin  $[\text{Na}^+]$  is associated with increased mortality and MACE. Dialysate  $[\text{Na}^+]$ , corrected serum  $[\text{Na}^+]$ , serum albumin and congestive heart failure were significant clinical predictors of skin  $[\text{Na}^+]$  in dialysis patients.

The main finding of this study is that skin sodium accumulation is associated with worse clinical outcomes, potentially as the result of a combination of processes depositing sodium within tissues. The simplest explanation for this finding is that noninvasive tissue sodium detection by  $^{23}\text{Na}$  MRI reflects the degree of tissue congestion/edema. From a mechanistic perspective, this explanation is supported by previous experimental evidence. A recent comprehensive study in rats and humans showed that tissue  $[\text{Na}^+]$  in rats and skin  $[\text{Na}^+]$  in humans is paralleled by water content (“isotonic” sodium accumulation) as a direct function of ECV expansion, and inversely with intracellular volume and potassium concentration.<sup>13</sup> Similar data have been shown in a mathematical model relating total tissue  $[\text{Na}^+]$  with ECV.<sup>2</sup> However, these observations are derived from animals/subjects without significant CKD and impaired ability to excrete sodium.

Noninvasive, human-based  $^{23}\text{Na}$  MRI studies confirmed the close relationship between sodium and water at the tissue level: both diuretics<sup>6,7</sup> and ultrafiltration with HD<sup>8</sup> have been associated with tissue  $[\text{Na}^+]$  reduction. At the epidemiological level, clinical outcomes are correlated with surrogate measures of ECV expansion, such as fluid overload detected with bioimpedance spectroscopy<sup>3,4</sup> and lung ultrasound.<sup>14</sup>

In the present study, the hypothesis of the relationship between sodium and water at the skin level is supported by the significant explanatory role of serum albumin and comorbid congestive heart failure on skin  $[\text{Na}^+]$ . Indeed, these two factors are associated with positive net capillary filtration,

according to the Starling equation: increased plasma hydrostatic pressure (congestive heart failure) and reduced plasma oncotic pressure (hypoalbuminemia).

However, the additional, explanatory role of dialysate  $[\text{Na}^+]$  suggests that sodium accumulation may also occur in excess of water, as shown by several preclinical studies.<sup>15</sup> Increased sodium intake in rats was associated with increased skin  $[\text{Na}^+]$  and followed by lymph capillary expansion, via macrophage-mediated, tonicity-sensitive VEGF-C secretion; dysfunction in this system was associated with increased skin  $[\text{Na}^+]$  and the downregulation of the endothelial nitric oxide synthase.<sup>16</sup> In humans, we recently showed that chronic HD patients receiving a dialysate  $[\text{Na}^+]$  of 140 mmol/L had larger skin  $[\text{Na}^+]$  compared with patients receiving a dialysate  $[\text{Na}^+]$  of 137 mmol/L, based on different unit prescription protocols.<sup>17</sup> This evidence suggests that skin  $[\text{Na}^+]$  accumulation resulting from intradialytic positive diffusive sodium balance may be an additional factor leading to worse clinical outcomes. Although we cannot discern the pathophysiological mechanisms linking water-free skin  $[\text{Na}^+]$  with increased mortality and cardiovascular events, recent studies have suggested that skin  $[\text{Na}^+]$  may exert “toxic” effects on the cardiovascular system, such as BP and left ventricular mass, independently of ECV.<sup>5,16</sup>

Hypoalbuminemia is a well-known predictor for all-cause mortality in dialysis patients; according to our results, we speculate that the relationship between low serum albumin and clinical outcomes is mediated by overt or subclinical tissue congestion. Indeed, we showed a continuous negative relationship between serum albumin and skin  $[\text{Na}^+]$ , so that even small reductions in serum albumin were associated with larger skin  $[\text{Na}^+]$  – likely as the result of reduced plasma oncotic pressure.<sup>18</sup> Other potential mechanisms linking hypoalbuminemia with clinical outcomes in chronic dialysis patients may be related with reduced albumin synthesis due to inflammation and reduced protein-calorie intake,<sup>19</sup> and impaired endothelial barrier with resulting transcapillary

escape rate of albumin and intercompartmental albumin redistribution.<sup>20</sup> Differently than previous studies,<sup>8,12</sup> we did not find a significant correlation between age and skin  $[\text{Na}^+]$ , as well as clinical outcomes. This is likely the result of several combined factors: (a) small study sample, (b) limited age range in the study population, (c) the greater influence of other clinical and sodium-related variables, suggesting the primary relevance of volume and sodium balance in the dialysis population.

Several limitations must be considered when interpreting the present study findings. This is an observational, exploratory study and other potentially relevant confounders associated with outcomes have not been included in the statistical models due to the small sample size and related lack of statistical power. Eight out of 42 HD patients were receiving individualized dialysate  $[\text{Na}^+]$  prescription: although dialysate  $[\text{Na}^+]$  was significantly associated with skin  $[\text{Na}^+]$ , it is possible the clinical factors underlying dialysate  $[\text{Na}^+]$  individualization may have influenced outcomes. We assumed that an interdialytic, cross-sectional evaluation of skin  $[\text{Na}^+]$  would be associated with clinical outcomes, assuming no longitudinal changes in skin  $[\text{Na}^+]$  during the follow-up period. Evaluation of all-cause mortality and MACE was limited by the small number of patients included in the study, right censoring by kidney transplantation and short follow-up times.

Due to the small and unequal sample size it was not possible to differentiate the impact of different dialytic techniques (HD vs PD) on skin  $[\text{Na}^+]$  and clinical outcomes. Inherently different volume and sodium removal strategies associated with these techniques, however, might have a separate impact on skin  $[\text{Na}^+]$  and clinical outcomes. Additional studies are required to confirm this hypothesis.

In conclusion, higher skin  $[\text{Na}^+]$  (as quantified with  $^{23}\text{Na}$  MRI) was associated with worse clinical outcomes in dialysis patients. Although potential unaccounted confounding effects may be at play,

these findings suggest sodium balance may play an important role in the care of dialysis patients, from both a traditional view (with expansion of ECV) and as a function of our evolving understanding of water-free sodium accumulation within tissues. Future studies investigating the role of skin  $[\text{Na}^+]$  as a quantitative imaging biomarker for risk stratification, therapy optimization and as a potential direct therapeutic target are necessary.

## 5.5 Bibliography

1. Kopp C, Linz P, Wachsmuth L, et al. (23)Na magnetic resonance imaging of tissue sodium. *Hypertens (Dallas, Tex 1979)*. 2012;59(1):167-172. doi:10.1161/HYPERTENSIONAHA.111.183517
2. Rossitto G, Touyz RM, Petrie MC, Delles C. “Much ado about N . . . Atrium: Modelling tissue sodium as a highly sensitive marker of subclinical and localised oedema.” *Clin Sci*. 2018;132(24):2609-2613. doi:10.1042/CS20180575
3. Zoccali C, Moissl U, Chazot C, et al. Chronic fluid overload and mortality in ESRD. *J Am Soc Nephrol*. 2017;28(8):2491-2497. doi:10.1681/ASN.2016121341
4. Dekker MJE, Marcelli D, Canaud BJ, et al. Impact of fluid status and inflammation and their interaction on survival: a study in an international hemodialysis patient cohort. *Kidney Int*. 2017;91(5):1214-1223. doi:10.1016/j.kint.2016.12.008
5. Schneider MP, Raff U, Kopp C, et al. Skin Sodium Concentration Correlates with Left Ventricular Hypertrophy in CKD. *J Am Soc Nephrol*. 2017;28(6):1867-1876. doi:10.1681/asn.2016060662
6. Hammon M, Grossmann S, Linz P, et al. <sup>23</sup>Na magnetic resonance imaging of the lower leg of acute heart failure patients during diuretic treatment. *PLoS One*. 2015;10(10):1-13. doi:10.1371/journal.pone.0141336
7. Karg M V., Bosch A, Kannenkeril D, et al. SGLT-2-inhibition with dapagliflozin reduces tissue sodium content: A randomised controlled trial. *Cardiovasc Diabetol*. 2018;17(1):1-8. doi:10.1186/s12933-017-0654-z
8. Dahlmann A, Dörfelt K, Eicher F, et al. Magnetic resonance-determined sodium removal from tissue stores in hemodialysis patients. *Kidney Int*. 2015;87(2):434-441.

doi:10.1038/ki.2014.269

9. Nagel AM, Laun FB, Weber MA, Matthies C, Semmler W, Schad LR. Sodium MRI using a density-adapted 3D radial acquisition technique. *Magn Reson Med*. 2009;62(6):1565-1573. doi:10.1002/mrm.22157
10. Qirjazi E, Salerno FR, Akbari A, et al. Tissue sodium concentrations in chronic kidney disease and dialysis patients by lower leg sodium-23 magnetic resonance imaging. *Nephrol Dial Transplant*. 2020;Apr 6. doi:10.1093/ndt/gfaa036
11. Katz MA. Hyperglycemia-induced hyponatremia--calculation of expected serum sodium depression. *N Engl J Med*. 1973;289(16):843-844. doi:10.1056/NEJM197310182891607
12. Sahinoz M, Tintara S, Deger SM, et al. Tissue sodium stores in peritoneal dialysis and hemodialysis patients determined by 23-sodium magnetic resonance imaging. *Nephrol Dial Transplant*. 2020. doi:10.1093/ndt/gfaa350
13. Rossitto G, Mary S, Chen JY, et al. Tissue sodium excess is not hypertonic and reflects extracellular volume expansion. *Nat Commun*. 2020;11(1):1-9. doi:10.1038/s41467-020-17820-2
14. Zoccali C, Tripepi R, Torino C, Bellantoni M, Tripepi G, Mallamaci F. Lung congestion as a risk factor in end-stage renal disease. *Blood Purif*. 2014;36(3-4):184-191. doi:10.1159/000356085
15. Titze J, Lang R, Ilies C, et al. Osmotically inactive skin Na<sup>+</sup> storage in rats. *Am J Physiol Physiol*. 2003;285(6):F1108-F1117. doi:10.1152/ajprenal.00200.2003
16. MacHnik A, Neuhofer W, Jantsch J, et al. Macrophages regulate salt-dependent volume and blood pressure by a vascular endothelial growth factor-C-dependent buffering mechanism. *Nat Med*. 2009;15(5):545-552. doi:10.1038/nm.1960

17. Lemoine S, Salerno FR, Akbari A, McIntyre CW. Influence of Dialysate Sodium Prescription on Skin and Muscle Sodium Concentration. *Am J Kidney Dis.* 2021;Jan 8:S0272-6386(21)00005-6. doi:10.1053/j.ajkd.2020.11.025
18. Bhave G, Neilson EG. Body fluid dynamics: Back to the future. *J Am Soc Nephrol.* 2011;22(12):2166-2181. doi:10.1681/ASN.2011080865
19. Gama-Axelsson T, Heimbürger O, Stenvinkel P, Bárány P, Lindholm B, Qureshi AR. Serum albumin as predictor of nutritional status in patients with ESRD. *Clin J Am Soc Nephrol.* 2012;7(9):1446-1453. doi:10.2215/CJN.10251011
20. Yu Z, Tan BK, Dainty S, Matthey DL, Davies SJ. Hypoalbuminaemia, systemic albumin leak and endothelial dysfunction in peritoneal dialysis patients. *Nephrol Dial Transplant.* 2012;27(12):4437-4445. doi:10.1093/ndt/gfs075

# Chapter 6

## 6.1 Overview and Research Questions

ECV expansion in CKD has been known to be associated with adverse cardiovascular effects such as hypertension and left ventricular hypertrophy, as well as adverse clinical outcomes such as myocardial infarction, heart failure and death, since the earlier days of renal replacement therapy.<sup>1–</sup>

<sup>4</sup> According to compartment physiology, ECV expansion is mostly made of water, sodium and its counter anions chloride and bicarbonate.<sup>5–7</sup> Recent studies have also identified the human body's capability to store sodium without commensurate water retention, mainly at the skin dermis level, where sodium's main counter anion would be negatively-charged sulfated proteoglycans.<sup>8,9</sup> These studies suggests that the toxic effects of sodium may be beyond ECV expansion. <sup>23</sup>Na MRI has the ability to visualize tissue sodium directly, and is currently the most accurate way to estimate total body sodium *in vivo*.

Although ECV control is a fundamental target of renal replacement therapy,<sup>10</sup> achieving optimal balance with current dialysis practices is challenging – removal of large volumes of water and sodium within a standard four-hour HD treatment is frequently burdened by cardiovascular complications.<sup>11,12</sup> This required HD clinical practice to change by increasing dialysate [Na<sup>+</sup>], improving intradialytic hemodynamic stability, which in turn resulted in increased total body sodium and cardiovascular adverse effects.<sup>13</sup>

In this setting, the goal of this work was to exploit <sup>23</sup>Na MRI to investigate the relationship between tissue [Na<sup>+</sup>] and CKD, with a particular focus on patients receiving chronic renal replacement

therapy, with particular regards to the associated predictors of tissue  $[Na^+]$  and its effects on cardiovascular surrogates (left ventricular mass) and clinical outcomes.

The following research questions were addressed by this work:

- **Chapter 2.** How does tissue  $[Na^+]$  relate to CKD, HD and PD in adult individuals? Are there any relevant clinical predictors relating to tissue  $[Na^+]$ ?
- **Chapter 3.** How does tissue  $[Na^+]$  relate to kidney disorders in childhood? What are its clinical predictors?
- **Chapter 4.** How does tissue  $[Na^+]$  relate to cardiac structural parameters and geometrical abnormalities in HD patients?
- **Chapter 5.** How does tissue  $[Na^+]$ , particularly at the skin level, relate to clinical outcomes in patients receiving dialysis? What are its main clinical predictors?

## 6.2 Summary and Conclusions

The findings of this thesis work may be summarized as follows:

- **Chapter 2:** Tissue  $[Na^+]$  in the skin and the soleus muscle were higher in HD and PD patients compared to controls. Serum albumin showed a strong, negative correlation with soleus  $[Na^+]$  in HD patients ( $r=-0.81$ ,  $p<0.01$ ). eGFR showed a negative correlation with tissue  $[Na^+]$  (Soleus:  $r=-0.58$ ,  $p<0.01$ , Tibia:  $r=-0.53$ ,  $p=0.01$ ) in merged Control-CKD patients.
- **Chapter 3:** No significant differences were found between healthy children/adolescents and CKD patients. In comparison, healthy adults had significantly higher tissue  $[Na^+]$  compared with pediatric groups, suggesting age is a strong predictor of tissue  $[Na^+]$ . Four CKD patients with glomerular disease and one kidney transplant recipient due to atypical

hemolytic-uremic syndrome had elevated whole-leg  $[\text{Na}^+]$  Z-scores. Reduced whole-leg  $[\text{Na}^+]$  Z-scores were found in two patients with tubular disorders (Fanconi syndrome, proximal-distal renal tubular acidosis). All tissue  $[\text{Na}^+]$  measures had a significant positive association with proteinuria and negative association with serum albumin concentration

- **Chapter 4:** Both skin  $[\text{Na}^+]$  and whole-leg  $[\text{Na}^+]$  were positively associated with greater LVMI (Skin  $[\text{Na}^+]$ :  $r=0.425$ ,  $p<0.05$ ; whole-leg  $[\text{Na}^+]$ :  $r=0.480$ ,  $p<0.05$ ) and LVEDV/BSA (skin  $[\text{Na}^+]$ :  $r=0.494$ ,  $p<0.01$ ; whole-leg  $[\text{Na}^+]$ :  $r=0.447$ ,  $p<0.05$ ). Concentric hypertrophy (normal geometry vs concentric hypertrophy:  $19.2\pm 3.4$  mmol/L vs  $28.1\pm 6.9$  mmol/L,  $p<0.05$ ) and eccentric hypertrophy (normal geometry vs eccentric hypertrophy:  $19.2\pm 3.4$  mmol/L vs  $36.3\pm 12.5$  mmol/L,  $p<0.01$ ) were associated with higher skin  $[\text{Na}^+]$  compared to normal geometry.
- **Chapter 5:** Increasing skin  $[\text{Na}^+]$  quartiles were associated with significantly shorter overall and major cardiovascular adverse event-free survival (log-rank  $\chi^2(1) = 3.926$ , log-rank  $\chi^2(1) = 5.685$ ,  $p$  for trend  $<0.05$  in both instances). Skin  $[\text{Na}^+]$  was associated with all-cause mortality (HR 4.013, 95% CI: 1.988-8.101,  $p<0.001$ ) and composite events (HR 2.332, 95% CI: 1.378-3.945,  $p<0.01$ ), independently of age, sex, serum  $[\text{Na}^+]$  and serum albumin. In multiple regression models, dialysate  $[\text{Na}^+]$ , serum albumin and congestive heart failure were significant predictors of skin  $[\text{Na}^+]$  in HD patients ( $R^2_{adj}=0.62$ ).

In conclusion, this work provided evidence that (1) eGFR and CKD per se are marginally associated with increased tissue  $[\text{Na}^+]$ , whereas some specific etiologies are associated with either accumulation or depletion; (2) end-stage CKD requiring renal replacement therapy is associated with tissue sodium accumulation; (3) the main predictors of tissue  $[\text{Na}^+]$  (age, serum albumin,

dialysate  $[\text{Na}^+]$  and congestive heart failure) suggest a multitude of mechanisms of tissue sodium accumulation, including tissue composition, hydrostatic and oncotic forces and intradialytic sodium intake; (4) tissue  $[\text{Na}^+]$  is associated with left ventricular hypertrophy and dilatation in HD patients; (5) skin  $[\text{Na}^+]$  is associated with major cardiovascular adverse events and mortality in patients receiving renal replacement therapy.

### **6.3 Limitations**

As the main limitations associated with the individual studies were already covered in Chapters 2 to 5, only the general limitations associated with the study designs and methodology will be addressed below.

Generally, the studies of this work are characterized by an exploratory design and a small sample size. This may translate into false negative results due to the studies being underpowered. When possible, an a priori sample size calculation was performed (**Chapter 4**). The most evident example are: the relationship between eGFR and tissue  $[\text{Na}^+]$  in **Chapter 2**, and in **Chapter 3**, where each individual pediatric CKD etiology was modestly represented.

The studies were cross-sectional or observational in nature, and lack an interventional component. This was mainly due to the difficulties associated with designing clinical trials in the HD setting, requiring the recruitment and retention of a large number of participants and with complex treatment schedules.<sup>14,15</sup>

The  $^{23}\text{Na}$  MRI technique we employed comes with several limitations, that invite some degree of caution when interpreting the results from this study. First, image acquisition comes with a single 30 mm-slice and a  $3 \times 3 \text{ mm}^2$  planar resolution. This signifies that the  $^{23}\text{Na}$  signal from each

individual voxel will be the result of the average of sodium ions from all tissues contained within it, as a result of the partial volume effect. Indeed, a weak  $^{23}\text{Na}$  signal is therefore the result of different voxel compositions: interstitial tissue (high in sodium), cellular tissue and fat tissue (both low in sodium content). At the muscle level, a weak  $^{23}\text{Na}$  signal may reflect healthy muscle, whereas a strong  $^{23}\text{Na}$  signal may reflect muscle mass loss and interstitial tissue replacement (cachexia). Second, a recent study posited the possibility that UTE pulse sequences, such as the one we employed in this work, are unable to measure significant signal from the sodium bound to skin proteoglycans.<sup>16</sup> This would signify that the signal we detect does not include water-free sodium, but only sodium dissolved in water, mainly in the ECV. This observation, however, requires further confirmation and is, to our knowledge, limited to this report. Third, due to its limited availability, elevated cost and technical expertise, as well as prolonged scan time, the diffusion of  $^{23}\text{Na}$  MRI is going to be challenging, especially in the renal replacement therapy setting, where sodium measurements may be required to be repeated several times of the course of a year. This limits the use of this technique to the clinical trial setting or to selected clinical cases in third-level university hospital settings, in which the use of  $^{23}\text{Na}$  MRI may be deemed essential to make complex management and therapeutic decisions. Nonetheless, the potential clinical significance of tissue  $[\text{Na}^+]$  may encourage a wider implementation of  $^{23}\text{Na}$  MR technology to commercial MRI scanners and diffusion of this technology in daily clinical practice in the future.

#### **6.4 Significance of the Results**

Despite the initial focus on ECV balance, sodium restriction and BP control of the earlier renal replacement therapy days,<sup>1,13,17</sup> more recent HD practices have since focused on highly efficient blood depuration, based on urea clearance-derived measures (namely urea reduction ratio and

Kt/V), at the expense of less efficient fluid removal and higher dialysate  $[\text{Na}^+]$ .<sup>18</sup> This work provides evidence in support of the recent “Volume First” in dialysis policies proposed in the United States<sup>19</sup> and Canada.<sup>20</sup> Briefly, these policies support strict ECV and sodium balance as a vital goal for optimal dialysis, by exploiting HD treatment times no shorter than 4 hours per session, use of dialysate  $[\text{Na}^+] < 139$  mmol/L and dietary counseling to limit salt intake.

This is fundamental as cardiovascular disease is the first cause of death in CKD, with CKD patients displaying both “traditional” and “atypical” risk factors for cardiovascular disease.<sup>21,22</sup>

A significant body of research by Christopher McIntyre et al was dedicated to demonstrating how hemodynamic instability during HD is responsible for the high cardiovascular morbidity and mortality observed in the HD population.<sup>23–27</sup> At the center of this idea, is that shortening HD treatment times, both a necessity motivated by the high demand of renal replacement therapy in developed countries and an opportunity made possible by the high depurative efficiency of modern HD, is one of the main factors associated with the “unphysiology” of HD,<sup>28</sup> concentrating a normally continuous renal function in the short space of four hours three times per week. Indeed, the cardiovascular system is often unable to tolerate large volumes of ECV removal without developing recurrent ischemia-reperfusion injury during short HD treatments.

The other side of intradialytic hemodynamic instability is ECV expansion, or tissue sodium accumulation. While the notion that ECV expansion is highly prevalent in CKD – especially if requiring renal replacement therapy – is not new,<sup>29</sup> this work points at tissue sodium accumulation as the main target for future research and treatment strategies.

Other research groups have shown that CKD, HD and PD are associated with increased tissue  $[\text{Na}^+]$ ;<sup>30,31</sup> in **Chapter 2**, we confirm these findings relative to HD and PD patients. To this body of research, we add preliminary observations on pediatric CKD (**Chapter 3**), where we suggest

that specific causes of kidney disease may lead to tissue sodium depletion (tubular disorders) or tissue sodium accumulation (nephrotic syndrome). The significance of this observation is uncertain, as we were unable to establish the clinical consequences of these findings, which require further confirmation.

A German group has shown a linear relationship between skin  $[\text{Na}^+]$  and left ventricular mass (using cardiac MRI) in patients with CKD.<sup>32</sup> Similarly, we have shown that tissue  $[\text{Na}^+]$  is positively associated with left ventricular mass and dilatation in CKD patients requiring HD (**Chapter 4**). To our knowledge, however, this work is the first to show a direct relationship between skin sodium accumulation with adverse clinical outcomes (**Chapter 5**). This observation requires further and independent confirmation and poses the fundamental question of whether tissue  $[\text{Na}^+]$  reduction would translate into more favorable clinical outcomes.

## 6.5 Future Steps

This work set the basis for new promising lines of research that will be delineated below.

Hypothesizing a more extensive application of  $^{23}\text{Na}$  MRI in the clinical field, being able to define what  $[\text{Na}^+]$  values can be considered normal for each tissue becomes essential. This requires scanning healthy individuals at a population scale, likely in the order of several thousands. As sex and age have been shown to be significant predictors of tissue  $[\text{Na}^+]$ , normal values would be defined according to sex and age for each tissue, in a manner similar to dual-energy x-ray absorptiometry for the definition of osteoporosis or cardiac MRI for the definition of left ventricular hypertrophy. This will allow to compute the Z-scores of the subject of interest against the standard sex- and age-specific healthy tissue  $[\text{Na}^+]$  value. Subsequently, a wider, population scale application of  $^{23}\text{Na}$  MRI in specific patient groups (e.g. CKD not requiring dialysis, stratified

by eGFR stage) will allow to define clearly whether significant deviations from normality have an outcome significance, and establish useful surrogate outcomes for future tissue  $[\text{Na}^+]$ -directed interventional clinical trials.

As mentioned in the conclusion to the previous paragraph, interventions are necessary to test the effect of tissue sodium reduction on clinical outcomes. In CKD patients receiving HD, the impact of more frequent and/or prolonged HD schedules, addressing the “unphysiology” of HD by allowing for more lenient ultrafiltration rates and lower dialysate  $[\text{Na}^+]$  (thus achieving diffusive sodium removal rather than accumulation), requires further testing. Indeed, frequent and prolonged HD schedules have already been shown to be associated with a lesser degree of cardiac ischemia-reperfusion injury,<sup>33</sup> lower left ventricular mass,<sup>34</sup> and a survival similar to the general population.<sup>3</sup> In this setting, tissue sodium reduction may be more easily achievable due to better intradialytic hemodynamic stability, and may be the main mechanism leading to improved left ventricular mass and better survival.

Improved sodium removal strategies have also been recently designed in the setting of PD, with specifically designed sodium-free hypertonic solutions (either containing 10% dextrose solution or 30% icodextrin/10% dextrose solution), either in the setting of hybrid dialysis (i.e. using both HD and PD sequentially to improve ECV management) or continuous ambulatory PD. Two clinical trials are currently ongoing from our group (ClinicalTrials.gov Identifiers: NCT04603014 and NCT05185999).

In paragraph 6.3, we mentioned the inability of UTE pulse sequences for  $^{23}\text{Na}$  MRI to detect the signal of sodium bound to proteoglycans, as it occurs at the dermal skin level.<sup>16</sup> The potential for triple quantum filtering  $^{23}\text{Na}$  MRI to detect these deposits opens up to a very interesting line of research, allowing – from a physiological standpoint – to visually identify and quantify water-free

tissue sodium deposits *in vivo*. Moving to the clinical setting, investigating the variability of dermal skin sodium deposits between disease groups, the conditions associated with them, their clinical significance and potential for clearance through specific treatment strategies would follow, similarly to the structure of the present work.

The potential of  $^{23}\text{Na}$  MRI in CKD includes its application to other organs, especially the kidneys. Here, the ratio between the sodium signal in the cortex and the medulla (sodium corticomedullary ratio) has been associated with the kidneys' capacity to concentrate the urine<sup>35</sup>

Figure 6.1: Anatomic  $^1\text{H}$  (A) and  $^{23}\text{Na}$  (B) MRI scans in a healthy volunteer and (C) corresponding overlaid  $^1\text{H}$  and  $^{23}\text{Na}$  images for region of interest analysis.

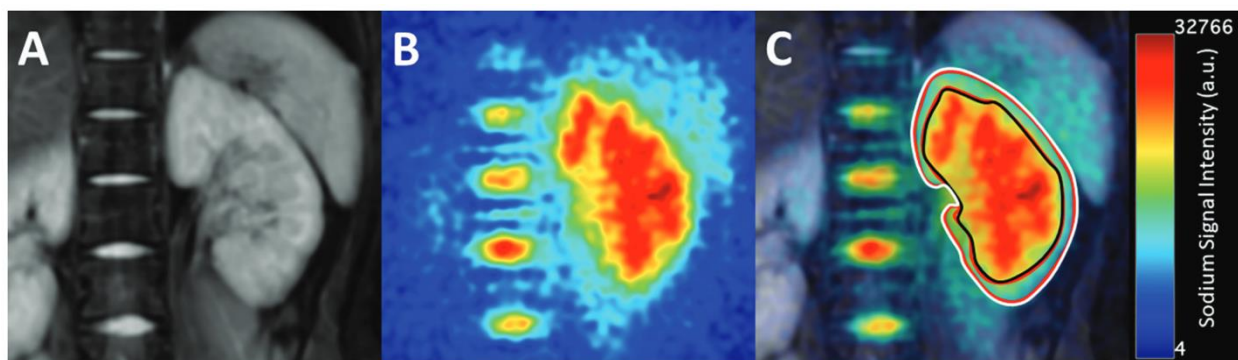


Image reproduced with permission<sup>35</sup>

and may be employed, in perspective, as a sensitive biomarker of kidney injury in the critical care setting, differentiating organic and irreversible tubular damage (acute tubular necrosis) from functional and reversible forms of kidney failure (prerenal azotemia), or allowing the quantification of residual kidney function in the CKD and dialysis settings.

## 6.6 Bibliography

1. Scribner BH, Buri R, Caner JEZ, Hegstrom R, M BJ. The Treatment of Chronic Uremia by

- Means of Intermittent Hemodialysis: a Preliminary Report. *Trans Am Soc Artif Intern Organs*. 1960;6:114-122.
2. Chazot C, Charra B, Laurent G, et al. Interdialysis blood pressure control by long haemodialysis sessions. *Nephrol Dial Transplant*. 1995;10(6):831-837. doi:10.1093/oxfordjournals.ndt.a091231
  3. Charra B, Terrat JC, Vanel T, et al. Long thrice weekly hemodialysis: The Tassin experience. *Int J Artif Organs*. 2004;27(4):265-283. doi:10.1177/039139880402700403
  4. Krautzig S, Janssen U, Koch KM, Granolleras C, Shaldon S. Dietary salt restriction and reduction of dialysate sodium to control hypertension in maintenance haemodialysis patients. *Nephrol Dial Transplant*. 1998;13(3):552-553. doi:10.1093/ndt/13.3.552
  5. Bhawe G, Neilson EG. Body fluid dynamics: Back to the future. *J Am Soc Nephrol*. 2011;22(12):2166-2181. doi:10.1681/ASN.2011080865
  6. FORBES GB, LEWIS AM. Total sodium, potassium and chloride in adult man. *J Clin Invest*. 1956;35(6):596-600. doi:10.1172/JCI103313
  7. Edelman IS, Leibman J, O'Meara MP, Birkenfeld LW. Interrelations between serum sodium concentration, serum osmolarity and total exchangeable sodium, total exchangeable potassium and total body water. *J Clin Invest*. 1958;37(9):1236-1256. doi:10.1172/JCI103712
  8. Titze J. Water-free Na<sup>+</sup> retention: Interaction with hypertension and tissue hydration. *Blood Purif*. 2008;26(1):95-99. doi:10.1159/000110573
  9. Titze J. Water-free sodium accumulation. *Semin Dial*. 2009;22(3):253-255. doi:10.1111/j.1525-139X.2009.00569.x
  10. Flythe JE, Chang TI, Gallagher MP, et al. Blood pressure and volume management in

- dialysis: conclusions from a Kidney Disease: Improving Global Outcomes (KDIGO) Controversies Conference. *Kidney Int.* 2020;97(5):861-876. doi:10.1016/j.kint.2020.01.046
11. McIntyre CW. Recurrent Circulatory Stress: The Dark Side of Dialysis. *Semin Dial.* 2010;23(5):449-451. doi:10.1111/j.1525-139X.2010.00782.x
  12. Huang SHS, Filler G, Lindsay R, McIntyre CW. Euvolemia in Hemodialysis Patients: A Potentially Dangerous Goal? *Semin Dial.* 2015;28(1):1-5. doi:10.1111/sdi.12317
  13. Sellars L, Robson V, Wilkinson R. Sodium retention and hypertension with short dialysis. *Br Med J.* 1979;1(6162):520-521. doi:10.1136/bmj.1.6162.520
  14. Baigent C, Herrington WG, Coresh J, et al. Challenges in conducting clinical trials in nephrology: conclusions from a Kidney Disease—Improving Global Outcomes (KDIGO) Controversies Conference. *Kidney Int.* 2017;92(2):297-305. doi:10.1016/j.kint.2017.04.019
  15. Natale P, Gutman T, Howell M, et al. Recruitment and retention in clinical trials in chronic kidney disease: Report from national workshops with patients, caregivers and health professionals. *Nephrol Dial Transplant.* 2020;35(5):755-764. doi:10.1093/ndt/gfaa044
  16. Hanson P, Philp CJ, Randeve HS, et al. Sodium in the dermis colocalizes to glycosaminoglycan scaffold, with diminishment in type 2 diabetes mellitus. *JCI Insight.* 2021;6(12):1-16. doi:10.1172/jci.insight.145470
  17. Charra B, Calemard E, Ruffet M, et al. Survival as an index of adequacy of dialysis. *Kidney Int.* 1992;41(5):1286-1291. doi:10.1038/ki.1992.191
  18. Flythe JE, Mc Causland FR. Dialysate Sodium: Rationale for Evolution over Time. *Semin Dial.* 2017;30(2):99-111. doi:10.1111/sdi.12570
  19. Weiner DE, Brunelli SM, Hunt A, et al. Improving clinical outcomes among hemodialysis patients: A proposal for a “volume First” approach from the chief medical officers of us

- dialysis providers. *Am J Kidney Dis.* 2014;64(5):685-695. doi:10.1053/j.ajkd.2014.07.003
20. Blum D, Beaubien-Souligny W, Silver SA, Wald R. Thinking Volume First: Developing a Multifaceted Systematic Approach to Volume Management in Hemodialysis. *Can J Kidney Heal Dis.* 2019;6. doi:10.1177/2054358119879776
  21. Mark PB, Johnston N, Groenning BA, et al. Redefinition of uremic cardiomyopathy by contrast-enhanced cardiac magnetic resonance imaging. *Kidney Int.* 2006;69(10):1839-1845. doi:10.1038/sj.ki.5000249
  22. Gross M-L, Ritz E. Hypertrophy and fibrosis in the cardiomyopathy of uremia--beyond coronary heart disease. *Semin Dial.* 2008;21(4):308-318. doi:10.1111/j.1525-139X.2008.00454.x
  23. Selby NM, Burton JO, Chesterton LJ, McIntyre CW. Dialysis-induced regional left ventricular dysfunction is ameliorated by cooling the dialysate. *Clin J Am Soc Nephrol.* 2006;1(6):1216-1225. doi:10.2215/CJN.02010606
  24. Burton JO, Jefferies HJ, Selby NM, McIntyre CW. Hemodialysis-induced repetitive myocardial injury results in global and segmental reduction in systolic cardiac function. *Clin J Am Soc Nephrol.* 2009;4(12):1925-1931. doi:10.2215/CJN.04470709
  25. Burton JO, Jefferies HJ, Selby NM, McIntyre CW. Hemodialysis-induced cardiac injury: Determinants and associated outcomes. *Clin J Am Soc Nephrol.* 2009;4(5):914-920. doi:10.2215/CJN.03900808
  26. McIntyre CW, Burton JO, Selby NM, et al. Hemodialysis-induced cardiac dysfunction is associated with an acute reduction in global and segmental myocardial blood flow. *Clin J Am Soc Nephrol.* 2008;3(1):19-26. doi:10.2215/CJN.03170707
  27. Marants R, Qirjazi E, Grant CJ, Lee TY, McIntyre CW. Renal Perfusion during

- Hemodialysis: Intradialytic Blood Flow Decline and Effects of Dialysate Cooling. *J Am Soc Nephrol.* 2019;30(6):1086-1095. doi:10.1681/ASN.2018121194
28. Kim GH. Dialysis unphysiology and sodium balance. *Electrolyte Blood Press.* 2009;7(2):31-37. doi:10.5049/EBP.2009.7.2.31
  29. Zoccali C, Moissl U, Chazot C, et al. Chronic fluid overload and mortality in ESRD. *J Am Soc Nephrol.* 2017;28(8):2491-2497. doi:10.1681/ASN.2016121341
  30. Sahinoz M, Tintara S, Deger SM, et al. Tissue sodium stores in peritoneal dialysis and hemodialysis patients determined by sodium-23 magnetic resonance imaging. *Nephrol Dial Transplant.* 2021;36(7):1307-1317. doi:10.1093/ndt/gfaa350
  31. Dahlmann A, Dörfelt K, Eicher F, et al. Magnetic resonance-determined sodium removal from tissue stores in hemodialysis patients. *Kidney Int.* 2015;87(2):434-441. doi:10.1038/ki.2014.269
  32. Schneider MP, Raff U, Kopp C, et al. Skin Sodium Concentration Correlates with Left Ventricular Hypertrophy in CKD. *J Am Soc Nephrol.* 2017;28(6):1867-1876. doi:10.1681/asn.2016060662
  33. Jefferies HJ, Virk B, Schiller B, Moran J, McIntyre CW. Frequent hemodialysis schedules are associated with reduced levels of dialysis-induced cardiac injury (myocardial stunning). *Clin J Am Soc Nephrol.* 2011;6(6):1326-1332. doi:10.2215/CJN.05200610
  34. Chan CT, Greene T, Chertow GM, et al. Effects of frequent hemodialysis on ventricular volumes and left ventricular remodeling. *Clin J Am Soc Nephrol.* 2013;8(12):2106-2116. doi:10.2215/CJN.03280313
  35. Akbari A, Lemoine S, Salerno F, et al. Functional Sodium MRI Helps to Measure Corticomedullary Sodium Content in Normal and Diseased Human Kidneys. *Radiology.*



# Appendices

## Appendix A: HSREB Full Board Initial Approval Notice.

Appendix A: HSREB Full Board Initial Approval Notice.



**Western  
Research**

Western University Health Science Research Ethics Board  
HSREB Full Board Initial Approval Notice

**Principal Investigator:** Dr. Christopher McIntyre

**Department & Institution:** Schulich School of Medicine and Dentistry\Medicine-Dept of,London Health Sciences Centre

**Review Type:** Full Board

**HSREB File Number:** 108765

**Study Title:** Evaluation of Sodium Deposition in Soft Tissues of Patients with Kidney Disease and its Association with Patient Symptomatology

**HSREB Initial Approval Date:** January 06, 2017

**HSREB Expiry Date:** January 06, 2018

**Documents Approved and/or Received for Information:**

Document Name	Comments	Version Date
Data Collection Form/Case Report Form	Case report form-Received Nov 23, 2016	
Instruments	5-D Pruritus Scale-Received Nov 23, 2016	2016/11/12
Instruments	HADS-Received Nov 23, 2016	
Instruments	Survey- restless legs-Received Nov 23, 2016	
Instruments	Survey - SF 36-Received Nov 23, 2016	
Instruments	Survey - SNAQ-Received Nov 23, 2016	
Western University Protocol	Received Jan 3, 2017	
Letter of Information & Consent		2017/01/03
Other	Study Protocol - Received for Information-Received on Dec 20, 2016	2016/12/19

The Western University Health Science Research Ethics Board (HSREB) has reviewed and approved the above named study, as of the HSREB Initial Approval Date noted above.

HSREB approval for this study remains valid until the HSREB Expiry Date noted above, conditional to timely submission and acceptance of HSREB Continuing Ethics Review.

The Western University HSREB operates in compliance with the Tri-Council Policy Statement Ethical Conduct for Research Involving Humans (TCPS2), the International Conference on Harmonization of Technical Requirements for Registration of Pharmaceuticals for Human Use Guideline for Good Clinical Practice Practices (ICH E6 R1), the Ontario Personal Health Information Protection Act (PHIPA, 2004), Part 4 of the Natural Health Product Regulations, Health Canada Medical Device Regulations and Part C, Division 5, of the Food and Drug Regulations of Health Canada.

Members of the HSREB who are named as Investigators in research studies do not participate in discussions related to, nor vote on such studies when they are presented to the REB.

The HSREB is registered with the U.S. Department of Health & Human Services under the IRB registration number IRB 00000940.

## Appendix B: Oxford University press license – Nephrology Dialysis

### Transplantation.

*Appendix B: Oxford University press license – Nephrology Dialysis Transplantation*

OXFORD UNIVERSITY PRESS LICENSE

TERMS AND CONDITIONS

Aug 11, 2022

---

---

This Agreement between Dr. Fabio Salerno ("You") and Oxford University Press ("Oxford University Press") consists of your license details and the terms and conditions provided by Oxford University Press and Copyright Clearance Center.

License Number	5351531230596
License date	Jul 17, 2022
Licensed content publisher	Oxford University Press
Licensed content publication	Nephrology Dialysis Transplantation
Licensed content title	Tissue sodium concentrations in chronic kidney disease and dialysis patients by lower leg sodium-23 magnetic resonance imaging
Licensed content author	Qirjazi, Elena; Salerno, Fabio R
Licensed content date	Apr 6, 2020
Type of Use	Thesis/Dissertation
Institution name	
Title of your work	Noninvasive Quantification of Tissue Sodium Concentration in the Kidney Disease Spectrum using 23Na Magnetic Resonance Imaging
Publisher of your work	University of Western Ontario
Expected publication date	Oct 2022
Permissions cost	0.00 CAD
Value added tax	0.00 CAD
Total	0.00 CAD
Title	Noninvasive Quantification of Tissue Sodium Concentration in the Kidney Disease Spectrum using 23Na Magnetic Resonance Imaging
Institution name	University of Western Ontario

Expected presentation date Oct 2022  
Portions Full article for thesis chapter  
Dr. Fabio Salerno

Requestor Location

Attn: Dr. Fabio Salerno  
Publisher Tax ID GB125506730  
Billing Type Invoice  
Dr. Fabio Salerno

Billing Address

Attn: Dr. Fabio Salerno  
Total 0.00 CAD

Terms and Conditions

**STANDARD TERMS AND CONDITIONS FOR REPRODUCTION OF MATERIAL FROM AN OXFORD UNIVERSITY PRESS JOURNAL**

1. Use of the material is restricted to the type of use specified in your order details.
2. This permission covers the use of the material in the English language in the following territory: world. If you have requested additional permission to translate this material, the terms and conditions of this reuse will be set out in clause 12.
3. This permission is limited to the particular use authorized in (1) above and does not allow you to sanction its use elsewhere in any other format other than specified above, nor does it apply to quotations, images, artistic works etc that have been reproduced from other sources which may be part of the material to be used.
4. No alteration, omission or addition is made to the material without our written consent. Permission must be re-cleared with Oxford University Press if/when you decide to reprint.
5. The following credit line appears wherever the material is used: author, title, journal, year, volume, issue number, pagination, by permission of Oxford University Press or the sponsoring society if the journal is a society journal. Where a journal is being published on behalf of a learned society, the details of that society must be included in the credit line.
6. For the reproduction of a full article from an Oxford University Press journal for whatever purpose, the corresponding author of the material concerned should be informed of the proposed use. Contact details for the corresponding authors of all Oxford University Press journal contact can be found alongside either the abstract or full text of the article concerned, accessible from [www.oxfordjournals.org](http://www.oxfordjournals.org) Should there be a problem clearing these rights, please contact [journals.permissions@oup.com](mailto:journals.permissions@oup.com)

7. If the credit line or acknowledgement in our publication indicates that any of the figures, images or photos was reproduced, drawn or modified from an earlier source it will be necessary for you to clear this permission with the original publisher as well. If this permission has not been obtained, please note that this material cannot be included in your publication/photocopies.

8. While you may exercise the rights licensed immediately upon issuance of the license at the end of the licensing process for the transaction, provided that you have disclosed complete and accurate details of your proposed use, no license is finally effective unless and until full payment is received from you (either by Oxford University Press or by Copyright Clearance Center (CCC)) as provided in CCC's Billing and Payment terms and conditions. If full payment is not received on a timely basis, then any license preliminarily granted shall be deemed automatically revoked and shall be void as if never granted.

Further, in the event that you breach any of these terms and conditions or any of CCC's Billing and Payment terms and conditions, the license is automatically revoked and shall be void as if never granted. Use of materials as described in a revoked license, as well as any use of the materials beyond the scope of an unrevoked license, may constitute copyright infringement and Oxford University Press reserves the right to take any and all action to protect its copyright in the materials.

9. This license is personal to you and may not be sublicensed, assigned or transferred by you to any other person without Oxford University Press's written permission.

10. Oxford University Press reserves all rights not specifically granted in the combination of (i) the license details provided by you and accepted in the course of this licensing transaction, (ii) these terms and conditions and (iii) CCC's Billing and Payment terms and conditions.

11. You hereby indemnify and agree to hold harmless Oxford University Press and CCC, and their respective officers, directors, employees and agents, from and against any and all claims arising out of your use of the licensed material other than as specifically authorized pursuant to this license.

12. Other Terms and Conditions:

v1.4

## Appendix C: Springer Nature press licence – Pediatric Nephrology.

*Appendix C: Springer Nature press licence – Pediatric Nephrology.*

### SPRINGER NATURE LICENSE TERMS AND CONDITIONS

Aug 11, 2022

---

---

This Agreement between Dr. Fabio Salerno ("You") and Springer Nature ("Springer Nature") consists of your license details and the terms and conditions provided by Springer Nature and Copyright Clearance Center.

License Number	5351520636451
License date	Jul 17, 2022
Licensed Content Publisher	Springer Nature
Licensed Content Publication	Pediatric Nephrology
Licensed Content Title	Effects of pediatric chronic kidney disease and its etiology on tissue sodium concentration: a pilot study
Licensed Content Author	Fabio R. Salerno et al
Licensed Content Date	Jun 2, 2022
Type of Use	Thesis/Dissertation
Requestor type	academic/university or research institute
Format	print and electronic
Portion	full article/chapter
Will you be translating?	no
Circulation/distribution	1 - 29
Author of this Springer Nature content	yes
Title	Noninvasive Quantification of Tissue Sodium Concentration in the Kidney Disease Spectrum using <sup>23</sup> Na Magnetic Resonance Imaging
Institution name	University of Western Ontario
Expected presentation date	Oct 2022 Dr. Fabio Salerno
Requestor Location	
Billing Type	Attn: Dr. Fabio Salerno Invoice

Dr. Fabio Salerno

Billing Address

Attn: Dr. Fabio Salerno

Total

0.00 CAD

Terms and Conditions

**Springer Nature Customer Service Centre GmbH  
Terms and Conditions**

This agreement sets out the terms and conditions of the licence (the **Licence**) between you and **Springer Nature Customer Service Centre GmbH** (the **Licensor**). By clicking 'accept' and completing the transaction for the material (**Licensed Material**), you also confirm your acceptance of these terms and conditions.

**1. Grant of License**

1. The Licensor grants you a personal, non-exclusive, non-transferable, world-wide licence to reproduce the Licensed Material for the purpose specified in your order only. Licences are granted for the specific use requested in the order and for no other use, subject to the conditions below.
2. The Licensor warrants that it has, to the best of its knowledge, the rights to license reuse of the Licensed Material. However, you should ensure that the material you are requesting is original to the Licensor and does not carry the copyright of another entity (as credited in the published version).
3. If the credit line on any part of the material you have requested indicates that it was reprinted or adapted with permission from another source, then you should also seek permission from that source to reuse the material.

**2. Scope of Licence**

1. You may only use the Licensed Content in the manner and to the extent permitted by these Ts&Cs and any applicable laws.
2. A separate licence may be required for any additional use of the Licensed Material, e.g. where a licence has been purchased for print only use, separate permission must be obtained for electronic re-use. Similarly, a licence is only valid in the language selected and does not apply for editions in other languages unless additional translation rights have been granted separately in the licence. Any content owned by third parties are expressly excluded from the licence.
3. Similarly, rights for additional components such as custom editions and derivatives require additional permission and may be subject to an additional fee.

4. Where permission has been granted **free of charge** for material in print, permission may also be granted for any electronic version of that work, provided that the material is incidental to your work as a whole and that the electronic version is essentially equivalent to, or substitutes for, the print version.
5. An alternative scope of licence may apply to signatories of the [STM Permissions Guidelines](#), as amended from time to time.

**Duration of Licence**

1. A licence for is valid from the date of purchase ('Licence Date') at the end of the relevant period in the below table:

Scope of Licence	Duration of Licence
Post on a website	12 months
Presentations	12 months
Books and journals	Lifetime of the edition in the language purchased

**Acknowledgement**

1. The Licensor's permission must be acknowledged next to the Licenced Material in print. In electronic form, this acknowledgement must be visible at the same time as the figures/tables/illustrations or abstract, and must be hyperlinked to the journal/book's homepage. Our required acknowledgement format is in the Appendix below.

**Restrictions on use**

1. Use of the Licensed Material may be permitted for incidental promotional use and minor editing privileges e.g. minor adaptations of single figures, changes of format, colour and/or style where the adaptation is credited as set out in Appendix 1 below. Any other changes including but not limited to, cropping, adapting, omitting material that affect the meaning, intention or moral rights of the author are strictly prohibited.
2. You must not use any Licensed Material as part of any design or trademark.
3. Licensed Material may be used in Open Access Publications (OAP) before publication by Springer Nature, but any Licensed Material must be removed from OAP sites prior to final publication.

**Ownership of Rights**

1. Licensed Material remains the property of either Licensor or the relevant third party and any rights not explicitly granted herein are expressly reserved.

**Warranty**

IN NO EVENT SHALL LICENSOR BE LIABLE TO YOU OR ANY OTHER PARTY OR ANY OTHER PERSON OR FOR ANY SPECIAL, CONSEQUENTIAL, INCIDENTAL OR INDIRECT DAMAGES, HOWEVER CAUSED, ARISING OUT OF OR IN CONNECTION WITH THE DOWNLOADING, VIEWING OR USE OF THE MATERIALS REGARDLESS OF THE FORM OF ACTION, WHETHER FOR BREACH OF CONTRACT, BREACH OF WARRANTY, TORT, NEGLIGENCE, INFRINGEMENT OR OTHERWISE (INCLUDING, WITHOUT LIMITATION, DAMAGES BASED ON LOSS OF PROFITS, DATA, FILES, USE, BUSINESS OPPORTUNITY OR CLAIMS OF THIRD PARTIES), AND WHETHER OR NOT THE PARTY HAS BEEN ADVISED OF THE POSSIBILITY OF SUCH DAMAGES. THIS LIMITATION SHALL APPLY NOTWITHSTANDING ANY FAILURE OF ESSENTIAL PURPOSE OF ANY LIMITED REMEDY PROVIDED HEREIN.

#### □ **Limitations**

1. **BOOKS ONLY:** Where 'reuse in a dissertation/thesis' has been selected the following terms apply: Print rights of the final author's accepted manuscript (for clarity, NOT the published version) for up to 100 copies, electronic rights for use only on a personal website or institutional repository as defined by the Sherpa guideline ([www.sherpa.ac.uk/romeo/](http://www.sherpa.ac.uk/romeo/)).
2. For content reuse requests that qualify for permission under the [STM Permissions Guidelines](#), which may be updated from time to time, the STM Permissions Guidelines supersede the terms and conditions contained in this licence.

#### □ **Termination and Cancellation**

1. Licences will expire after the period shown in Clause 3 (above).
2. Licensee reserves the right to terminate the Licence in the event that payment is not received in full or if there has been a breach of this agreement by you.

### **Appendix 1 — Acknowledgements:**

#### **For Journal Content:**

Reprinted by permission from [the Licensor]: [Journal Publisher (e.g. Nature/Springer/Palgrave)] [JOURNAL NAME] [REFERENCE CITATION (Article name, Author(s) Name), [COPYRIGHT] (year of publication)]

#### **For Advance Online Publication papers:**

Reprinted by permission from [the Licensor]: [Journal Publisher (e.g. Nature/Springer/Palgrave)] [JOURNAL NAME] [REFERENCE CITATION (Article name, Author(s) Name), [COPYRIGHT] (year of publication), advance online publication, day month year (doi: 10.1038/sj.[JOURNAL ACRONYM].)]

#### **For Adaptations/Translations:**

Adapted/Translated by permission from [the Licensor]: [Journal Publisher (e.g.

Nature/Springer/Palgrave)] [JOURNAL NAME] [REFERENCE CITATION  
(Article name, Author(s) Name), [COPYRIGHT] (year of publication)

**Note: For any republication from the British Journal of Cancer, the following credit line style applies:**

Reprinted/adapted/translated by permission from [the Licensor]: on behalf of Cancer Research UK: : [Journal Publisher (e.g. Nature/Springer/Palgrave)] [JOURNAL NAME] [REFERENCE CITATION (Article name, Author(s) Name), [COPYRIGHT] (year of publication)

For **Advance Online Publication** papers:

Reprinted by permission from The [the Licensor]: on behalf of Cancer Research UK: [Journal Publisher (e.g. Nature/Springer/Palgrave)] [JOURNAL NAME] [REFERENCE CITATION (Article name, Author(s) Name), [COPYRIGHT] (year of publication), advance online publication, day month year (doi: 10.1038/sj.[JOURNAL ACRONYM])

**For Book content:**

Reprinted/adapted by permission from [the Licensor]: [Book Publisher (e.g. Palgrave Macmillan, Springer etc) [Book Title] by [Book author(s)] [COPYRIGHT] (year of publication)

**Other Conditions:**

Version 1.3

## Appendix D: Oxford University press licence – Clinical Kidney Journal.

*Appendix D: Oxford University press licence – Clinical Kidney Journal.*

### OXFORD UNIVERSITY PRESS LICENSE TERMS AND CONDITIONS

Aug 11, 2022

---

---

This Agreement between Dr. Fabio Salerno ("You") and Oxford University Press ("Oxford University Press") consists of your license details and the terms and conditions provided by Oxford University Press and Copyright Clearance Center.

License Number	5351531448560
License date	Jul 17, 2022
Licensed content publisher	Oxford University Press
Licensed content publication	Clinical Kidney Journal
Licensed content title	Outcomes and predictors of skin sodium concentration in dialysis patients
Licensed content author	Salerno, Fabio R; Akbari, Alireza
Licensed content date	Jan 28, 2022
Type of Use	Thesis/Dissertation
Institution name	
Title of your work	Noninvasive Quantification of Tissue Sodium Concentration in the Kidney Disease Spectrum using <sup>23</sup> Na Magnetic Resonance Imaging
Publisher of your work	University of Western Ontario
Expected publication date	Oct 2022
Permissions cost	0.00 CAD
Value added tax	0.00 CAD
Total	0.00 CAD
Title	Noninvasive Quantification of Tissue Sodium Concentration in the Kidney Disease Spectrum using <sup>23</sup> Na Magnetic Resonance Imaging
Institution name	University of Western Ontario
Expected presentation date	Oct 2022

Portions Full article for thesis chapter  
Dr. Fabio Salerno

Requestor Location

Attn: Dr. Fabio Salerno  
Publisher Tax ID GB125506730  
Billing Type Invoice  
Dr. Fabio Salerno

Billing Address

Attn: Dr. Fabio Salerno  
Total 0.00 CAD

Terms and Conditions

**STANDARD TERMS AND CONDITIONS FOR REPRODUCTION OF  
MATERIAL FROM AN OXFORD UNIVERSITY PRESS JOURNAL**

1. Use of the material is restricted to the type of use specified in your order details.
2. This permission covers the use of the material in the English language in the following territory: world. If you have requested additional permission to translate this material, the terms and conditions of this reuse will be set out in clause 12.
3. This permission is limited to the particular use authorized in (1) above and does not allow you to sanction its use elsewhere in any other format other than specified above, nor does it apply to quotations, images, artistic works etc that have been reproduced from other sources which may be part of the material to be used.
4. No alteration, omission or addition is made to the material without our written consent. Permission must be re-cleared with Oxford University Press if/when you decide to reprint.
5. The following credit line appears wherever the material is used: author, title, journal, year, volume, issue number, pagination, by permission of Oxford University Press or the sponsoring society if the journal is a society journal. Where a journal is being published on behalf of a learned society, the details of that society must be included in the credit line.
6. For the reproduction of a full article from an Oxford University Press journal for whatever purpose, the corresponding author of the material concerned should be informed

of the proposed use. Contact details for the corresponding authors of all Oxford University Press journal contact can be found alongside either the abstract or full text of the article concerned, accessible from [www.oxfordjournals.org](http://www.oxfordjournals.org) Should there be a problem clearing these rights, please contact [journals.permissions@oup.com](mailto:journals.permissions@oup.com)

7. If the credit line or acknowledgement in our publication indicates that any of the figures, images or photos was reproduced, drawn or modified from an earlier source it will be necessary for you to clear this permission with the original publisher as well. If this permission has not been obtained, please note that this material cannot be included in your publication/photocopies.

8. While you may exercise the rights licensed immediately upon issuance of the license at the end of the licensing process for the transaction, provided that you have disclosed complete and accurate details of your proposed use, no license is finally effective unless and until full payment is received from you (either by Oxford University Press or by Copyright Clearance Center (CCC)) as provided in CCC's Billing and Payment terms and conditions. If full payment is not received on a timely basis, then any license preliminarily granted shall be deemed automatically revoked and shall be void as if never granted. Further, in the event that you breach any of these terms and conditions or any of CCC's Billing and Payment terms and conditions, the license is automatically revoked and shall be void as if never granted. Use of materials as described in a revoked license, as well as any use of the materials beyond the scope of an unrevoked license, may constitute copyright infringement and Oxford University Press reserves the right to take any and all action to protect its copyright in the materials.

9. This license is personal to you and may not be sublicensed, assigned or transferred by you to any other person without Oxford University Press's written permission.

10. Oxford University Press reserves all rights not specifically granted in the combination of (i) the license details provided by you and accepted in the course of this licensing transaction, (ii) these terms and conditions and (iii) CCC's Billing and Payment terms and conditions.

11. You hereby indemnify and agree to hold harmless Oxford University Press and CCC, and their respective officers, directors, employs and agents, from and against any and all claims arising out of your use of the licensed material other than as specifically authorized pursuant to this license.

12. Other Terms and Conditions:

v1.4

## Appendix E: Radiology licence.

Appendix E: Radiology licence.

### Permission to reproduce figure for doctoral dissertation

 Permissions      

To: Fabio Salerno Fri 14/10/2022 13:34

Dear Doctor Salerno,

Thank you for your permission request. As an author of the original article, you may re-use the figure in other works without obtaining formal permission from RSNA. We do ask, however, that you please cite the original source of the figure.

Please let me know if you have any questions or require further assistance.

Kind regards,  
Marta Jendra



---

**From:** Fabio Salerno  
**Sent:** Thursday, October 13, 2022 8:29 AM  
**To:** Permissions  
**Subject:** Permission to reproduce figure for doctoral dissertation

Dear RSNA Staff,

I am reaching out to ask for permission to reproduce Figure 2 from the following article of which I am a co-author, for use in my doctoral dissertation titled "**Noninvasive Quantification of Tissue Sodium Concentration in the Kidney Disease Spectrum using <sup>23</sup>Na Magnetic Resonance Imaging**", for the department of Medical Biophysics, Western University, London, ON, Canada.

Akbari A, Lemoine S, Salerno F, Marcus TL, Duffy T, Scholl TJ, Filler G, House AA, McIntyre CW. Functional Sodium MRI Helps to Measure Corticomedullary Sodium Content in Normal and Diseased Human Kidneys. *Radiology*. 2022 May;303(2):384-389. doi: 10.1148/radiol.211238. Epub 2022 Feb 8. PMID: 35133199.

## Appendix F: Curriculum Vitae

*Appendix F: Curriculum Vitae*

### Education

Sept 2018 – active: **PhD Candidate, Medical Biophysics**

Western University, Department of Medical Biophysics. London, ON, Canada.

Supervisors: Christopher W. McIntyre, MBBS, DM; Grace Parraga, PhD.

Aug 2013 – Aug 2018: **Nephrology Fellow**

School of Specialization in Nephrology – Milan-Bicocca University, Via Cadore 48, 20900 Monza, Italy. Department of Clinical Nephrology, San Gerardo Hospital, Monza, Italy. Mark: 70/70.

Sep 2006 - Jul 2012: **Doctor of Medicine and Surgery**

School of Medicine and Surgery, Milano-Bicocca University, Monza, Italy. Mark: 110/110 cum laude.

### Professional Experience and Training

April 19<sup>th</sup> 2022 – Active: **Consultant Nephrologist**, A. Manzoni Hospital, Lecco, ASST Lecco, Italy.

March 24<sup>th</sup> 2020 – June 30<sup>th</sup> 2020: **Nephrologist and Internal Medicine physician** for the COVID-19 emergency. ASST Monza, San Gerardo Hospital, Monza, Italy.

Feb 2016 – Dec 2016; Jul 2017 – Dec 2017: **Visiting Clinical Research Fellow**

Western University, Schulich School of Medicine & Dentistry. London, ON, Canada.

Kidney Clinical Research Unit, Victoria Hospital, London, ON, Canada.

Feb 2013: **Medical License Exam (Italy)**

Milano-Bicocca University, Monza, Italy. Mark: 268.75/270.

Mar 2010 – Jul 2013: **Nephrology Intern Student**

Department of Clinical Nephrology, San Gerardo Hospital, Monza, Italy.

May 2009 – Sept 2009: **Gerontology Intern Student**

Department of Gerontology, Bassini Hospital, Cinisello Balsamo, Italy.

### Dissertations

Nephrology Fellowship Dissertation: “Acute Myocardial Injury Induced by Continuous Renal Replacement Therapy in Critically Ill Patients”. School of Specialization in Nephrology, Milano-Bicocca University. Supervisor: Renato Alberto Sinico. Co-supervisor: Christopher W. McIntyre.

Medical Doctor Dissertation: “[Renal Denervation for the Treatment of Resistant Arterial Hypertension]”, in Italian. School of Medicine and Surgery, Milano-Bicocca University. Supervisor: Andrea Stella, MD, PhD. Co-Supervisor: Federico Pieruzzi, MD, PhD.

## Scholarships

- Selected as candidate for the Vanier Canada Graduate Scholarship 2019 – **Not awarded**.
- Western University Dean’s Research Scholarship (DRS) 2020: **Awarded**; total value: 14,000 Canadian dollars per year for two years.

## Awards

February 15<sup>th</sup>-17<sup>th</sup> 2019. Award for best abstract (250\$ USD): “Varying Intensity of Remote Ischemic Preconditioning to Prevent Hemodialysis-Induced Cardiac Injury: a Randomized Controlled Trial”. **Salerno FR**, Crowley L, Tamasi T, Penny JD, McIntyre CW. The 1<sup>st</sup> International University of Florida Nephrocardiology Conference 2019” Orlando, FL, US.

March 13<sup>th</sup>-15<sup>th</sup> 2015. Commendation for best oral presentation. “Alpha-galactosidase activity, high-sensitivity troponin T and myocardial fibrosis in Fabry disease: a case series”. **Salerno FR**, Pieruzzi F, Di Gennaro F, Binaggia A, Di Giacomo A, Torti G, Stella A. “PhD Fabry Research Initiative”, 14<sup>th</sup> European Round Table on Fabry disease, Paris, France.

November 21<sup>st</sup>-22<sup>nd</sup> 2014. Commendation for best abstract. "Association between Anderson-Fabry disease clinical severity and high-sensitivity troponin-T levels”. **Salerno F**, Pieruzzi F, Binaggia A, Di Giacomo A, Torti G, Parini R, Rigoldi M, Stella A. “European Symposium on Lysosomal Storage Disorders”, London, UK.

October 3<sup>rd</sup>-5<sup>th</sup> 2013. Award for best poster (300 Euros). “[Effect of blood pressure on left ventricular mass, diastolic function and cardiac geometry in children]”. **Salerno F**, Pieruzzi F, Antolini L, Giussani M, Brambilla P, Galbiati S, Frizziero D, Mastriani S, Stella A, Valsecchi MG, Genovesi S. 30<sup>th</sup> congress of the Italian Society of Arterial Hypertension (SIIA), Rome, Italy.

## Ph.D. Courses

2018 Fall Term:

- BIOPHYS 9513A: Preparing for Scientific Research (Compulsory, Grade 86/100)
- BIOPHYS 9515A: Introduction to Medical Imaging (Audit)
- BIOPHYS 9700: Biophysics Graduate Seminars (Compulsory)

2019 Winter Term

- BIOPHYS 9514B: Preparing for Scientific Research (Compulsory, Grade 84/100)

- BIOPHYS 9700: Biophysics Graduate Seminars (Compulsory)

2019 Fall Term

- BIOPHYS 9650A: Conceptual MRI (Grade 93/100)
- BIOPHYS 9700: Biophysics Graduate Seminars (Compulsory)

2020 Winter Term

- BIOPHYS 9522B: Inferencing from data analysis (Withdrawn due to leave of absence)
- BIOPHYS 9700: Biophysics Graduate Seminars (Compulsory)

2020 Fall Term

- BIOPHYS 9700: Biophysics Graduate Seminars (Compulsory)

2021 Winter Term

- BIOPHYS 9522B: Inferencing from data analysis (Grade 91/100)
- BIOPHYS 9700: Biophysics Graduate Seminars (Compulsory)

2021 Fall Term

- BIOPHYS 9700: Biophysics Graduate Seminars (Compulsory)

2022 Winter Term

- BIOPHYS 9700: Biophysics Graduate Seminars (Compulsory)

## **Attended Conferences**

- American Society of Nephrology Conference November 5<sup>th</sup>-10<sup>th</sup> 2019, Washington, DC, US.
- London Health Research Day, April 30<sup>th</sup> 2019, London, ON, Canada
- The 1<sup>st</sup> International University of Florida Nephrocardiology Conference, February 15<sup>th</sup>-17<sup>th</sup> 2019, Orlando, FL, US.
- American Society of Nephrology Conference October 25<sup>th</sup>-28<sup>th</sup> 2018, San Diego, CA, US.

## **Original Publications**

- 1) **Salerno FR**, Akbari A, Lemoine S, Filler G, Scholl TJ, McIntyre CW. Outcomes and predictors of skin sodium concentration in dialysis patients. *Clin Kidney J.* 2022 Jan 28;15(6):1129-1136. doi: 10.1093/ckj/sfac021. PMID: 35664280; PMCID: PMC9155229.
- 2) Filler G, Schott C, **Salerno FR**, Ens A, McIntyre CW, Díaz González de Ferris ME, Stein R. Growth hormone therapy in HHRH. *Bone Rep.* 2022 May 18;16:101591. doi: 10.1016/j.bonr.2022.101591. PMID: 35663378; PMCID: PMC9156862.
- 3) **Salerno FR**, Akbari A, Lemoine S, Scholl TJ, McIntyre CW, Filler G. Effects of pediatric chronic kidney disease and its etiology on tissue sodium concentration: a pilot study. *Pediatr Nephrol.* 2022 Jun 2. doi: 10.1007/s00467-022-05600-7. Epub ahead of print. PMID: 35655040.
- 4) Schorr M, Zalitach M, House C, Gomes J, Wild CJ, **Salerno FR**, McIntyre C. Cognitive Impairment Early After Initiating Maintenance Hemodialysis: A Cross Sectional Study. *Front Neurol.* 2022 Mar 15;13:719208. doi: 10.3389/fneur.2022.719208. PMID: 35370903; PMCID: PMC8964944.
- 5) Akbari A, Lemoine S, **Salerno F**, Marcus TL, Duffy T, Scholl TJ, Filler G, House AA, McIntyre CW. Functional Sodium MRI Helps to Measure Corticomedullary Sodium Content in Normal and Diseased Human Kidneys. *Radiology.* 2022 May;303(2):384-389. doi: 10.1148/radiol.211238. Epub 2022 Feb 8. PMID: 35133199.
- 6) **Salerno FR**, Roggero L, Rossi F, Binaggia A, Bertoli S, Pieruzzi F. Relapsing minimal change disease superimposed on late-onset p.N215S Fabry nephropathy. *Clin Kidney J.* 2021 Aug 13;15(1):171-173. doi: 10.1093/ckj/sfab148. Erratum in: *Clin Kidney J.* 2022 Jan 19;15(4):839. PMID: 35035949; PMCID: PMC8757417.
- 7) Penny JD, Jarosz P, **Salerno FR**, Lemoine S, McIntyre CW. Impact of Expanded Hemodialysis Using Medium Cut-off Dialyzer on Quality of Life: Application of Dynamic Patient-Reported Outcome Measurement Tool. *Kidney Med.* 2021 Jul 29;3(6):992-1002.e1. doi: 10.1016/j.xkme.2021.05.010. PMID: 34939008; PMCID: PMC8664707.
- 8) Lemoine S, **Salerno FR**, Akbari A, McKelvie RS, McIntyre CW. Tissue Sodium Storage in Patients With Heart Failure: A New Therapeutic Target? *Circ Cardiovasc Imaging.* 2021 Nov;14(11):e012910. doi: 10.1161/CIRCIMAGING.121.012910. Epub 2021 Nov 16. PMID: 34784242.
- 9) Filler G, **Salerno F**, McIntyre CW, de Ferris MED. Animal, Human, and <sup>23</sup>Na MRI Imaging Evidence for the Negative Impact of High Dietary Salt in Children. *Curr Pediatr Rep.* 2021;9(4):110-117. doi: 10.1007/s40124-021-00249-6. Epub 2021 Sep 18. PMID: 34567839; PMCID: PMC8449209.
- 10) Filler G, Geda R, **Salerno F**, Zhang YC, de Ferris MED, McIntyre CW. Management of severe polyuria in idiopathic Fanconi syndrome. *Pediatr Nephrol.* 2021 Nov;36(11):3621-3626. doi: 10.1007/s00467-021-05213-6. Epub 2021 Aug 24. PMID: 34427794.

- 11)“Influence of Dialysate Sodium Prescription on Skin and Muscle Sodium Concentration.” Lemoine S, **Salerno FR**, Akbari A, McIntyre CW. *Am J Kidney Dis*. 2021 Jan 8:S0272-6386(21)00005-6. doi: 10.1053/j.ajkd.2020.11.025. Epub ahead of print. PMID: 33428998.
- 12)“Pruritus: Is there a grain of salty truth?” Penny JD, **Salerno FR**, Akbari A, McIntyre CW. *Hemodial Int*. 2020 Sep 29. doi: 10.1111/hdi.12885. Epub ahead of print.
- 13)“Tissue sodium concentrations in chronic kidney disease and dialysis patients by lower leg sodium-23 magnetic resonance imaging.”. Qirjazi E, **Salerno FR**, Akbari A, Hur L, Penny J, Scholl T, McIntyre CW. *Nephrol Dial Transplant*. 2020 Apr 6. Epub ahead of print]
- 14)“Remote Ischemic Preconditioning Protects against Hemodialysis-Induced Cardiac Injury.” **Salerno FR**, Crowley LE, Odudu A, McIntyre CW. *Kidney Int Rep*. 2019. *Kidney Int Rep*. 2019 Aug 30;5(1):99-103.
- 15)“Continuous renal replacement therapy is associated with acute cardiac stunning in critically ill patients”. Slessarev M, **Salerno F**, Ball IM, McIntyre CW. *Hemodial Int*. 2019 Jul;23(3):325-332.
- 16)“Intradialytic exercise preconditioning: an exploratory study on the effect on myocardial stunning.” Penny JD, **Salerno FR**, Brar R, Garcia E, Rossum K, McIntyre CW, Bohm CJ. *Nephrol Dial Transplant*. 2019 Nov 1;34(11):1917-1923.
- 17)“Renal transplants from older deceased donors: Is pre-implantation biopsy useful? A monocentric observational clinical study.” Colussi G, Casati C, Colombo VG, Camozzi MLP, **Salerno FR**. *World J Transplant*. 2018 Aug 9;8(4):110-121.
- 18)“Computational Assessment of Blood Flow Heterogeneity in Peritoneal Dialysis Patients' Cardiac Ventricles.” Kharche SR, So A, **Salerno F**, Lee TY, Ellis C, Goldman D, McIntyre CW. *Front Physiol*. 2018 May 17;9:511.
- 19)“Diagnosis and Treatment of Intradialytic Hypotension in Maintenance Hemodialysis Patients.” McIntyre CW, **Salerno FR**. *Clin J Am Soc Nephrol*. 2018 Mar 7;13(3):486-489.
- 20)“Percutaneous perfusion monitoring for the detection of hemodialysis induced cardiovascular injury.” Penny JD, Grant C, **Salerno F**, Brumfield A, Mianulli M, Poole L, McIntyre CW. *Hemodial Int*. 2018 Jul;22(3):351-358.
- 21)“Why Is Your Patient Still Short of Breath? Understanding the Complex Pathophysiology of Dyspnea in Chronic Kidney Disease.” **Salerno FR**, Parraga G, McIntyre CW. *Semin Dial*. 2017 Jan;30(1):50-57.

- 22)“The role of blood pressure, body weight and fat distribution of left ventricular mass, diastolic function and cardiac geometry in children.” Pieruzzi F, Antolini L, **Salerno FR**, Galbiati S, Giussani M, Stella A, Genovesi S. *J Hypertens*. 2015 Jun;33(6):1182-92.
- 23)“[Clinical and histological findings in Fabry nephropathy].” Pieruzzi F, **Salerno F**, Di Giacomo A, Torti G, Ferrario F, Pagni F, Stella A. *G Ital Nefrol* 2013 Nov-Dec;30(6). Review article in Italian.

## Book Chapters

Christopher W McIntyre, **Fabio R Salerno**. Avoidance and treatment of cardiovascular disease in dialysis. 2023/1/1, *Handbook of dialysis therapy*, 421-429. Elsevier

## Abstracts

*Accepted:*

- “Associations of muscle sodium deposition with sodium-23 MRI in hemodialysis patients”. Salerno FR, Akbari A, Lemoine S, Scholl T, McIntyre CW. [Oral presentation]. European Renal Association – European Dialysis and Transplantation Association (ERA-EDTA), Virtual Congress 2020.
- “Noninvasive assessment of pulmonary hypertension using quantitative imaging in hemodialysis patients”. Salerno FR, Lindenmaier T, Matheson A, Eddy RL, McIntosh M, Dorie J, Parraga G, McIntyre CW. [e-poster]. European Renal Association – European Dialysis and Transplantation Association (ERA-EDTA), Virtual Congress 2020.
- “Is Tissue Sodium Storage Driving Systemic Inflammation in Chronic Kidney Disease? A Sodium Magnetic Resonance Imaging Study”. Akbari A, Hur L, Penny J, Qirjazi E, **Salerno FR**, McIntyre CW. American Society of Nephrology Conference 2019, Washington, DC, US.
- “A Novel Magnetic Resonance Imaging Biomarker of Tibial Bone Quality in Chronic Kidney Disease”. **Salerno FR**, Akbari A, Hur LY, McIntyre CW. American Society of Nephrology Conference 2019, Washington, DC, US.
- “Lung Ventilation Abnormalities in Chronic Hemodialysis Patients with Hyperpolarized <sup>129</sup>Xe Gas Magnetic Resonance Imaging”. **Salerno FR**, Eddy RL, Matheson AM, Parraga G, McIntyre CW. American Society of Nephrology Conference 2019, Washington, DC, US.
- “Muscle Quality Assessment by Texture Analysis of 1H-Magnetic Resonance Images in Chronic Kidney Disease Patients”. Hur LY, **Salerno FR**, Akbari A, McIntyre CW. American Society of Nephrology Conference 2019, Washington, DC, US.

- February 15<sup>th</sup>-17<sup>th</sup> 2019: “Varying Intensity of Remote Ischemic Preconditioning to Prevent Hemodialysis-Induced Cardiac Injury: a Randomized Controlled Trial”. **Salerno FR**, Crowley L, Tamasi T, Penny JD, McIntyre CW. The 1<sup>st</sup> International University of Florida Nephrocardiology Conference 2019, Orlando, FL, US.
- October 25<sup>th</sup>-28<sup>th</sup> 2018: “Dose-Effect Response of Remote Ischemic Preconditioning for the Prevention of Hemodialysis-Induced Myocardial Stunning: Preliminary Results of a Randomized Controlled Trial”. **Salerno FR**, Crowley L, Penny JD, McIntyre CW. American Society of Nephrology Conference 2018, San Diego, CA, US.
- March 13<sup>th</sup>-15<sup>th</sup> 2015. “Alpha-galactosidase activity, high-sensitivity troponin T and myocardial fibrosis in Fabry disease: a case series”. **Salerno FR**, Pieruzzi F, Di Gennaro F, Binaggia A, Di Giacomo A, Torti G, Stella A. “PhD Fabry Research Initiative”, 14<sup>th</sup> European Round Table on Fabry disease, Paris, France.
- November 21<sup>st</sup>-22<sup>nd</sup> 2014: "Association between Anderson-Fabry disease clinical severity and high-sensitivity troponin-T levels". **Salerno F**, Pieruzzi F, Binaggia A, Di Giacomo A, Torti G, Parini R, Rigoldi M, Stella A. “European Symposium on Lysosomal Storage Disorders”, London, UK.
- October 3<sup>rd</sup>-5<sup>th</sup> 2013: “[Effect of blood pressure on left ventricular mass, diastolic function and cardiac geometry in children]”. **Salerno F**, Pieruzzi F, Antolini L, Giussani M, Brambilla P, Galbiati S, Frizziero D, Mastriani S, Stella A, Valsecchi MG, Genovesi S. 30<sup>th</sup> congress of the Italian Society of Arterial Hypertension (SIIA), Rome, Italy.

## Oral Presentations

“Associations of muscle sodium deposition with sodium-23 MRI in hemodialysis patients”. **Salerno FR**, Akbari A, Lemoine S, Scholl T, McIntyre CW. European Renal Association – European Dialysis and Transplantation Association (ERA-EDTA), Virtual Congress 2020, June 6<sup>th</sup>-9<sup>th</sup> 2020.

“Varying Intensity of Remote Ischemic Preconditioning to Prevent Hemodialysis-Induced Cardiac Injury: a Randomized Controlled Trial”. **Salerno FR**, Crowley L, Tamasi T, Penny JD, McIntyre CW. “The 1<sup>st</sup> International University of Florida Nephrocardiology Conference 2019”, Orlando, FL, US. February 15<sup>th</sup>-17<sup>th</sup> 2019.

“Alpha-galactosidase activity, high-sensitivity troponin T and myocardial fibrosis in Fabry disease: a case series”. **Salerno FR**, Pieruzzi F, Di Gennaro F, Binaggia A, Di Giacomo A, Torti G, Stella A. “PhD Fabry Research Initiative”, 14<sup>th</sup> European Round Table on Fabry disease, Paris, March 13<sup>th</sup>-15<sup>th</sup> 2015.

"Association between Anderson-Fabry disease clinical severity and high-sensitivity troponin-T levels". **Salerno F**, Pieruzzi F, Binaggia A, Di Giacomo A, Torti G, Parini R, Rigoldi M, Stella A. “European Symposium on Lysosomal Storage Disorders”, London, November 21<sup>st</sup>-22<sup>nd</sup> 2014.

## Lectures

### *Academic lectures:*

- May 7<sup>th</sup> 2018. [Acute Kidney Injury in the Intensive Care Unit], in Italian. Elective course “Dialysis”. School of Medicine and Surgery, Milano-Bicocca University, Monza, Italy.
- April 11<sup>th</sup> 2017. [Acute Kidney Injury, Sepsis and Renal Replacement Therapy], in Italian. Elective course “Dialysis”. School of Medicine and Surgery, Milano-Bicocca University, Monza, Italy.
- April 6<sup>th</sup> 2017. [Elements of Plasmapheresis and Vascular Access for Hemodialysis], in Italian. Elective course “Dialysis”. School of Medicine and Surgery, Milano-Bicocca University, Monza, Italy.

### *Contract lectures – Sponsored by Genzyme, a Sanofi Company.*

- June 12<sup>th</sup>-13<sup>th</sup> 2018. [The Role of High-Sensitivity Troponin T in Fabry Cardiomyopathy], in Italian. “Fabry Excellence Meeting”, Naples, Italy.
- May 23<sup>rd</sup>-24<sup>th</sup> 2017. [Fabry disease: how to predict renal outcomes], in Italian. “Master School: advanced course on Fabry disease”, Monza, Italy.
- February 9<sup>th</sup>-10<sup>th</sup> 2016. [The Role of High-Sensitivity Troponin T in Fabry Cardiomyopathy], in Italian. “Fabry Excellence Meeting”, Baggiovara, Italy.
- May 6<sup>th</sup>-7<sup>th</sup> 2015. [The role of the cardiologist: clinical cases], in Italian. “Master School: advanced course on Fabry disease”, Monza, Italy.
- September 18<sup>th</sup>-19<sup>th</sup> 2014. [The role of the cardiologist: clinical cases], in Italian. “Master School: advanced course on Fabry disease”, Monza, Italy.

### *Clinical lectures:*

- July 7<sup>th</sup> 2015. [Use of Biofeedback Mechanisms in Hemodialysis], in Italian. Update course for dialysis nurses. San Gerardo Hospital, Monza, Italy.

### *Online lectures:*

- 2017. Salerno FR, Slessarev M. Authored informative Powerpoint slides and video tutorials for cardiac ultrasound image acquisition and interpretation with the Echopac GE software. (<https://sites.google.com/scary/view/mcvaderlab/echo-tutorial>)

## Editorial Activity

**Review Editor** for *Frontiers in Medicine* (2021 IF: 5.058), section Nephrology, since August 2022.

## Peer Review Activity

Peer reviewer for the following Peer-Reviewed journals: *Scientific Reports* (2021 IF: 4.996), *Clinical Journal of the American Society of Nephrology* (2021 IF: 10.671), *Frontiers in Medicine* (2021 IF: 5.058), *Frontiers in Neurology* (2021 IF: 4.086), *Hemodialysis International* (2021 IF: 1.543), *BMC Nephrology* (2021 IF: 2.585).

## Mentorship Activity

- 2018 Miss Martina Milani, medical student. MD dissertation: [Volume Depletion Induced by Hemodialysis: a Model for the Echocardiographic Study of the Complex Relationship Between Pump Function and Myocardial Function], in Italian.
- 2017 Miss Veronica Evasi, medical student. MD dissertation: [Role of Cardiac Biomarkers and Imaging Techniques for the Evaluation of Cardiac Involvement in Patients Affected by Fabry Disease], in Italian.
- Miss Francesca Pescatore, medical student. MD dissertation: [The Burden of Childhood Abuse: Personality Disorders and Potential Psychiatric Perinatal Relapses], in Italian.
- 2016 Miss Anna Calastri, medical student. MD dissertation: [Post-Tonsillectomy Bleeding: Literature Review and Case Analysis], in Italian.

## Volunteer Activity

April 2019 – February 2020: **Chess Instructor** at the Spriet Family Children's Library, London Public Library, London, ON, Canada.

2016-2017: **Chess Classes for Beginner Players** London Chess Club, Kiwanis Seniors' Community Centre, London, ON, Canada.

2003-2007: **Summertime caregiver at a seaside residence for people with disabilities** at the UNITALSI Association, Borghetto Santo Spirito, Italy.